Politecnico di Torino

Master of Science program

Architecture Construction City

Thesis of Master’s Degree:

Layers of Past and Future
Geomatics applied to Archaeological Sites, a case study: Hierapolis of Phrygia, Turkey

Supervisors:

Prof. Giulio Tonolo Fabio

Prof. Spanò Antonia

Co-supervisor:

Dr. Patrucco Giacomo

Candidate:

Avivit Levy

Academic year: 2020-2021

This thesis is a result of my life-long passion for architecture which has introduced me to the concept of restoration and nostalgia. I strongly believe that history and architecture go hand in hand where the act of designing a building or a city starts from the history of the place and is conducted by the architect. The work on an archaeological site opened my eyes to a new field which I found fascinating and connected with the work of the architect, both in theory and practice. I hope that the investigations of new technologies in this work will serve both fields and will contribute to further research and discoveries.

Astract

My thesis will focus on the role of Geomatics in supporting the analysis and documentation of archaeological sites with geomatics technologies. More specifically, assessing the possibility to extract and investigate additional valuable information based on multi-temporal imagery acquired by UAVs (Unmanned Aerial Vehicles) with visible and NIR (Near-Infrared) sensors. The case study selected for the investigations is Hierapolis of Phrygia, Turkey.

The main issues discussed in the work are the evaluation of positional and thematic accuracy of the generated data, the impact of extracting relevant information from NIR and DSM (Digital Surface Model) data, the assessment of the performance of the different software involved in the various processes and the creation of a GIS of the area of interest. The main objective of this thesis is to suggest different geomatics methods and technologies for analysing and monitoring archaeological sites. Additionally, it attempts to demonstrate which of the methods might contribute to- and support the documentation of these sites as well as urban areas in general. The focus is on the needs of archaeologists, along with the idea that these technologies could be reinforced and more widespread in the world of urban designers.

The research process consisted of two main stages. Firstly, the detecting of changes in the Hierapolis site over time through the multi-temporal imagery acquired by the Laboratory of geomatics for Cultural Heritage with UAVs in the years 2015 and 2019. The detective work was done by extracting, processing and presenting the 3D data in different ways using various tools related to geospatial analysis and photogrammetry. In the second step, after discovering the main areas excavated in the period 2015-2019, an examination is made to derive information that supports archaeologists in planning the areas to be 'excavated' with non-invasive means.

The central structure of the thesis starts from the description of the historical, cultural and natural values of the Hierapolis site with a focus on the North Necropolis – the area of interest. Then, the available materials that were used in the different phases of the work have been introduced. The materials mainly include multispectral images acquired by a UAV from a survey conducted in 2015, and an orthomosaic and related DSM from a survey carried out in 2019. An updated CAD dataset of the area for 2015 and relevant literature were also valuable to my research. Based on the available materials, a review of various

methods was performed. These methods concentrate on the types of information that can be extracted from the raster products (orthomosaic and DSM) and the vector products (CAD files or GIS features). Using these two types of materials allows to examine the effectiveness of the different bands acquired by the UAV, the importance of multispectral information and the usage of vector features in a GIS environment.

Most of the obtained results represented in the paper indeed support the general claim. It can be deduced that recent Geomatics technological tools may provide possible scientific solutions for assisting the archaeologists with monitoring and documentation of the site. The research encourages a consistent development of geomatics in the archaeological field, hand in hand with gradually enhancing its technologies in many other fields of application such as the world of urban design.

Contents

01 Introduction

01 Introduction

The preservation and restoration of heritage sites have been undertaken around the world for a long time and are considered challenging tasks because the required geospatial and geophysical data are usually incomplete and complex. These data are collected using multiple disciplines and techniques from Geomatics science, such remote sensing and photogrammetry[1], in order to record and document the most up-to-date and accurate information that can assist in both theory and practice (Al-Ruzouq et al. 2018). GIS (Geographic Information System) is exploited to integrate the aforementioned data with other geospatial data to extract added value information.
My thesis will focus on the role of Geomatics in supporting the analysis and documentation of archaeological sites with new technologies by extracting and investigating additional valuable information to assist the archaeological research. This work is mainly based on multi-temporal imagery acquired by UAVs (Unmanned Aerial Vehicles) with visible and NIR (Near-Infrared) sensors, taken from a selected case study: Hierapolis of Phrygia, Turkey.
As a general term, a UAV, better known as a drone, is an aircraft that can fly without a pilot, guided autonomously and/or with remote control by using digital sensors and a ground control station. This platform has been adapted for many applications, such as military ones, agriculture, product delivery and aerial photography (Daniel Câmara et al. 2015). In recent years, UAV technology has become a useful and even essential tool for archaeologists, due to the non-intrusive studies that it can provide for the entire archaeological site with more rapid and cheaper procedures than ground-based surveys (Spanò et al. 2018; Chiabrando et al. 2018). The main issues discussed in the work are the geometric and thematic accuracy of the generated data; the results and the impact of exploiting NIR and DSM (Digital Surface Model) data when extracting thematic information in relation to archaeological interpretations and assumptions, the assessment of the abilities of the different software involved in the various processes, and the creation of a GIS of the area of interest.
This thesis was written as part of my Master’s Degree in Architecture Construction City, and although the topic of the documentation of archaeological sites may seem somewhat not close to my field of studies, more related to a modern design approach, there are some strong connections between the two, at both a local and global level.

[1] Photogrammetry – Deriving accurate and reliable 3D measurements from images. (Granshaw 2020)

From the local point of view, the North Necropolis is an integral part of the ancient city of Hierapolis, and as with any human settlement, regardless of the time, there are urban, cultural and environmental aspects that need to be studied carefully and preserved by architects, urban designers and conservation scientists together with the archaeologists when intervening on the existing fabric. Reconstruction and redesign play a critical role, especially nowadays when cities and landscapes are transforming rapidly (Kealy et al. 2011). Moreover, from the outset of the mission to survey the site, which was initially directed by Paolo Verzone, an architect, engineer and expert in the history of ancient architecture from the Polytechnic of Turin, the cooperation between archaeologists and architects has been particularly significant. In fact, the first significant restoration carried out in Hierapolis, regarding the great Flavian theatre, highlights the close connection between the main components of the scientific team, the archaeologists, the epigraphists and the scholars of the history of ancient architecture (D’Andria et al. 1985; Daria De Bernardi Ferrero, 1993).

The case study of Hierapolis provides a clear demonstration of how best to intervene in a sensitive area and which archaeological tools to use when coping with the constant tension between the demands for economic and social development on the one hand, and the need to preserve the heritage of a past rich with history and the physical evidence of this on the other. Furthermore, the importance of documentation and the need for technical improvement and innovation for surveying and research purposes arise from this case.

In his article from 2018, Francesco D’Andria, the Italian archaeologist who was the director of the Hierapolis archaeological mission for many years, highlights the negative impact of mass tourism on the site and the pressure from different public entities to accelerate the excavation activities, restoring and reusing the ancient buildings as fast as possible to attract more visitors and increase the regional economy, all this at the expense of scientific research and at times going against international restoration charters. The author identifies five macro-scale activities related to any archaeological site: *'preservation, conservation, archaeological fieldwork, research and presentation to the public of museums, sites and monuments'* (D’andria 2018: 205). The latter activity would seem to be the one most significantly associated with the architect and the urban designer. In fact, it is their responsibility to support preservation and developments. In addition, they have the competence and the duty to protect the ancient physical and spiritual assets in a modern city for future generations, as D’Andria stresses in his paper, similarly to other contributions (Boito et al. 2009; Waterson et al. 2019).

D'Andria considers the whole Hierapolis site as a potential economic asset and suggests increasing the cultural quality and the balance between the current 'fast tourism' and 'slow tourism' by further developments that will fit the existing environment. Among the solutions mentioned in his text, some themes are associated with the role of the architect and designer and can be divided into three main elements: regulations, urban planning and landscape design.

One example of the regulatory aspects involved in the architectural intervention in Hierapolis is the Preservation and Development plan created in 1991, which was added to the master plan from 1969 and was later supported by the Yönetim ve Sunum Planıs plan in 2007, which paid more attention to the historic and natural values. At this point it is also important to mention the inscription of the site in the World Heritage list in 1988, which most likely constituted the basis for the modification of the master plan in 1991. The World Heritage committee chose the Hierapolis site as a result of it meeting three of its criteria[2]:

(iii) To bear a unique or at least exceptional testimony to a cultural tradition or to a civilization which is living or which has disappeared: Hierapolis is an exceptional example of a Greco-Roman thermal installation established on an extraordinary natural site. The therapeutic virtues of the waters were exploited at the various thermal installations, the temple of Apollo, the theatre, which dates from the time of Severus and the necropolis, which extends over two kilometres, with a panorama of the funerary practices of the Greco-Roman era.

(iv) To be an outstanding example of a type of building, architectural or technological ensemble or landscape which illustrates a significant stage in human history: The Christian monuments of Hierapolis, erected between the 4th and the 6th centuries, are an outstanding example of an Early Christian architectural group with a cathedral, baptistery and churches.

(vii) To contain superlative natural phenomena or areas of exceptional natural beauty and aesthetic importance: Calcite-laden waters from hot springs, emerging from a cliff almost two hundred metres high overlooking the plain, have created a visually stunning landscape at Pamukkale.

The need to resolve conflicting ideas about the land use and the selection of the functions of the archaeological site while avoiding unsympathetic development are crucial issues raised in D'Andria's article. Regarding the Hierapolis site, the dilemma of attracting tourists to the existing ancient facilities, such as the theater, and the additional new features, like a museum or an archaeo-seismological park that can also host large events, stands in contrast to the sustainable approach of preserving the vulnerable

---

[2] From the official website of UNESCO: https://whc.unesco.org/en/list/485/

ancient buildings and their original purpose as heritage for future generations. According to the author, the building of a new bridge and paths on the site was a solution for controlling both the flow of the visitors and the restoration procedures that are constantly being done on the site, an action that strengthens the connection with the architecture field.

From a more global point of view, there are some notable similarities between the fields of archaeology and architecture, where creativity, precision and the ability to visualize the finished structure seem to be the common key features. These characteristics are required of both the architect and the archaeologist when beginning a new project on a site. Furthermore, when it comes to dealing with the cultural heritage of an archaeological site, more profound knowledge of matters such as the history, culture, society, politics and environment of the ancient city is required. This study is essential to know what has remained intact and what has been destroyed in order to guarantee better future preservation.
The common way to explore the story of the past is by the act of excavation in the archaeological site. The excavations are crucial for understanding the phases of the buildings, the urban space, and the lifestyle of the human community that inhabited in them.

The common way to explore the story of the past is by the act of excavation on the archaeological site. Excavations are crucial for understanding the urban space, the phases of the buildings and the lifestyle of the human community that inhabited them. However, at the end of the 80s, geomatics technology (based on metric measurements), was already being used by archaeologists. At that time, it was adopted for the purpose of surveying cultural heritage to foster preservation and risk prevention through a graphical visualisation of the site. In fact, the acts of archaeological digging and core sampling rely on various plans and maps for exploiting vector cartographic data such as cadastre, geological and landscape maps and also use raster data from aerial photographs, satellite images or any other set of digitalized images to create the operation report (Djindjian 1998).
The use of geomatics technology is constantly developing. There is no doubt that 3D geoinformation based on geomatic techniques and, in particular, UAV photogrammetry will provide a meaningful contribution to the Construction City theme as well. Thanks to this innovative technology, it is possible to document accurately large areas at different scales and levels of detail, detect developments and changes over time, extract topographic heights and generate a 3D model by simply using aerial photogrammetry technology, GIS systems and photogrammetric processing software.

The main objective of this thesis is to suggest different methods and new technologies for analysing and monitoring archaeological sites and to demonstrate which of these might contribute to and support the documentation of these sites and urban areas in general. The focus is on the needs of archaeologists, along with the idea that these technologies could be reinforced and more widespread in the world of urban designers. Other goals I focus on are, firstly, detecting the changes in the Hierapolis site over time through the multi-temporal imagery acquired by the UAVs in the years 2015 and 2019, by extracting, processing and presenting the 3D data in different ways using various tools related to geospatial analysis and photogrammetry. After discovering the main areas excavated in the period 2015-2019, the second goal is to investigate the possibility of deriving information to support archaeologists in planning the areas to be 'excavated' with non-invasive means.

After presenting the area under study, the following parts of the work are divided into three main topics. Firstly, I will explain the different methodologies I used in order to achieve the main goals mentioned above, from the creation of a 3D model in order to permit various visual investigations to a presentation of the GIS techniques that can support archaeological research. Subsequently I will examine the different results I obtained using the methodologies presented, while I will conclude by discussing the different methods used and the results obtained.

02 Study Area

02 Study Area

Site Description

The Hierapolis archaeological site is a UNESCO world heritage site due to its impressive archaeological remains and the unique formation of white natural travertine pools[3]. The area is also considered one of the most extensively excavated areas in Phrygia region, southwestern Anatolia, Turkey (Fig. 1).
The main excavation activities started in the late 50s under the management of the Italian Archaeological Mission of Hierapolis (MAIER). In the recent years the place became an area of interest for new technologies such as UAV in order to document and monitor the changes timeline in the area in a better and more consistent way (Castrianni et al. 2008; Chiabrando et al. 2018; Nuzzo et al. 2009).

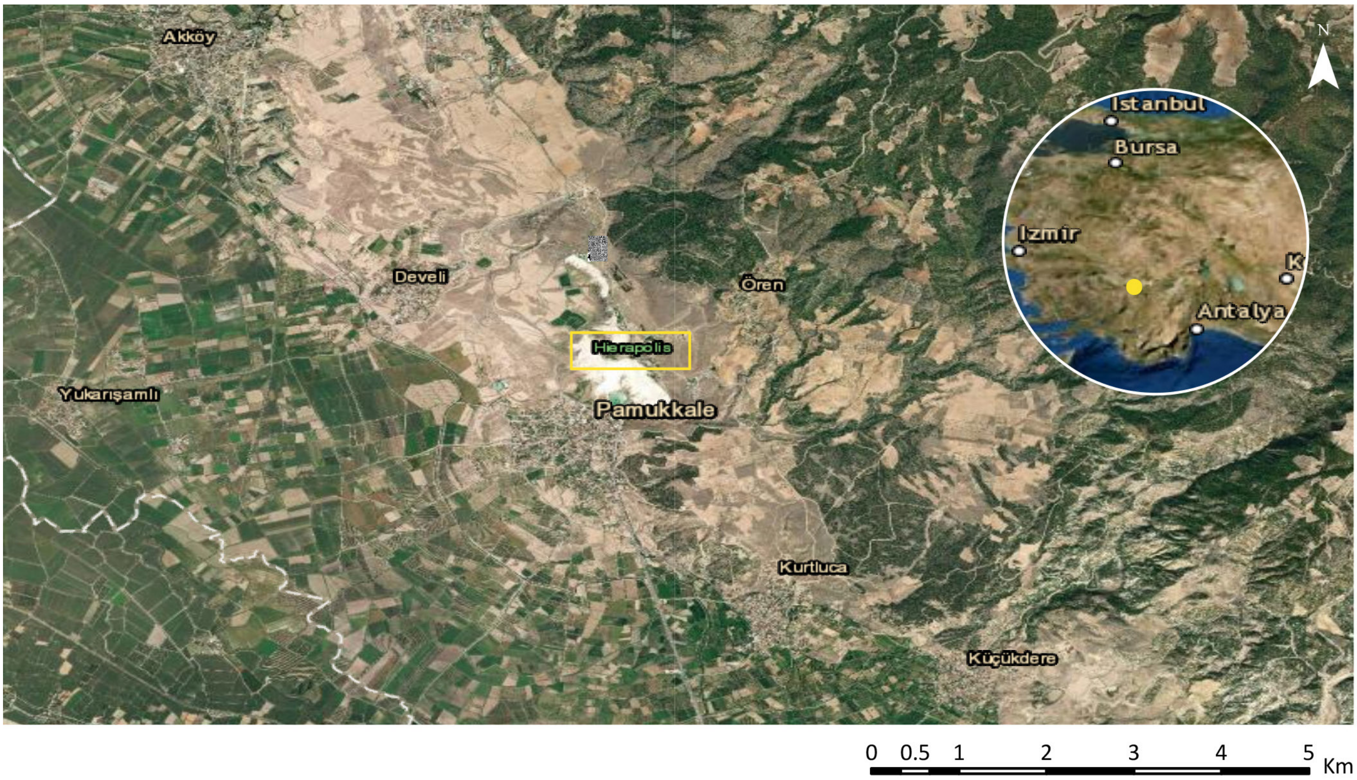

Fig. 1. A satellite image of the archaeological site, Hierapolis (Source: ArcGIS Pro, *WV03* satellite by *Maxar* technologies)

Hierapolis, which comes from the ancient Greek word for "Holy City", was structured and functioned as a Greek city from the 2nd century B.C until the 14th century A.D, and was founded on a calcareous shelf with many springs emerging from subterranean terraces. From a geological point of view, the site varies from clay to travertine stone, and with its ancient and current arrangements, the studies show that the

[3] From the official website of UNESCO: https://whc.unesco.org/en/list/485/

area was characterised by frequent destructive earthquakes, especially between the 4th-7th centuries. This phenomenon caused severe damage, followed by several urban transformations in the organization of the area (Negri et al. 2006; Vettori et al. 2019; Kumsar et al. 2016). The ancient city was characterised by Greek and first Roman imperial urban planning elements, such as grid roads with a main street: *Cardo-Maximus*, Agora, temples, theatre and other examples. Some important remains such as the temple of Apollo, Bath-church, Ploutonion, Nymphaeum and Necropolis were already studied in depth.

North Necropolis

In general, Necropolis is a large burial site, usually located outside of the settlement, in the Greek language the word means ‘city of dead’. In Hierapolis we can find one of the largest cemeteries in Anatolia, filled with sarcophagi and divided into several areas in the north, south and west (Fig. 2,3). In the late Hellenistic and early Imperial periods, tomb clusters were located along the main roads towards the town, as can be found in many Roman settlements. However, from the late 1st and early 2nd century AD, the hilltops in the north-east and east of the town became common areas for family tombs. The change with the topographical location may represent a different approach in the Greco-Romans period which tended to experience and use the surrounding landscape (Wenn et al. 2017).

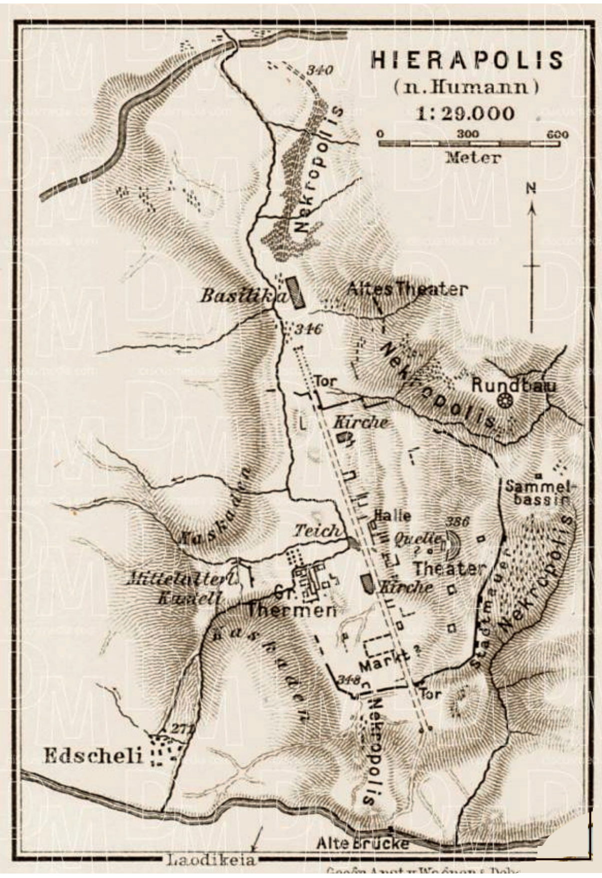

Fig. 2. The historical map of Hierapolis by Humann in 1914 (Source: https://www.discusmedia.com/maps/turkish_city_maps/5595/)

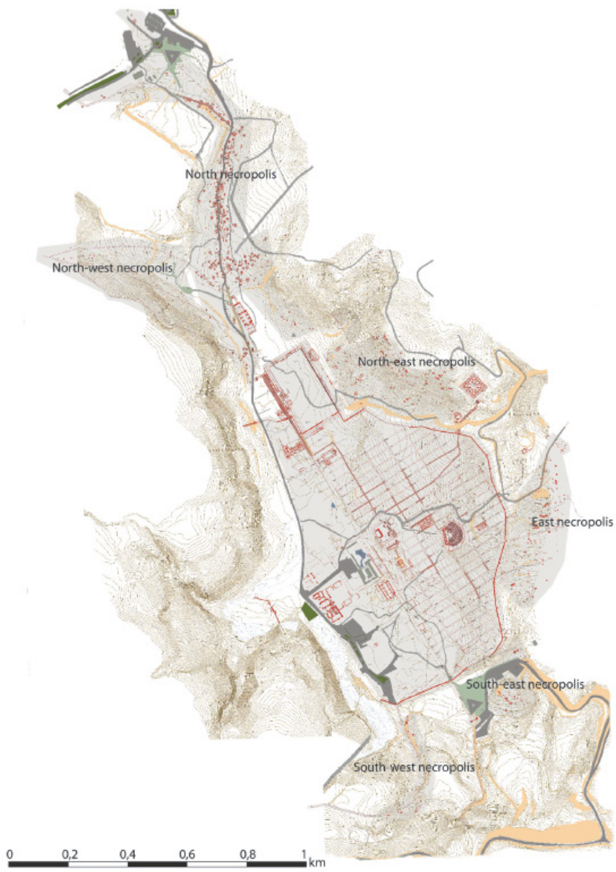

Fig. 3. The town plan of Hierapolis with the Necropoleis (Source: Atlante di Hierapolis di Frigia, 2008)

The graves can be classified by different periods which reflects the religious and socio-economic status of the dead. We can distinguish between four main types of architectural graves (Fig. 4):

a. Circular tumulus- a rounded and very large tomb, with a narrow passageway leading to a vaulted chamber inside. The structure used mainly as a family tomb with a division to some rooms. Dated from the 2nd century B.C. until the 1st century A.D.

b. Aedicule tomb - positioned on a podium with a pedimented roof. Considered as a monumental funerary structure with decorative features which emphasizes on the public remembrance of the buried and his lineage. Dated from the 1st century A.D. until the 2nd century.

c. Bomos - similar to the Aedicule tomb, characterized by a decorative, quadrangular geometric structure, with a flat roof that functions as a base for a sarcophagus. Dated from the 2nd century A.D. until the 3rd century.

d. Sarcophagi - some built on a substructure, others hollowed out from the rock made by marble or travertine. Many are covered with double pitched roof, decorated and enriched with inscriptions. (Ronchetta 2017).

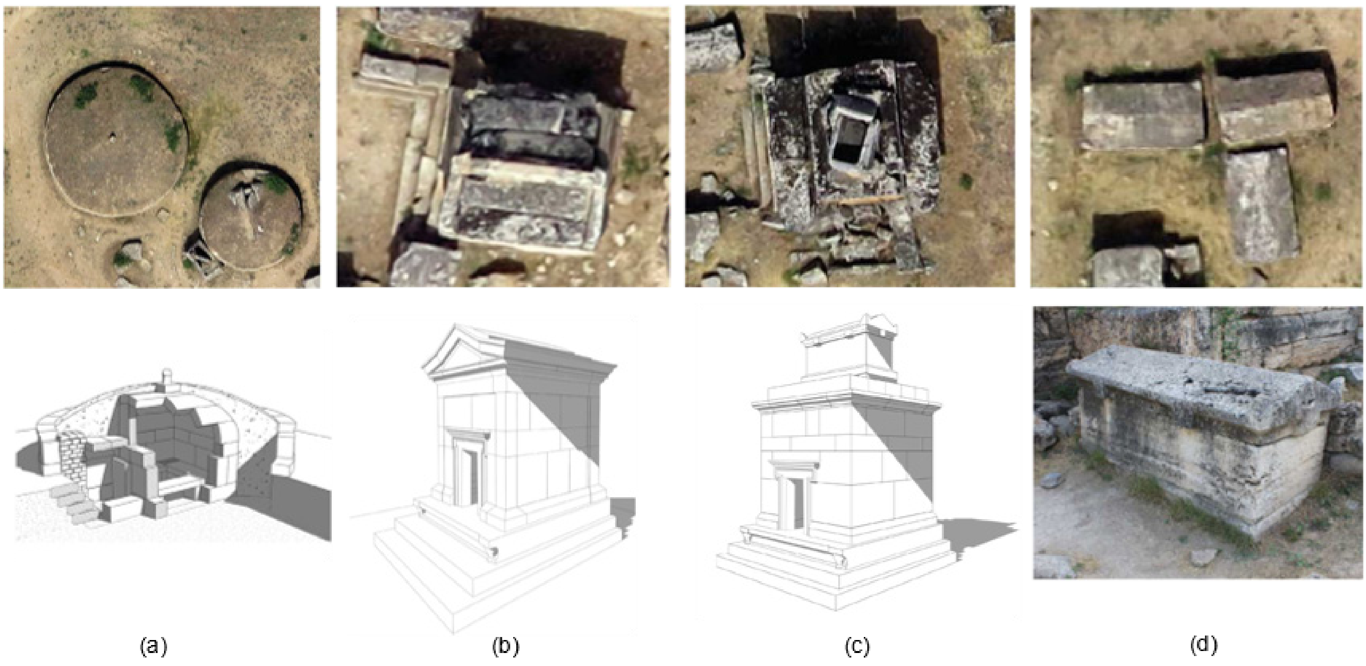

Fig.4. Classification of the common types of tombs in the Necropoleis from aerial view and 3D façade (Sources: images from a survey done in 2015, by the Cultural Heritage Lab in the Architecture and Design (DAD) department, Polytechnic of Turin, and Ronchetta 2017)

Of all mentioned above, the sarcophagi were the only type of tomb made from marble, while all the other forms usually made from limestone. Each tomb has an inscription with the name of the deceased, his social and political status and his activities (Wenn et al. 2017).

Among all burial zones, my study will focus on the Northern Necropolis area (Fig. 5,6) which is considered the largest one in Turkey with more than 1200 graves. The burial area composed of one main road around 500 meters in length and consists of two complexes from both sides. The parallel travertine blocks are arranged according to the length, which delimit the paving stones made up of compacted limestone. The main path was planned with access to both monumental tombs and sarcophagi with funerary inscriptions estimated from the mid 3rd century A.D. Some of the graves are set on a podium and some, on the ground level arranged along the main street and along internal lines. At times, they are organized as clusters which can help us to better understand the differences between families, temporal successions and religions (Chiabrando et al. 2018; Ritti et al. 2007).

The main reason for investigating the North Necropolis is because the area experienced fast transformations due to intense archaeological excavations that were executed and recorded between the years 2015- 2019. Therefore, the area is considered a good starting point for practicing the various technologies to achieve the different aims of the thesis.

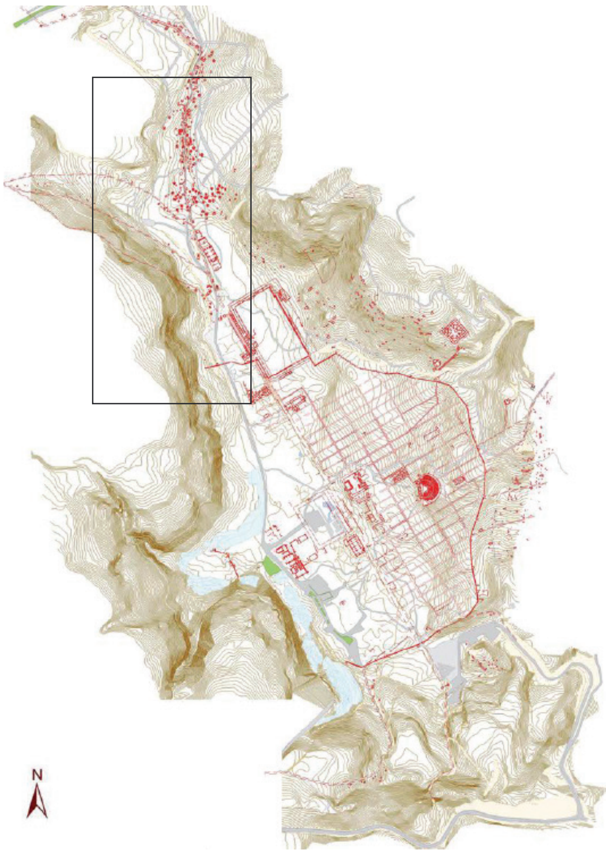

Fig. 5. (Above) A map of Hierapolis, the building layer is shown with red polygons superposed on a topographic map with brown contour lines for the land slopes and in grey the modern roads. The North Necropolis is highlighted with a black rectangle. (Source: Atlante di Hierapolis di Frigia, 2008).

Fig. 6. (Left) An orthoimage of 2019, North Necropolis- the study area.

03 Materials

03 Materials

Mapping Evolution

Since the 1950s, the Hierapolis site was intensively studied with the traditional archaeological method of manual excavations. From the 1960s to late 1990s, the city map was based on ground traditional surveys, gradually supported by topographic measurements and CAD archiving (Spanò 1999). During the years 1960s-1970s, the acquisition of remote sensing images using satellites such as the *Corona KH-4A* and *Hexagon* were performed with a ground resolution between 2.74 and 9 m, mainly for military purposes. Despite their medium spatial resolution, a couple of years after they were declassified in 1995 for civil use, researchers started to exploit the images. The images were a very useful tool for landscape archaeology which is important from a historical point of view. Using this technique allowed to supply important data about big patterns such as the ancient roads' networks and ancient orthogonal land divisions, which had better visibility than today. Furthermore, the analysis of the images is considered to be a fundamental tool for the reconstruction of the urban layout and the ancient topography. The reason is that they present the city and the surrounding landscape as it was before some of the modern transformations of the last decades. Modern transformations refer to the realization of infrastructure, the construction of new buildings above the ruins, the expansion of the modern towns in the surrounding areas, the diffusion of agriculture and such. This analysis was possible thanks to recent satellite images of *Ikonos-2* and *QuickBird-2* satellites which were taken at the beginning of the 2000s. As can be seen in figure 7, the modern technology made use of a ground resolution around 0.60 to 0.80 m for panchromatic[4] and 2.40 to 2.90 m for the multispectral[5] images, which is considered to be exceptionally high in accuracy. After verification in the field, the new orthoimages made a significant contribution to the discovery and extraction of street networks, country roads, fields, modern houses and more. In addition, the modern images acquired by the *Quickbird* satellite (nowadays not operational anymore), when compared to the medium scale images from 60s and 70s, are more efficient in the study of chronology. This comparison may also help detect anomalies related to buried archaeological structures and paleo-environmental elements (Castrianni et al. 2008; Scardozzi 2008; 2007; D'andria F et al. 2008).
Yet, using this method was not enough to generate an archaeological map of the ancient city since the task required a higher scale for measuring and studying the archaeological structures. Consequently, in

[4] Panchromatic-Black-and-white image usually consisting of one visible-light band (Granshaw 2020).
[5] Multispectral- Acquisition of several spectral bands relating to two or more ranges of frequencies or wavelengths in the electromagnetic spectrum (Granshaw, 2020; https://www.merriam-webster.com/dictionary/multispectral).

Fig. 7. Hierapolis in a *Corona KH-4A* photo taken in 1968 (left) and satellite *Quickbird-2* image of 2007 (right) (Source: Scardozzi 2008)

the 2000s, the first main digital map of Hierapolis with a scale of 1:1000 was generaned,using ground techniques in addition to the traditional ones.

During this process, precise topographical measurements with the use of Total Station and GNSS Control Points, allowed the recording of archaeological remains that were well-preserved and visible on the surface. Thereupon, it was possible to achieve a reliable and updated site plan with validated positional accuracy. In what followed, by using geometric objects as points, lines and polygons, which describe the elements of the ancient city, the cartographic items were sorted into main topics.

Automatic techniques of auto-correlation were applied on the images acquired by an aeroplane to create a digital photogrammetric map. Afterwards, by extraction of the terrain data from this map, a 3D model was created, which helps to accurately study the territory in the third dimension. The process involved the exploitation of contour lines and elevation points from some map's sheets which were updated in the 90s, provided by the Turkish government.

The orthoimages and the numerical derived maps, with technical specification of maps for archaeological research at 1:1000 map scale, became layers in the GIS including all the information already collected from the 1960s to the 2000s of Hierapolis and its territory. The data was stored in a database archive for future retrieval of spatial information and other data collections that will be accessible on the World Wide Web (Astori et al. 2003; Spanò et al. 2004; Castrianni et al. 2008; D'andria F et al. 2008).

Survey Planning and UAV Datasets Acquisition

In the last few years, the UAV technique has greatly expanded and became efficient with documentation of the archaeological site. This new technological improvement offers high-resolution remote sensing and provides the archaeologists further information regarding the landscape. In fact, this method assists them with a better understanding and interpreting of large archaeological sites, in high spatial and spectral resolutions over time. More than that, the possibility to perform surveys at regular intervals, useful for monitoring the territory with archaeological excavations constantly ongoing, and the ability to perform surveys in places that logistically difficult to access for measuring or organization photogrammetric flights, places the method in high priority due to its great efficiency.

The UAV surveys were carried out by the Geomatics for Cultural Heritage Lab in the Architecture and Design (DAD) department, Polytechnic of Turin in 2015 and 2019[6].

For each flight, different sensors, cameras and datasets have been used to create orthoimages and DSM (Digital Surface Model), and so, might display some differences in the quality and the accuracy of the outputs.

The UAV acquisition used an aerial photogrammetric technique, the term composed of the two words: 'photo' and 'meter' which means measurements from a photograph. As a definition: the art, science and technology of obtaining reliable information about physical objects and the environment, through processes of recording, measuring, and interpreting images on photographs.

The aerial digital photogrammetry is mostly used for 3D mapping with digital photographs taken from a camera mounted on the bottom of a UAV. The plane flies over the area following a pre-defined flight path so it can take overlapping photographs or videos of the entire area to get complete coverage (Pillay 2015).

The photogrammetric method used in the case of Hierapolis was the SfM (Structure from Motion) algorithm that allows the generation of a high-detailed 3D model of the area from overlapping multi-view 2D images to reconstruct the photographed scene.

No doubt that the combination of the UAV and the SfM technology provides a low-cost, rapid and efficient tool to obtain rich and accurate 3D data of the topography for credible surveys.

While preparing the UAV flight, some parameters are important to set by the user in order to acquire high- quality images. Factors such as flight height, shooting angles, the number of pictures and flight route affect the photos and the processed products, and for this reason, it is important to bring up some relevant terms that help understand the data acquired in the Hierapolis flights later in 2015 and 2019:

[6] The laboratory website: https://www.g4ch.polito.it

GSD (Ground Sample Distance) or the ground resolution distance is one of the most crucial elements for every photogrammetric project. By definition, the ground sample distance is the distance between two consecutive pixel centers measured on the ground[7], in other words, the size of a captured ground that represents one pixel in a raster image. With a high value of the GSD, the spatial resolution of the image will be low and fewer objects will be visible – and vice versa. This relation can be explained mathematically by looking at the formula below:

$$GSD = \frac{(H \cdot px)}{f}$$

Three variables affect the value of the GSD: ***H*** represents the flight altitude, ***px*** equals to the linear dimension of the pixel and ***f*** is the focal length of the sensor lens. The focal length is basically the distance between the sensor and its lens. It can be seen from the equation that the GSD has also a direct relation with the flight height, the higher the flight, the higher the GSD value. On the other hand, there is a reverse ratio between the GSD value and the focal length, with the high value of the focal length, the GSD value will be lower and this results in a more detailed and clear image. The schematic drawing below (Fig. 8) emphasizes the role of the focal length (*f*) in the GSD and so the accuracy of the image. When the value ***f*** is low, the angle of view is wide and the camera will capture more area, but at the same time, the pixel size will be bigger. With a high value of the focal length the captured image contains small pixels and therefore high-quality results.

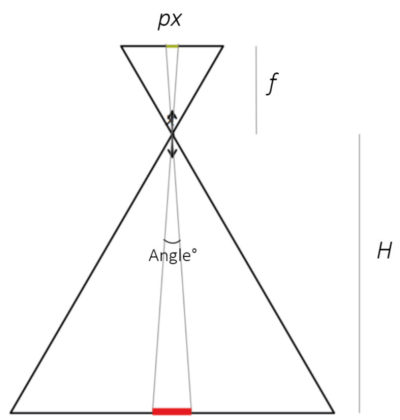

Fig. 8. A schematic drawing emphasizes the principle of the Focal Length of the lens (Source: http://gsp.humboldt.edu/OLM/Courses/GSP_216_Online/lesson2-2/scale.html)

It is worth mentioning that the variables above are not always set in their ideal mode, as each site has different requirements and constraints to be considered, such as the size of the area that needs to be

[7] Source: https://support.pix4d.com/hc/en-us/articles/202559809-Ground-sampling-distance-GSD

covered or the durability of the sensor's battery. These restraints lead to a compromise between features such as the overlapping percentages of the images when planning the flight path of the drone, or the hight of the flight for faster recording and and other factors.

At this point, it is also relevant to highlight the spectral and the radiometric resolutions, due to the significant role they play when using UAV technology. In general, the **spectral resolution** deals with the wavelength width and the number of bands in the electromagnetic energy that can be recorded by a device. Multispectral images grant a more complete view of the observed object and may provide a more accurate optical observation and reliable interpretation. Thus we learn that fused images can be acquired by sensors with sensitivity to visible and infrared ranges. Furthermore, additional information can be derived from integrated data with different characteristics, rather than each individual band data. Depending on the multispectral reflectivity of the target, these two factors can assist with detailed classification and analysis of the diverse elements which are captured in the scene (such as types of vegetation, water and soil). Moreover, thanks to the unique reflected radiation of each material on the ground, which is called the **spectral signature**, they can be identified more easily. The term will be explained in more details later on in the Methodologies section.

The **radiometric resolution** related to the levels of intensities of the radiation that the sensor can differentiate and measure by a number of bits. With a high number of bits, the image shows various shades, for example, 8-bit image can display 255 tones for each pixel. High resolution can be essential when analysing and classifying different materials in the site due to accurate match to their spectral signature and high contrast image (Pohl et al. 1998; Suárez et al. 2008). In the Hierapolis site, summarizing the information from both flights can help explain some of the differences in processes and results of the orthophotos, orthomosaic and the DSM by using the various software.

2015

Area: North Necropolis

Acquired data	Camera model	Focal length (mm)	Image resolution	N° of images	Estimated flighing altitude (m)	Coverage area (km²)	Estimated Ground resolution distance :GSD (cm/pix)
RGB	Canon PowerShot S110	5.2	4000*3000	148	104	0.246	3.29
NIR	Canon PowerShot S110	5.2	4000*3000	151	101	0.228	3.19

2019

Area: Hierapolis (all site)

Acquired data	Camera model	Focal length (mm)	Image resolution	N° of images	Estimated flighing altitude (m)	Coverage area (km²)	Estimated Ground resolution distance :GSD (cm/pix)
RGB	S.O.D.A 3D	10.6	5472*3648	3129	180	----	4<GSD <8.6

Table 1. Summary of the flights' main features acquired in 2015 and 2019 (Sources: Sammartano et al., 2020; Chiabrando et al., 2018; Dataset of images acquired in 2015).

Comparing the data in table 1 shows that the flight of 2015 included two different datasets that were acquired by two sensors. The first one, with a camera model *Canon PowerShot S110 RGB* for visible orthoimages with three bands (RGB) captured in the visible spectrum, with a central wavelength of 450 nm (Blue), 520 nm (Green) and 660 nm (Red)[8]. The second sensor acquired with *Canon PowerShot S110 NIR*, same as the first camera mentioned, but with a modified filter that allows obtaining data in the Near-Infrared band as well. Here, the NIR orthoimages are composed of three bands (RGN), acquired in the visible and the Near Infra-Red spectrum with a central wavelength of 550 nm (Green), 625 nm (Red) and 850 nm (NIR) (Fig. 9) (Chiabrando et al. 2018).

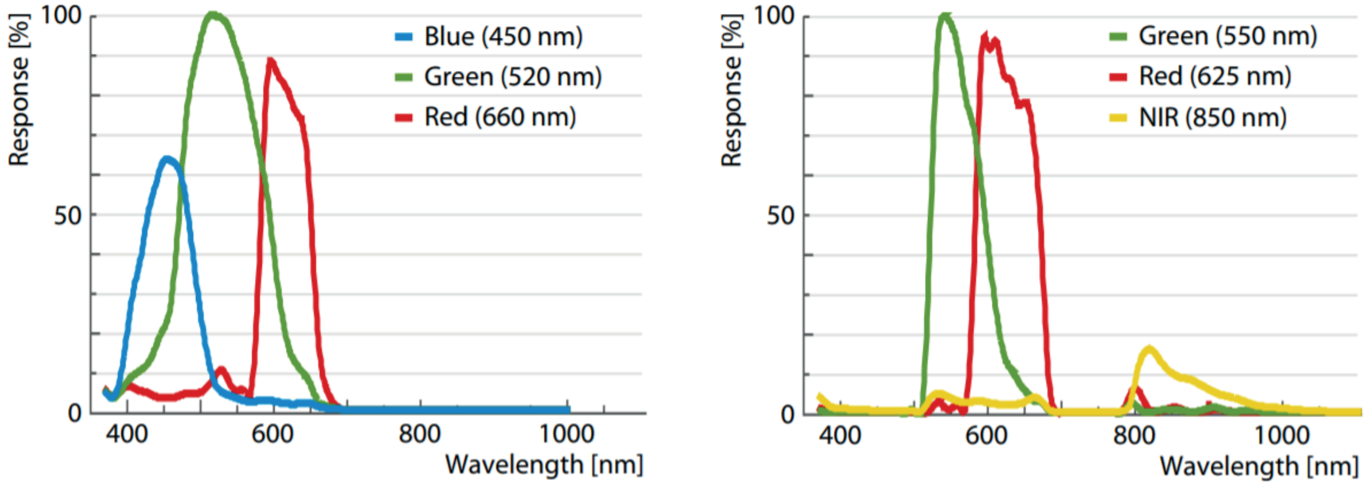

Fig. 9. The spectral response graphs for the *Canon S110 RGB* (left) and *Canon S110 NIR* (right), the cameras show different filter that can acquire information in different regions of the light spectrum (Source: http://95.110.228.56/documentUAV/camera%20manual/%5BENG%5D_2014_user_manual_s110_v3.pdf)

Fig. 10. An image aquired by the UAV during the flight over the Hierapolis site in 2015. using *Canon S110 RGB* camera (source: Cultural Heritage Lab in the Architecture and Design (DAD) department, Polytechnic of Turin)

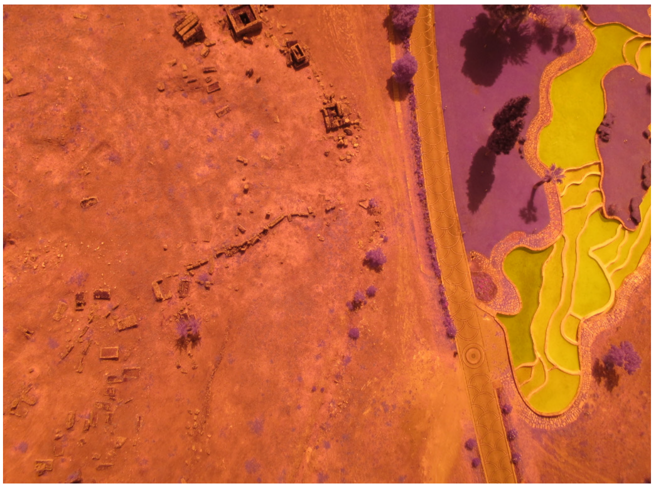

Fig. 11. An image aquired by the UAV during the flight over the Hierapolis site in 2015. using *Canon S110 NIR* camera (source: Cultural Heritage Lab in the Architecture and Design (DAD) department, Polytechnic of Turin)

[8] From the user manual of the camera Canon PowerShot S110: http://95.110.228.56/documentUAV/camera%20manual/%5BENG%5D_2014_user_manual_s110_v3.pdf

Examples for both cameras can be seen in figures 10 and 11. The images are part of a series of photos that were taken during the UAV flight in 2015 in the Necropolis. As can be seen in figure 11, the NIR sensor produces images with 'artificial' colours which do not reflect the reality, that will be explained later on, in the Methodologies section about the 'False colour' image and its contribution to my study.
The flight of 2019 contained only the visible spectrum with three bands (RGB) using *S.O.D.A 3D* camera[9] with the ability to change orientation during a flight. Moreover, the flight altitude and the Ground Resolution Distance are higher in this year than 2015 since the purpose of the mission was to cover the whole site and not just the northern Necropolis zone. Yet, the images obtained were still in a high spatial resolution due to the advanced abilities of the camera. (Sammartano et al. 2020).

Elevation Information

Thanks to the UAV method, it is possible to measure the elevation in the area of interest. This technique is considered to be an accurate and detailed way to represent the morphology of the terrain and infrastructures. It is mportant to mention the differences between DEM (Digital Elevation Model) and the DSM (Digital Surface Model): while the first one represents an elevation of the earth as a vertical distance between the bare-ground surface and a reference datum without including the natural and built surfaces, the second one, captures both the natural and built features (Fig. 12) (Granshaw 2020).
During the photogrammetric process of both flights, a DSM was produced, which as mentioned, capable of capturing both natural and artificial features of the environment.

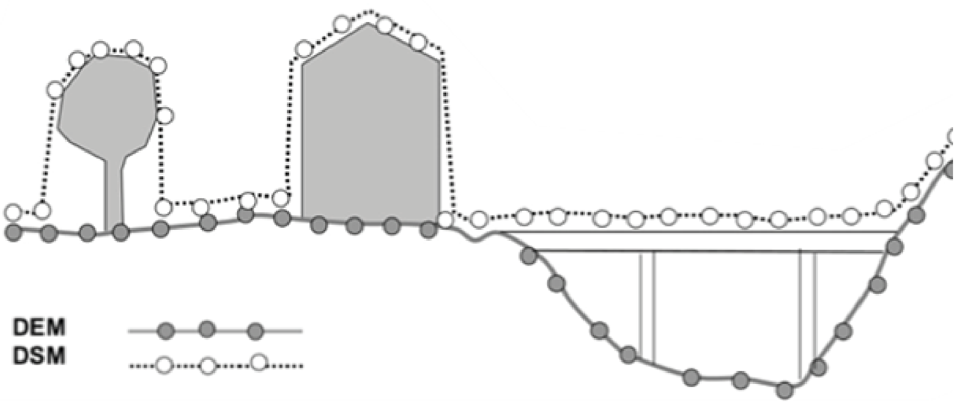

Fig. 12. A schematic drawing distinguishs between DSM (Digital Surface Model) and DEM (Digital Elevation Model) (Source: https://www.slideshare.net/3dgis/database-topografici-regole-e-strumenti-maurizio)

[9] The band responses are similar to the Canon PowerShot S110

There is no doubt that in the case of Hierapolis, the DSM has much more advantages than the DEM, since the elevation data also recognize the archaeological structures as well. This feature helps to discriminate between the soil and the tombs, and so, facilitates the documentation processes of the site. An example for the DSM can be seen in figure 13, a product of the UAV flight of 2019. The different colours on the map represent the changes with the topography. In the image, the burial area coloured in bright green is characterized by a mostly flat surface, while the east and west with increasing and decreasing of the elevation.

In the following part of the thesis, the DSM data from both years will help to understand the behaviour of the landscape with time and will assist with further investigations and anomalies that are linked to the elevation component.

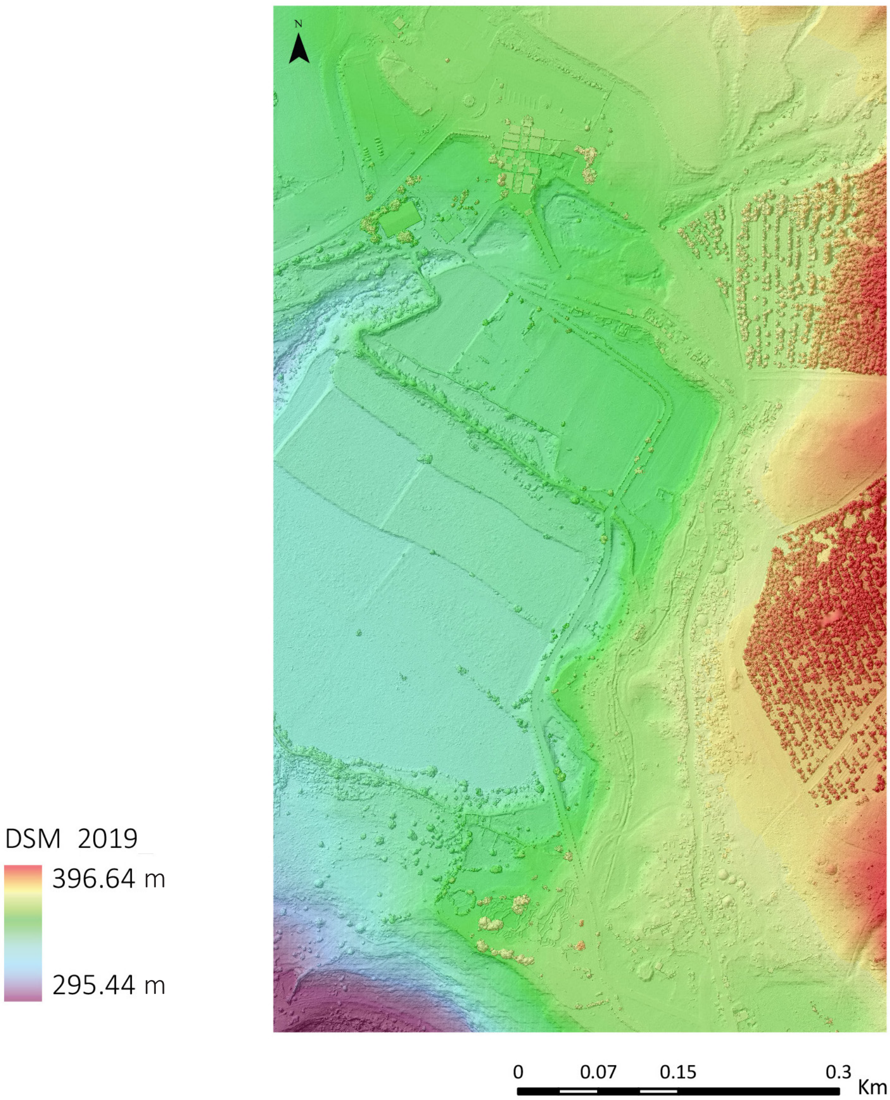

Fig. 13. DSM of 2019, extracted from *ArcGIS Pro* software

CAD data

In the previous paragraphs, the focus was on Raster data that was obtained by the UAV. Yet, additional material was needed in order to generate a GIS map for the Necropolis area which composed of lines and polygons. For that matter, I used a CAD file of the area which is a repository of the archaeological map and contains elements of the ancient city. The CAD data is a vector format, which allows in a GIS environment, to store and edit multiple information regarding each object on the map. The file derives from the '*Atlante di Hierapolis di Frigia*', Atlas of Hierapolis of Phrygia I (2008) and the following version, Atlas I (2015). The CAD dataset (Fig. 14) consists of maps and surveys created in earlier years and contains various layers related to different types of tombs, topographic lines, water bodies and modern roads made of lines, polylines, arches, circles and hatches (Astori et al. 2003; Spanò et al. 2004; Castrianni et al. 2008; D'andria et al. 2008).

Later on, this data will be converted to GIS components by using the ArcGIS software.

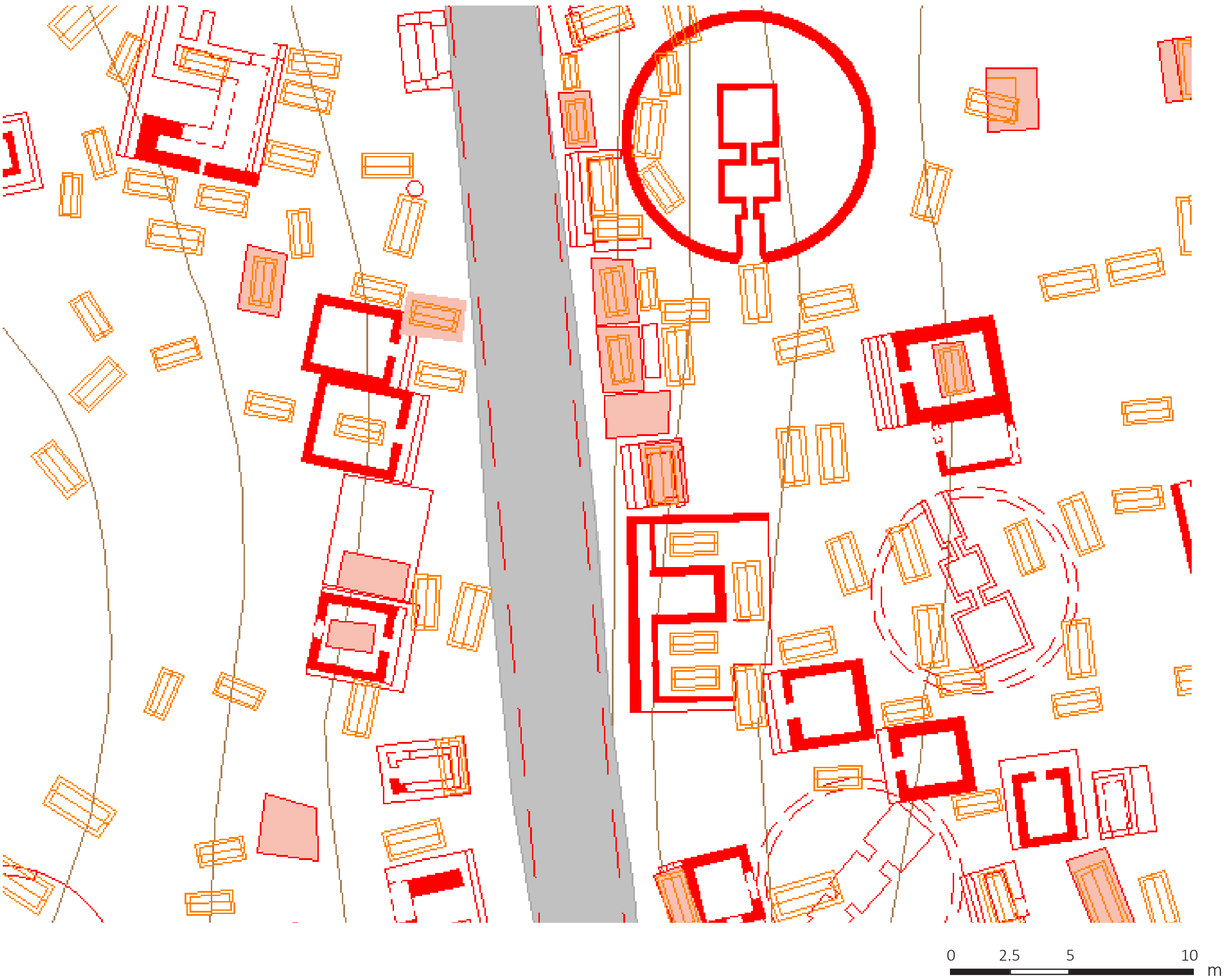

Fig. 14. A segment from a DWG plan of the Hierapolis site, updated to 2015 (source: Cultural Heritage Lab in the Architecture and Design (DAD) department, Polytechnic of Turin)

04 Methodologies

04 Methodologies

Preface

The chart below (Fig. 15) summarizes the steps for achieving the main goals of the thesis. Starting from generating a 3D model from series of images taken with a sensor, during the flights over the archaeological site in 2015 and 2019. All photogrammetric processing was done by using *Agisoft Metashape Pro* software. Later, continuing with different analyses of the available data as well as the implementation of a GIS demonstrator, both done by using *ArcGIS Pro* software.

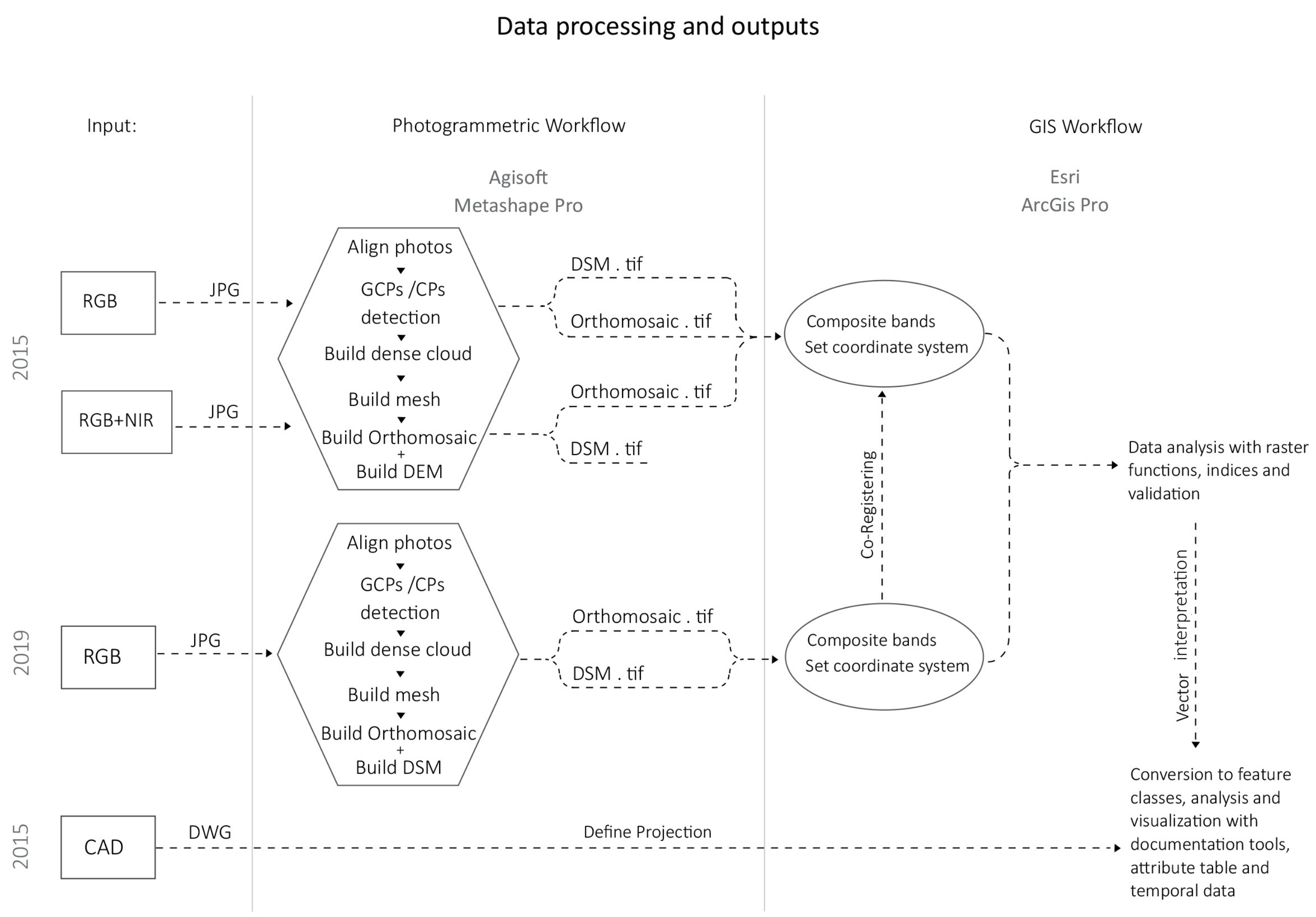

Fig. 15. Scheme summarizes the data processing and information extraction workflow.

Photogrammetric Workflow

Before the data acquisition, a number of artificial targets to be used as GCPs-Ground Control Points (Fig. 16,17) were well-distributed on the terrain and measured by coordinates. The amount of the points was related to the size of the area of interest in order to ensure a high accuracy of the outcomes.

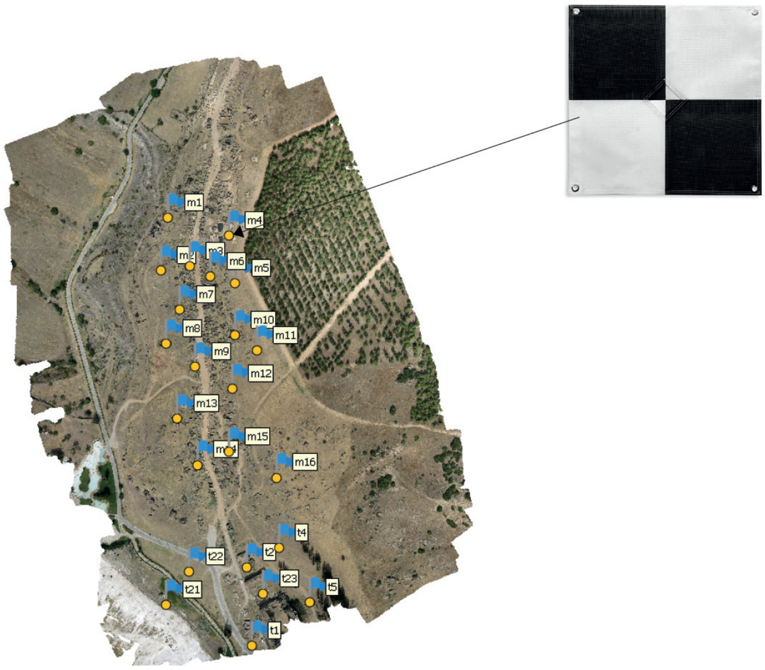

Fig. 16. Distribution of the GCPs in the site in 2015, background: orthomosaic from 2015, extrated from *Agisoft Metashape Pro*

Fig. 17. Location of one GCP on the ground in the archaeological site Hierapolis, background: image obtained by the UAV in 2015

The 3D aerial survey was managed with *eMotion* software which considered an automatic photogrammetric approach and required to set two parameters regarding the area of interest: the Ground Sample Distance (GSD), and the overlapping percentages among the images (side-lap and end-lap). After inserting the data, the software calculates the average flying height and the number of strips required to cover the area (Chiabrando et al. 2018; Nikolakopoulos et al. 2017). Figure 18 presents the location of the photos taken in the survey done in 2015 in the Necropolis. In the image, the blue colour in the center shows a high overlapping (with more than nine photos), which gradually reduced at the edges of the area with less overlapping – as can be seen in orange.

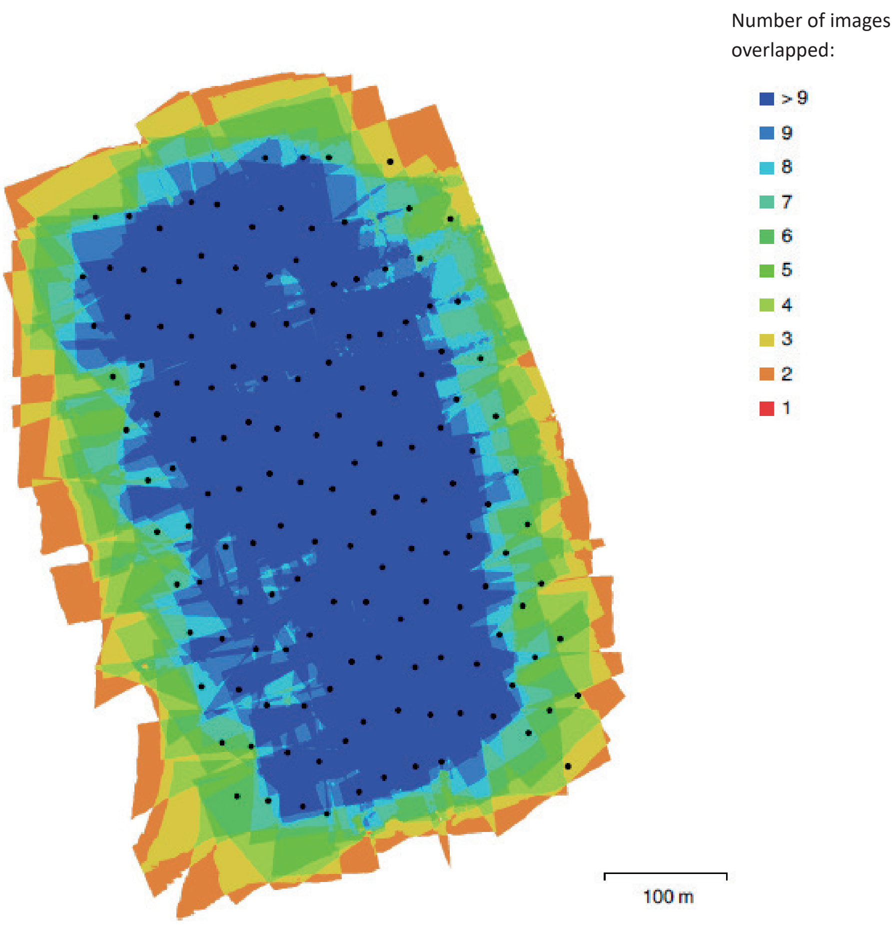

Fig. 18. Camera location and image overlap for the images acquired in 2015 in the Necropolis area, the blue colour represents the highest overlapping,extrated from the report of *Agisoft Metashape Pro*

My starting point in the thesis was by receiving multispectral images from the Geomatics laboratory for Cultural Heritage[10] acquired with UAV platforms in 2015 and a ready-made orthomosaic and DSM of a survey, which was taken in 2019. The first aim was to create a 3D model using Agisoft Metashape Pro software, which processed the aerial data and generated an orthomosaic and DSM from the orthophotos of 2015.

After the images were loaded, the program estimated the position and orientation of the camera of all the photos and aligned them automatically into a sparse point cloud composed of tie points (Fig. 19,21). Since each Ground Control Point located in the site was already defined by coordinates, the next step was to import an external CSV file with the available reference coordinate data for each point. Then, matching these points to their specific location (in each photo) of the preliminary model as markers, in order to set a precise geospatial location. In the *Metashape* program two types of markers are exist:

GCPs - optimise the bundle adjustment of the photogram process (Fig. 20) and georeference the model.

Check Points - validate the accuracy of the camera alignment and estimate the overall success of the

[10] https://www.g4ch.polito.it/wordpress/en/

photogrammetric method.

For both types of markers, an error estimation (RMSE[11]) was carried out (Fig. 22), and also can be seen in table 2. In relation to the area that was covered, optimal results were achieved for both years, with a RMSE in the range from few centimeters to 20 cm.

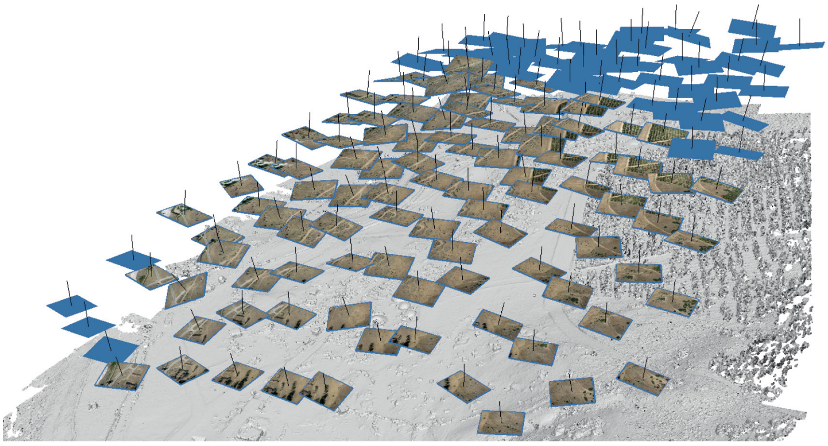

Fig. 19. Distribution of the orthophotos acquired by UAV in 2015, extrated from *Agisoft Metashape Pro*

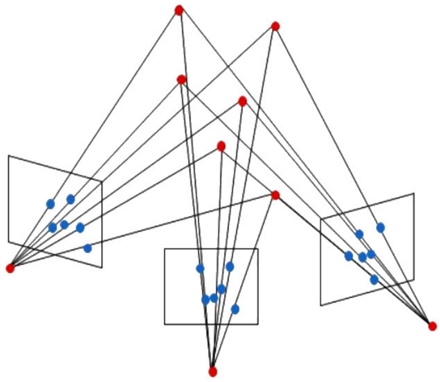

Fig. 20. A scheme shows the method of a bundle adjustment, which estimates the position of the photos by the camera parameters and 3D coordinates. (Source: https://graphicdesignjunction.com/2019/09/how-does-triangulation-in-photogrammetry-work/bundle_adjustment/)

Fig. 21. Result of the sparse point cloud using orthoimages of 2015, extrated from *Agisoft Metashape Pro*

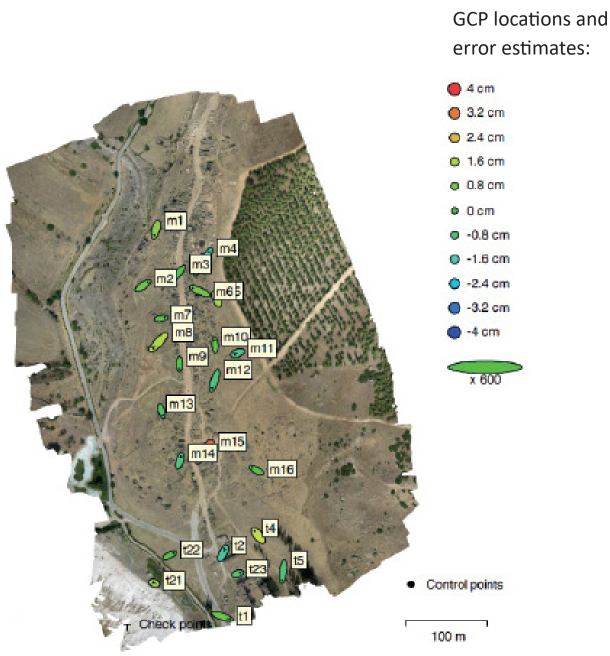

Fig. 22. Location of Ground Point Control and the Check Points and the estimation errors of orthomosaic of 2015. The colours show the error with the Z axis and the shapes of the ellipses represent the errors with X, Y axis.

[11] Root mean square deviation

2015

Acquired data	Tie points	Dense cloud	3D mesh triangles	N° Ground Control Points (GCP)	N° Check Point (CP)	RMSE GCPs (cm)	RMSE CPs (cm)
RGB	348,482	69,159,580	13,831,872	16	7	2.7	3
NIR	357,408	69,694,043	13,938,792	15	8	2.5	2.8

2019

Acquired data	Tie points	Dense cloud	3D mesh triangles	N° Ground Control Points (GCP)	N° Check Point (CP)	RMSE GCPs (cm)	RMSE CPs (cm)
RGB	----	------	------	35	10	10	23

Table 2. Summary of the flight's main features acquired in 2015 and 2019

In order to obtain a complete and efficient 3D model, a dense point cloud process was applied (Fig. 23). To do this, the program estimated the camera positions and calculated the information related to the distance between the actual surface of the site and the camera location for each image. Then, based on the cloud point information, the software was able to reconstruct a solid surface composed of polygons – a mesh model[12] (Fig. 24).

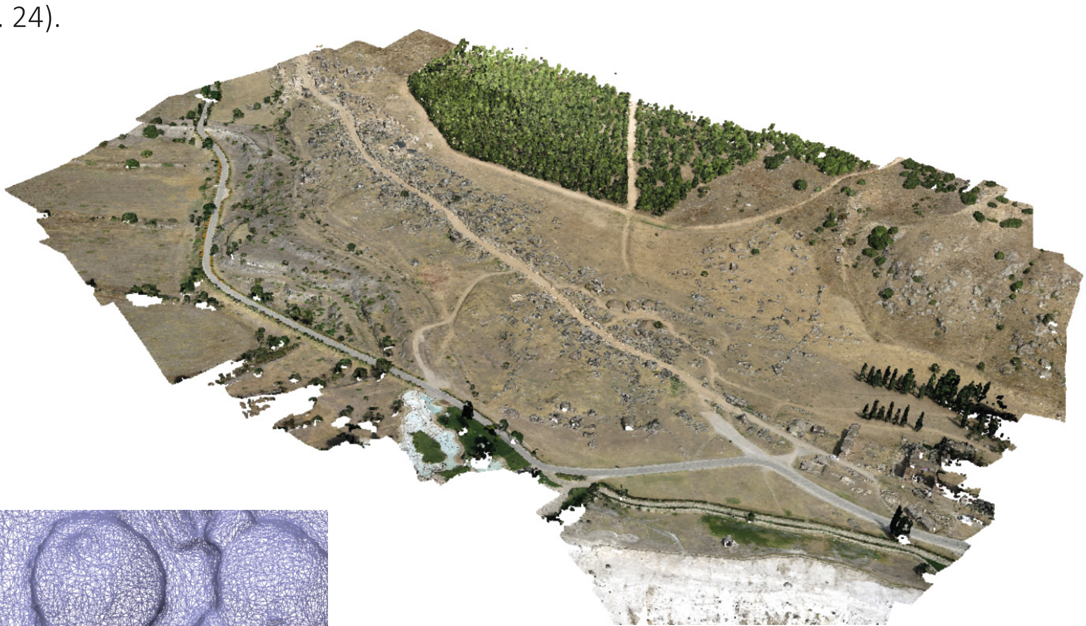

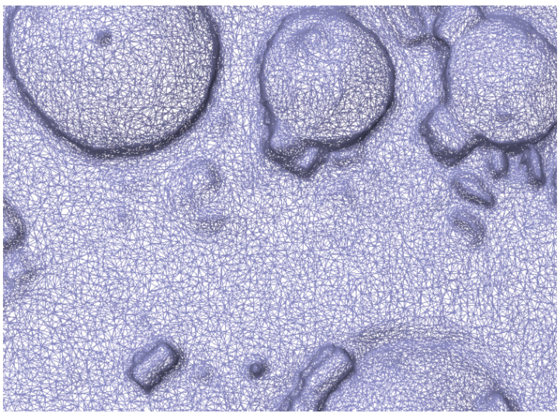

Fig. 23. (above) Result of the dense point cloud using orthoimages of 2015, extrated from *Agisoft Metashape Pro*

Fig. 24. (left) Close-up on the mesh model derived from the dense point cloud of The Necropolis area in 2015, extrated from *Agisoft Metashape Pro*

[12] Source: https://www.agisoft.com/pdf/metashape-pro_1_5_en.pdf

Image Co-registration

After exporting the orthomosaic and the DSM files of 2015 and 2019 from the *Agisoft Matashape pro*, the data was added as raster layers into the *ArcGIS Pro* software. That is for examining the possibility of extracting additional and valuable information from the different datasets, concentrating on the available bands from the visible and infrared spectrum together with the data from the DSM. In case that accurate GCPs or RTK[14] in a survey are not available in a project, there is a possibility to perform a Co-registration process between the different datasources. With this procedure we slightly adjust all the GIS data by decreasing deviations and improving the geo-position of all the raster data. At the end of the process, the different layers are better aligned for a clear and accurate comparisons and investigations that are crucial for future steps. This process is important especially when scanned maps and historical data are involved, because usually they do not contain spatial reference information and the applied processing and nominal accuracy are often unknown. The operation of aligning the raster data is executed by the *ArcGIS Pro* Software, using the *Georeference* tab. The principle based on adding manually control points to one of the raster layers that need to be aligned. Then, choosing the corresponding control point on the aligned target data as the target point. At the end, the system will shift the raster dataset from its existing location to the spatially correct location[13]. An example of Co-registration issues and the proper solution of adding manually Ground Control Points for aligning the different orthoimage layers can be seen in figures 25 and 26.

Fig. 25. An example of Co-registration issues between multispectral orthoimagery, extracted from *ArcGIS Pro*

Fig. 26. An example of three Ground Control Points added manually to one orthoimage in order to fit the second one, extracted from *ArcGIS Pro*

[13] From the official website of ArcGIS Pro: https://pro.arcgis.com/en/pro-app/latest/help/data/imagery/overview-of-georeferencing.htm

[14] RTK (Real Time Kinematic)- A GPS correction technology technique that provides real-time corrections to location data when the survey drone is capturing photos of a site. Source: https://www.identifiedtech.com/blog/drone-technology/gcps-ppk-rtk-best-receive-fast-accurate-data/

Visual Inspections of Temporal Changes

One of the objectives of the thesis is to assess the potential of the multispectral UAV imagery using the available data achieved in the previous phases. Thanks to the *ArcGIS* software, it was possible to use Raster functions and to apply several processing algorithms directly to the pixels of the raster datasets. The calculations are applied to the pixels of the original data of the raster that are displayed, so only pixels that are visible on the screen are processed. A raster function pattern can be also created as a chain of combined functions[15].

Naturally, the study started with understanding the developments through time by detecting the areas with the natural and artificial changes during the years 2015-2019 for further examinations.

For that, comparing and calculating the DSM datasets of the two years was a suitable solution with providing a fast visualization and quantification of the elevation differences.

As a start, a simple technique to compare between Z values of two Raster images is by the *Raster Calculator* tool which allows to create and execute sort of an algebraic map by applying mathematical calculation operations on the pixels.

But more than that, using build-in tools offered by the *ArcGIS* software such as *Compute change, Minus*, and *Cut-Fill* allows extraction of additional information with various visualizations to emphasize the changes. Here are the definitions I used as given by the formal website of *ArcGIS*[16]:

Compute Change - Computes the differences between two continuous raster datasets.

Minus - Subtracts the value of the second input raster from the value of the first input raster on a pixel-by-pixel basis (Fig. 27).

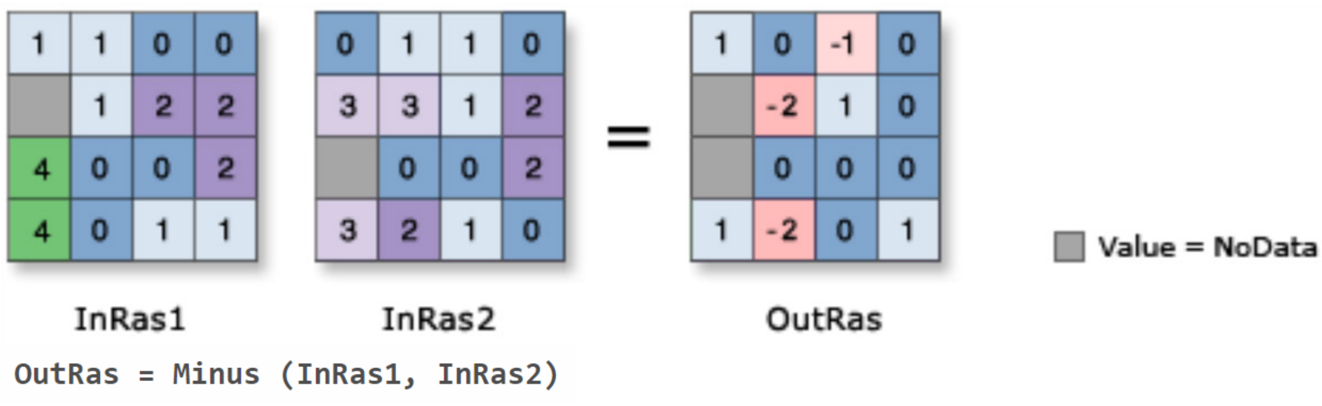

Fig. 27. A demonstration of the pixels' values of the new layer after applying *Minus* algorithm on two raster images (Source: https://desktop.arcgis.com/en/arcmap/10.3/tools/spatial-analyst-toolbox/minus.htm)

[15] From the official website of ArcGIS Pro: https://pro.arcgis.com/en/pro-app/latest/help/analysis/raster-functions/raster-functions.htm

[16] From https://pro.arcgis.com/en/pro-app/latest/help/analysis/raster-functions/list-of-raster-functions.htm

By comparing between these two raster functions, it could be stated that the *Minus* provides an absolute difference between the pixel values of two raster datasets. However, the *Compute Change* has the ability to calculate not only the absolute difference, but also the Relative difference which considers the quantities of the values being compared, and a Categorical difference which contains an attribute table with additional information about the changes of two rasters.

Cut-Fill- modified the elevation of a landform surface by removal (cut) or addition (fill) of surface material (Fig.28). The operation calculates the area and the volume that change between two surfaces of two raster databases. As can be seen in the example below (Fig. 29), The Raster output assigns three 'codes' according to the changes in the elevation as: 'Net Gain', 'Net Loss' and also 'Unchanged', and respectively display in three different colours.

Fig. 28. A demonstration of the pixels' values of the new layer after applying *Cut-Fill* algorithm on two raster images (Source: https://desktop.arcgis.com/en/arcmap/10.3/tools/spatial-analyst-toolbox/cut-fill.htm)

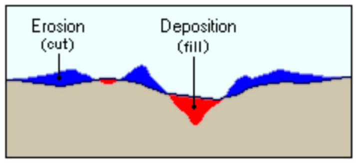

Fig. 29. A demonstration of the area and the volume that calculated with the *Cut-Fill* algorithm (Source: https://desktop.arcgis.com/en/arcmap/10.3/tools/spatial-analyst-toolbox/cut-fill.htm)

The functions explained above will be demonstrated in the Results chapter, by comparison and computation of the raster databases of the DSM of 2015 and 2019.

Exploring the Surface Geometry

The following step after distinguishing the new excavations areas in 2019, was to exploit the 3D and multispectral data to derive information that can be used as an indicator for buried elements. The first strategy was to highlight in different displays the surface geometry according to the given Z values in the DSM. Again, with the help of the Raster functions under '*Surface*' category, such as *Slope*, *Contour*, *shaded relief*, *Hillshade*, and *Aspect-Slope,* it was possible to gain visual and computed information for finding anomalies with the landform behaviour. The following are the descriptions of various operations that were performed with the *ArcGIS Pro* software[17], in order to explain better the differences between the functions I have used images of the same segment of the Necropolis area:

Slope - Displays the rate of change of the elevation for each cell in the DSM. The ranges of the heights and the colours can be modified by the user in order to highlight better the steepness and the moderation of the slopes.
The picture below (Fig. 30) demonstrates a portion of the DSM from 2019 of the Necropolis area after applying the *Slope* function. In the image, the colours represent the different degrees of the inclination of the elevation (natural or artificial), the darker the colour the steeper the surface. This function was found to be a useful tool for a fast and easy way to show the distinction of the objects from the soil. As it can be seen in the image, it is very easy to identify the archaeological ruins which are represented by the darkest outlines, and the soil which are represented by the lightest colours.

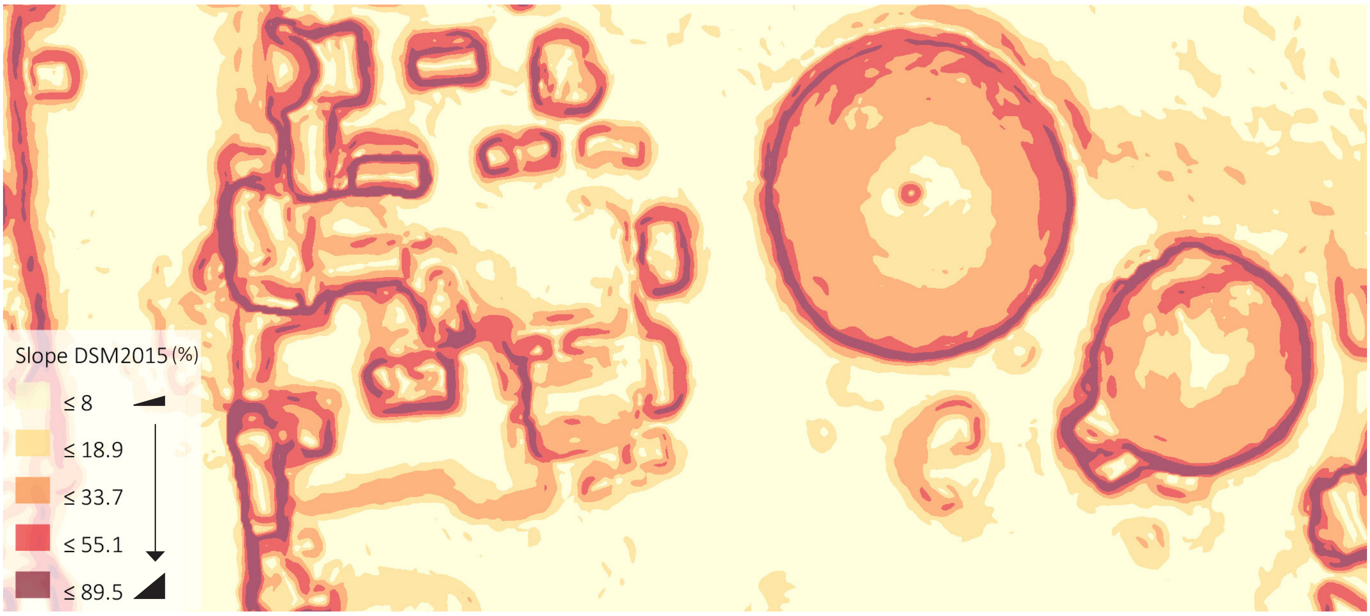

Fig. 30. A segment of a new layer that was created by applying the *Slope* function on a DSM of the Necropolis from 2019, extracted from *ArcGIS Pro*

[17] From the official website of ArcGIS: https://pro.arcgis.com/en/pro-app/latest/help/analysis/raster-functions/aspect-function.htm

Contour- generates contour lines by interpolating points with the same elevation value from a raster elevation dataset. The contours are isolines which were created as raster format for visualization, and later can be converted with another function into a vector format. Figure 31 below shows a portion of the DSM from 2019 of the Necropolis area after applying *Contour* function which highlights better the archaeological remains and the topography.

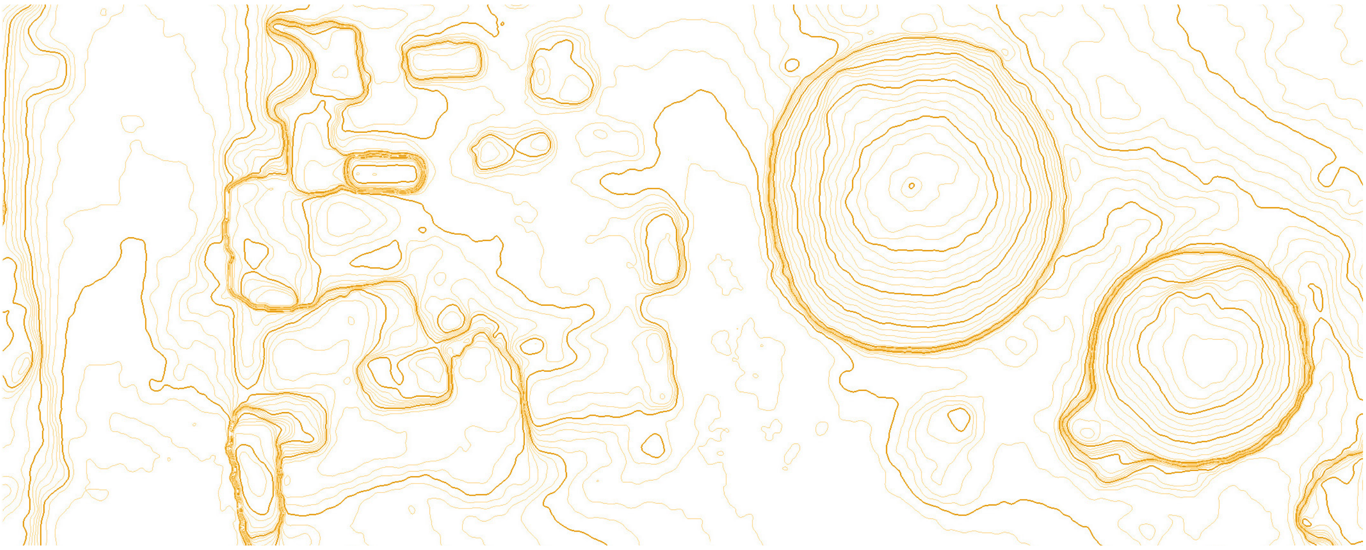

Fig. 31. A segment of a new layer that was created by applying the *Contour* function on a DSM of the Necropolis from 2019, extracted from *ArcGIS Pro*

Hillshade- Produces a grayscale 3D representation of the terrain surface. The outcome of this function is a shaded image that is created according to the position of the sun. This technique applies an illumination source from one direction, using altitude and azimuth values for each cell of the raster image to specify the position of the sun. The method is mostly qualitative for visualizing topography and does not give absolute elevation values. An example can be seen in figure 32 below, taken from the Necropolis area.

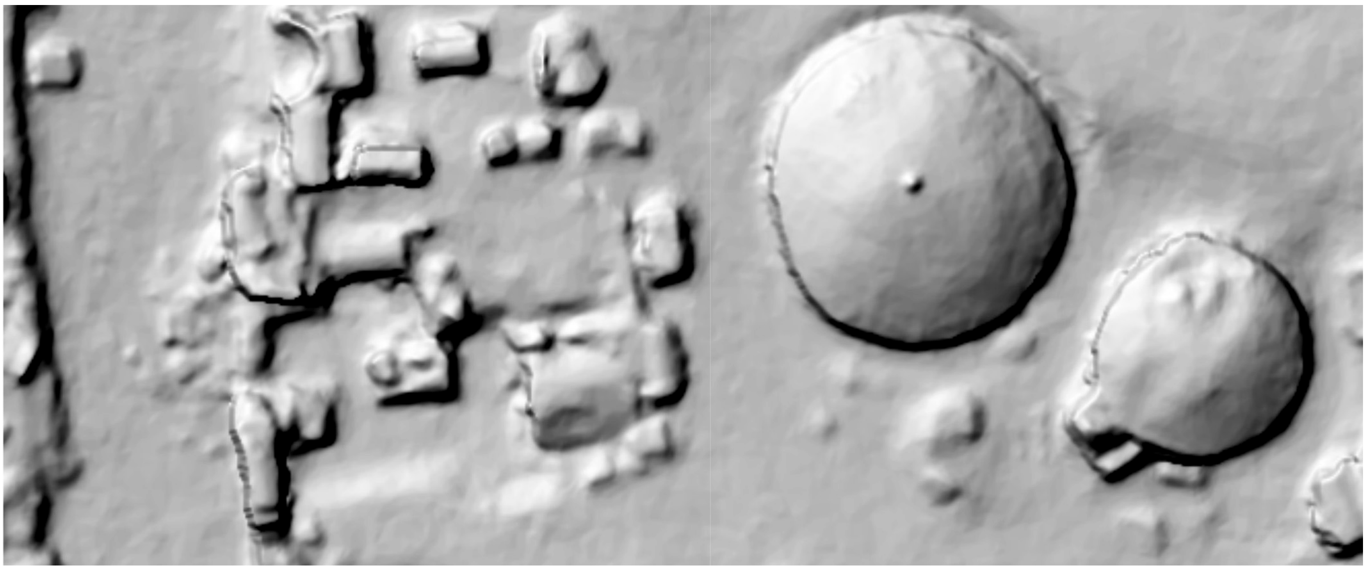

Fig. 32. A segment of a new layer that was created by applying the *Hillshade* function on a DSM of the Necropolis from 2019, extracted from *ArcGIS Pro*

Shaded Relief - A coloured 3D representation of the terrain is created by merging the images from the colour-coded and the *Hillshade* method. Also here, The function uses the altitude and azimuth properties to specify the position of the sun. Compared to the previous image, which was using the *Hillshade* function (Fig 32), the image below (Fig. 33) which was using the *Shaded Relief,* provides more information regarding the surface due to the coloured visualization.
Similar to the *Hillshade* function, the information that can be extracted using this function is qualitative without the possibility to measure the exact heights.

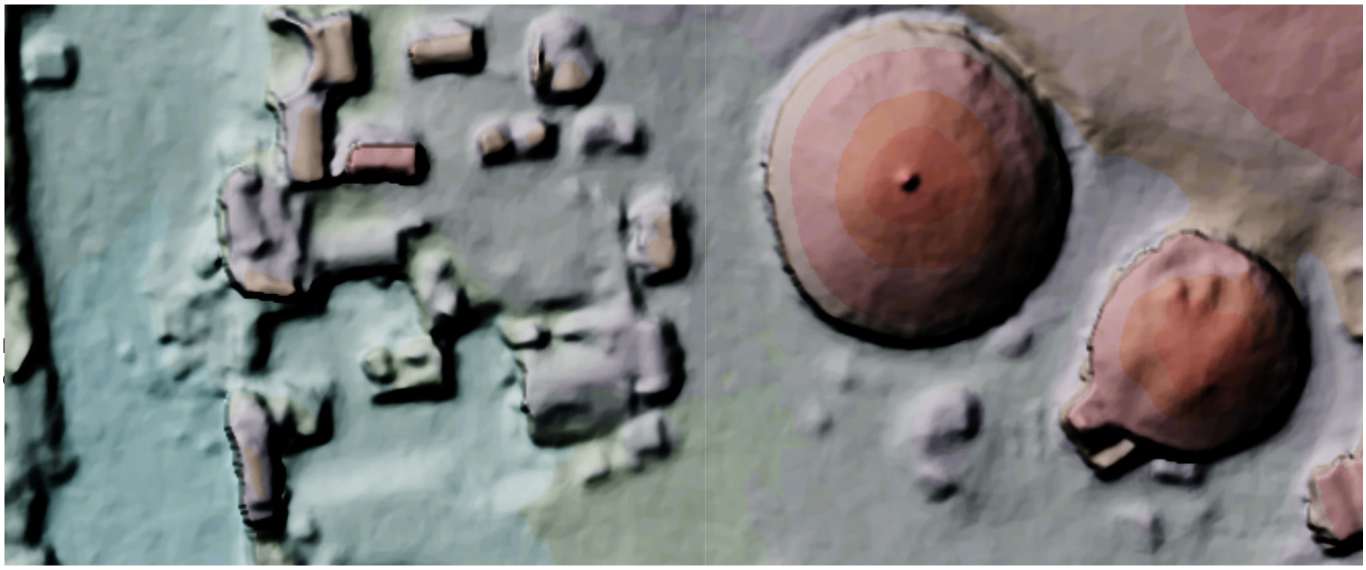

Fig. 33. A segment of a new layer that was created by applying the *Shaded Relief* function on a DSM of the Necropolis from 2019, extracted from *ArcGIS Pro*

Aspect-Slop- Creates a raster layer that simultaneously displays the *slope* and the *aspect* of a surface. The **Aspect** identifies the compass direction of the downslope from each pixel to its neighbors. The raster output is represented by a different Hue (colour). The **Slope**, which represents the steepness of the surface, is symbolised by the different colours tones. The combination of the two functions can be seen in the diagram below (Fig. 34). An example of this operation can be seen in figure 35, taken from the Necropolis area of the Hierapolis.

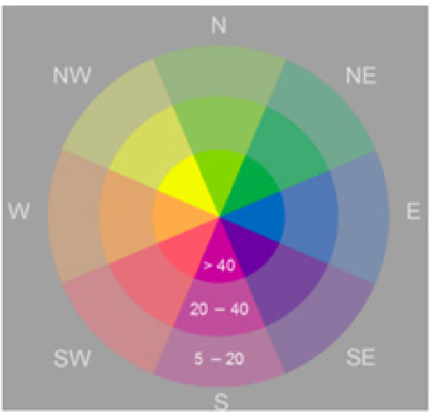

Fig. 34. A diagram demonstrates the colours apply for each compass direction and the different brightness for each slope rate (Source: https://www.esri.com/arcgis-blog/products/imagery/imagery/new-aspect-slope-raster-function-now-available/)

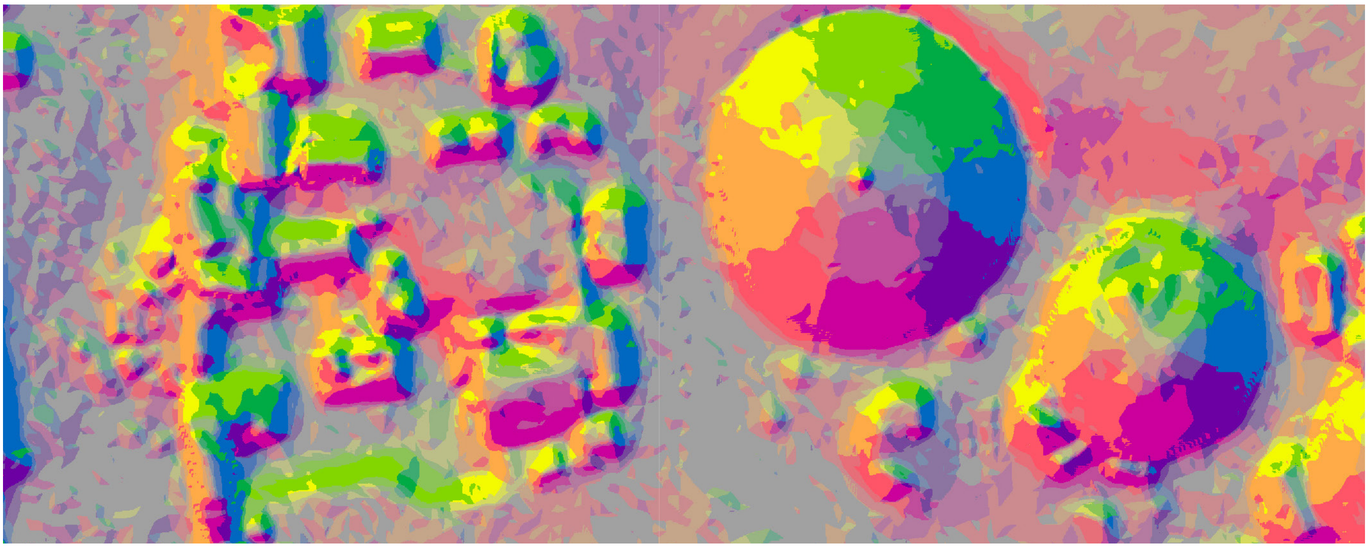

Fig. 35. A segment of a new layer that was created by applying the *Aspect-Slop* function on a DSM of the Necropolis from 2019, extracted from *ArcGIS Pro*

False Colour Composite

The sensors installed onboard UAVs are able to record data in different wavelengths, some are in the visible range and some are in the infrared range of the electromagnetic spectrum (Fig. 36).

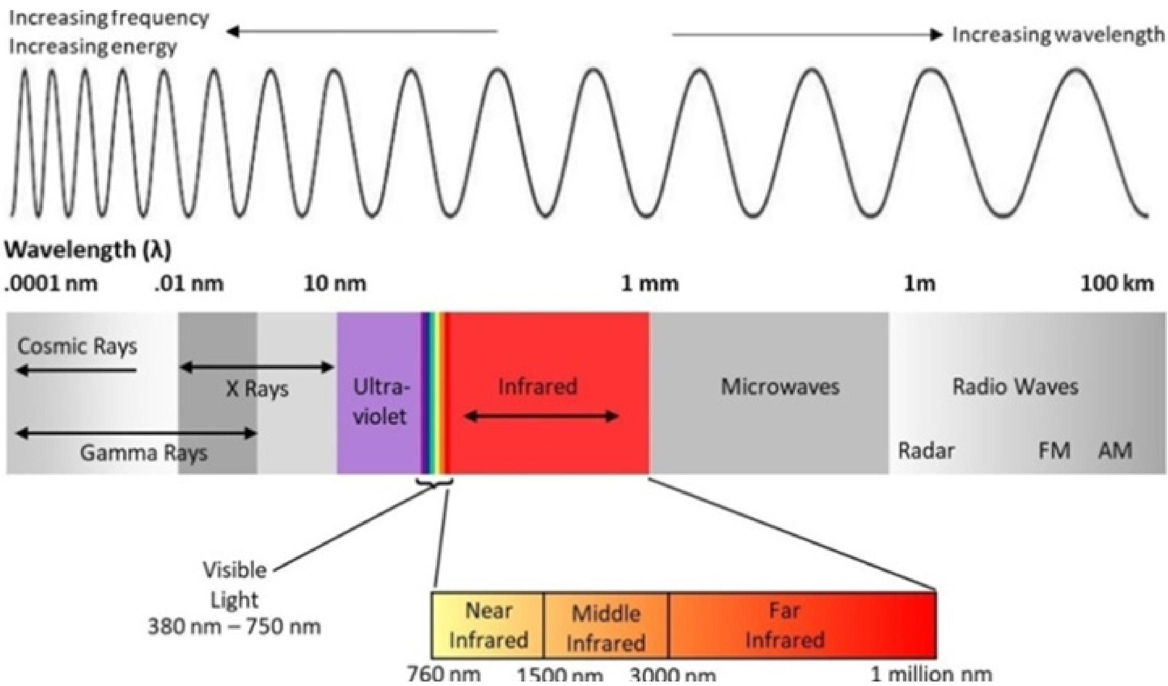

Fig. 36. Division of the different wavelengths in the electromagnetic spectrum (Source: https://www.azooptics.com/Article .aspx?ArticleID=1666)

As mentioned briefly before, the **multispectral image** is obtained by acquiring several bands by using a multispectral sensor. This sensor can record data in multiple regions of the electromagnetic spectrum. Each band that is acquired, can be displayed on a digital screen in two ways: one at a time as a greyscale image or as a combination of three bands at a time as a **colour composite image**. In this mode, each pixel of the three primary colours RGB (Red, Green, Blue), also called channels, can be used in various combinations. The channels contain different colours in the visible spectrum when assigning them to each spectral band (not necessarily from the visible range) (Fig. 37).

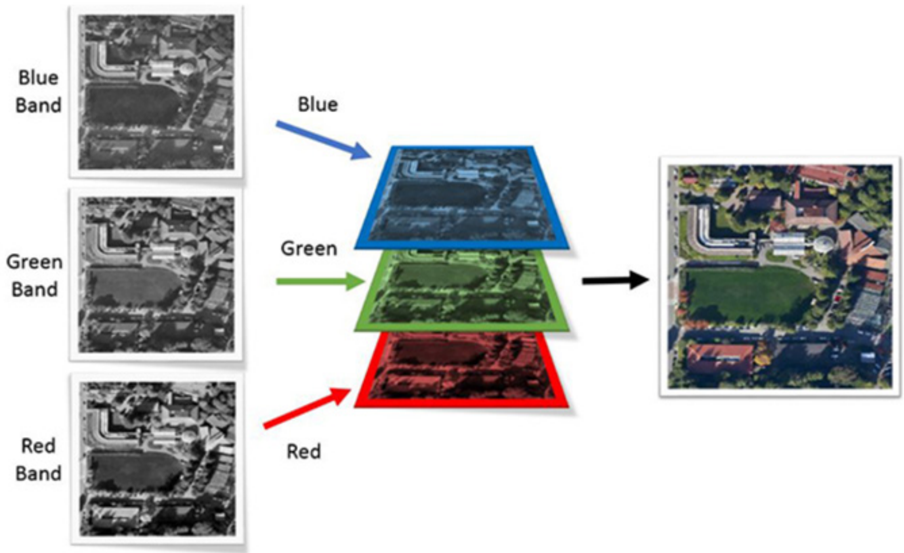

Fig. 37. A diagram shows a combination of the visible Blue, Green, Red bands assign to the corresponding channels in order to achieve a True Colour image (Source: https://gsp.humboldt.edu/OLM/Courses/GSP_216_Online/lesson3-1/bands.html)

The most common composition is the **True Colour** image, in other words the **Natural Colour** composite. This is the outcome when the composite image displays a combination of the Red-Green-Blue bands corresponding to the Red-Green-Blue channels on the computer screen. Examples can be seen in Fig. 37 and Fig. 38E.

In contrast, the **False composite** which uses other ranges than the visible one, is essential to create various depictions of the surface, and stress different spectral features of the earth. For instance, with the RGB channels, when assigning the bands Near infrared-Red-Green respectively, the image will show high contrast and will enhance different surface features of the crops compared to the True colour image[18] (Fig. 38F). The reason is that healthy vegetation reflects a lot of light in the Near-infrared band and therefore seen as red in the image.

[18] Source: https://crisp.nus.edu.sg/~research/tutorial/opt_int.htm

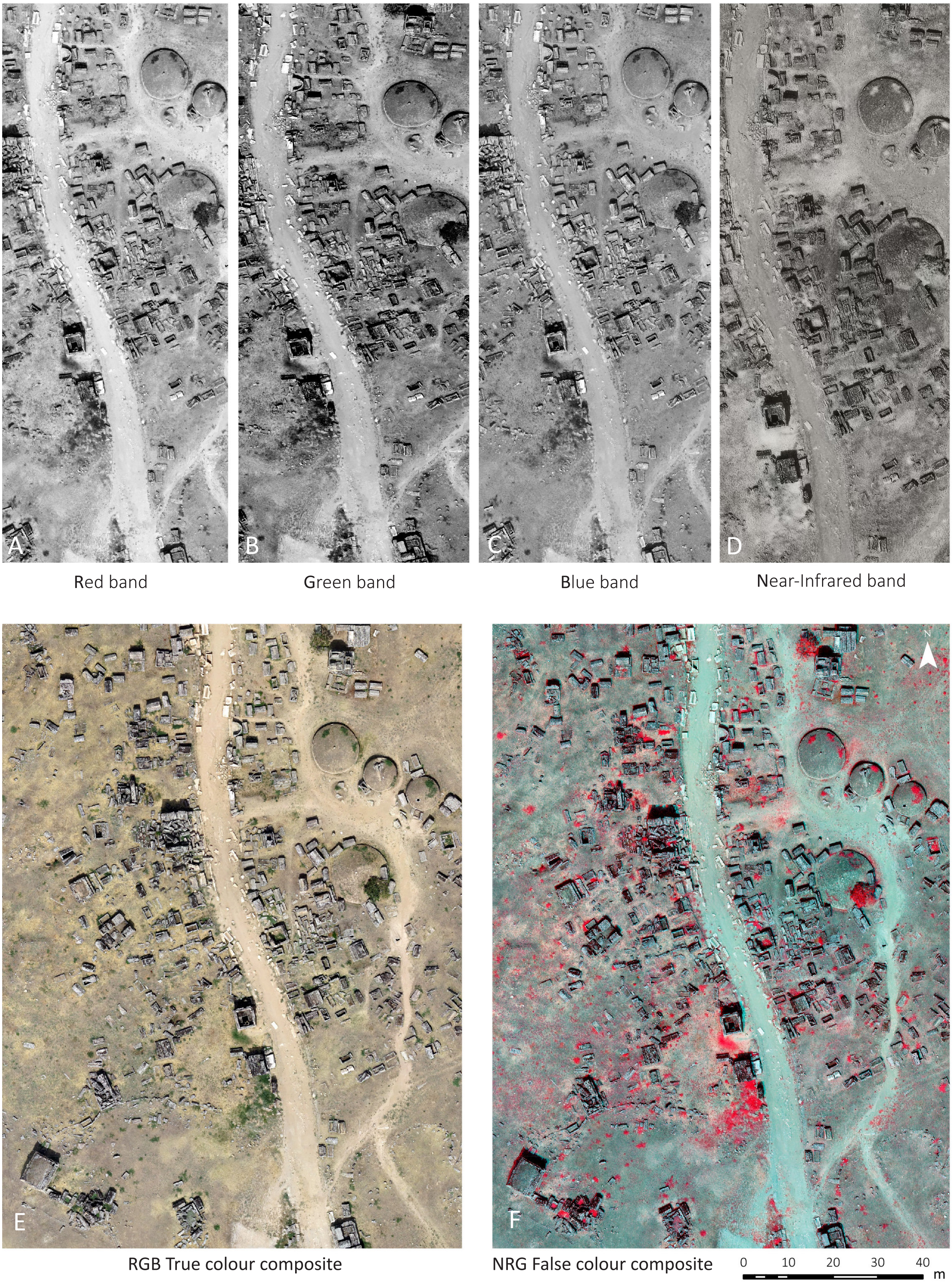

Fig. 38. A-F. The four bands recorded with UAV sensors in 2015 and two available colour composites, extracted from *ArcGIS Pro*

In fact, different types of surfaces with different colour, structure and texture, reflect the Infrared radiation in different ways. The reflected or emitted radiation versus the wavelength called 'Spectral Signature' of the surface. This principle can help to distinguish between different objects, materials, vegetation, humidity and etc.
The vegetation spectral signature can be explained from the graph below (Fig. 39). The red and the blue wavelengths in the visible spectrum are very sensitive to the energy absorbed by chlorophyll during photosynthesis and therefore, with low reflectance and high absorption. In contrast, in the Near-infrared, vegetation reflects more radiation and the energy released by the internal structure of the leaves is highlighted. (Geert J. Verhoeven 2007; Geert J. Verhoeven et al. 2009; Geert J. Verhoeven 2012).

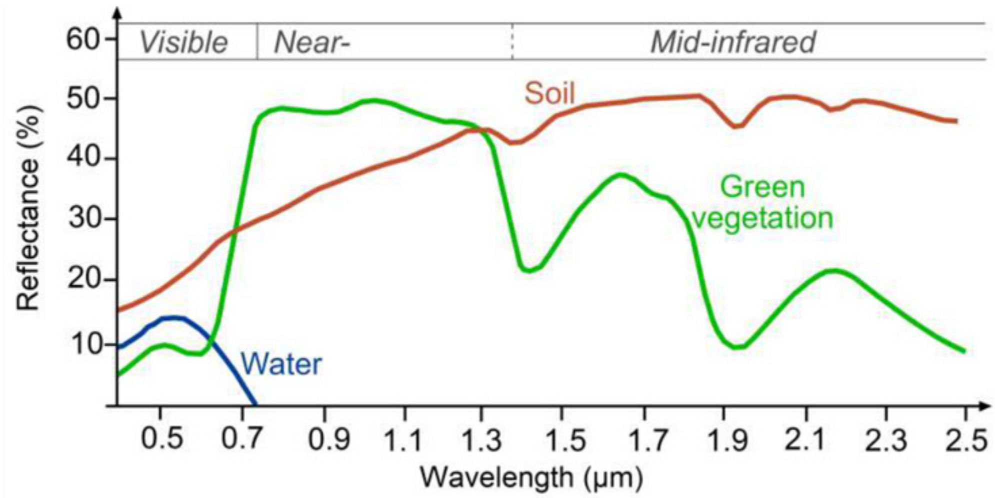

Fig. 39. 'Spectral signature', materials behave differently in the different ranges of the electromagnetic spectrum (Source: https://remotesensing529.wordpress.com/2016/05/25/spectral-signatures/)

Thus, we can learn that exploiting the multispectral information can assist in detecting anomalies in the different surfaces existing on the site, especially with vegetation if the NIR information is available.
In the Necropolis, the collection of the Near-infrared band, which was taken by the *Canon PowerShot S110* camera in 2015, was significant because of the possibility to visualize wavelengths that the human eye cannot see. The NIR band helps highlight additional spectral differences and increase the interpretability of the data. Therefore, it will be relevant to expand here more about the definition, features and advantages of this band.
The Infrared is a section of the electromagnetic spectrum which ranges from short wavelengths to long wavelengths. The infrared spectrum located between the Visible and the Microwave ranges with the wavelength between 0.7 µm to 1 million µm, and composed of the NIR-Infrared, Mid-Infrared and the Far-

infrared (see Fig. 36). The radiation of this spectrum is invisible to the human eye and can be seen only through a digital sensor. The Near-Infrared with the wavelength between 0.7 µm to 1.4 µm can be divided into two categories, reflected or emitted (thermal IR) radiation, depend on the sensor used.
When the (visible or) NIR energy encounters an object, this radiation can be absorbed, reflected or transmitted. Yet, only the reflected wavelengths that come out of the object can be measured by the sensor and used to create an image. The NIR spectral data can be used for varied analyses to get meaningful results on archaeological soils and sediments, especially in terms of understanding site development along with its phases and soil formation. Moreover, NIR radiation can penetrate a depth of a few mm into a powdered solid material, and may assist with detecting buried archaeological structures (Linderholm et al. 2019).

Spectral Indices

An index can be defined as an algebraic formula calculated per each pixel in a raster format, in short, a mathematical combination of different bands. The variables of the formula are the different spectral bands involved in a raster image (Abate et al. 2020). This visual inspection, based on the spectral reflectance of different organic substances, allows emphasizing a local phenomenon that related to a specific multispectral image. The idea of spectral indices is to neutralize and reduce the effect of other factors, such as shadows and clouds (which can lead to an inaccurate analysis). This process is usually done by adding and subtracting bands. The result is a single band which is generally displayed with a high contrast, grayscale or colour palette image.
Using this technique also allows a simple and a fast comparison over time, with only tracking the brightness changes in the one-band images.

With the help of *ArcGIS Pro* software, a fast and economic analysis can be done with multispectral images, producing different graphic representations by calculating several indexes. It is understandable that with more bands recorded by the sensor it is possible to obtain various band ratios. Thereby, a wider and more comprehensive study can be obtained about the materials above the ground and underground.
The indices can be divided into three main categories with different bands involved, according to the different optical reflectance from each material.

1. Vegetation Indices

As already mentioned, the NIR band has a strong connection with healthy vegetation. In fact, many indexes contain this band because of the high reflection of light in this range. In general, after applying a vegetation index on an image, a new layer will show healthy vegetation in bright, with high value of the digital number for each pixel in the image. On the contrary, the unhealthy vegetation as well as the terrain, will appear as dark due to their low values of their digital number. This type of indices considered an important archaeological tool since the differences in height, density and colour of vegetation might indicate the presence of a buried element. An example can be seen in the photos taken from two archaeological sites (Fig. 40,41). No doubt that this method eases the task of the archaeologist with a more concentrated investigation and excavation. Yet, it is also important to pay attention to the season that the images are acquired, since the natural seasonal changes with density and colour in the whole site may harden the mission of discovering these findings (Koucká et al. 2018; Salgado Carmona et al. 2020).

Fig. 40. An image taken from an archaeological site in Cyprus, shows different behavior of the vegetation probably due to buried structures underground (Source: Themistocleous et al., 2015)

Fig. 41. An image taken from an archaeological site in Prague, shows different behavior of the vegetation probably due to buried structures underground (Source: Koucká et al. 2018)

This anomaly in vegetation also called Crop Mark, as can be seen in the scheme on the next page (Fig. 42). According to this principle, the soil and moisture change around archaeological remains. In these places, there are changes in height or colour due to the lack of water and nutrients, which influences the vegetation patterns. This phenomenon can be seen as a 'negative crop mark' which appears above buried masonry, or as a 'positive crop mark', which occurs above damp and nutritious soil of buried pits (Lasaponara et al. 2007).

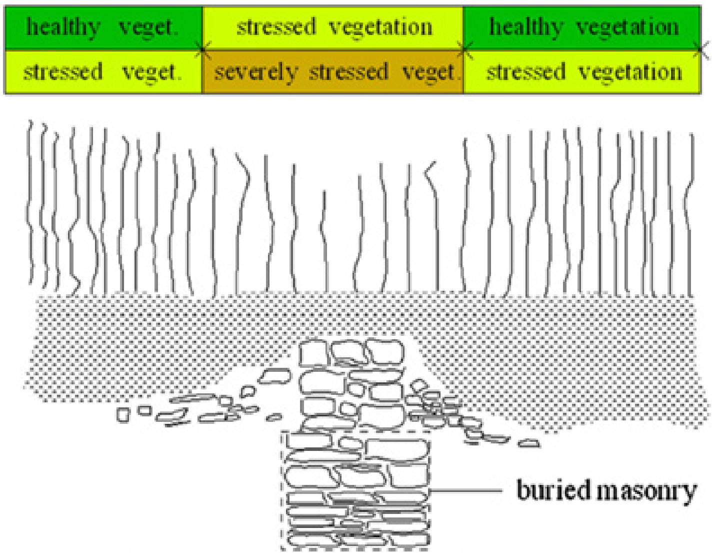

Fig. 42. A detail of the typical crop mark caused by the presence of buried structures (Source: Lasaponara et al. 2007)

The most widely used index is the NDVI (Normalised Difference Vegetation Index) which indicates different states of vegetation health. Healthy vegetation will be bright in the index image, whereas unhealthy vegetation, water and soil will be dark. The bands that participate in the formula are the Near-infrared and the Red, simply because of the high reflectivity of the radiation with vegetation in the NIR band, and the high absorption of vegetation in the red visible band. These contrasting properties of the two bands allow to generate a ratio between the red and the NIR bands with the following equation:

$$\frac{NIR - RED}{NIR + RED}$$

Each of the parameters above symbolizes the pixel value from its band. The index varies between the values -1 to +1. As a general rule, the digital number of the pixels that represent the dense and the green vegetation is between the range of 0.3 to 0.8. For more accurate results in a specific case, some samples can be collected manually from a specific image.

The ratio in this formula is necessary in order to normalized effects of shadows, snow and illumination that might reflect as bright with the red band. This way, the ratio helps to avoid misinterpretation and losses of valuable information on the investigated features (Aboutalebi et al. 2019).

An interesting example of this index is taken from the archaeological project in Álava, Spain. The main goal was to determine the course of an ancient Roman road that is now characterized as a rural area covered by vegetation.

The NDVI technique enhances the contrast for better interpretation since the crop marks seen clearer than conventional photography. Figure 43 below shows the assumption of the Roman roads after applying the NDVI index (Fuldain González et al. 2019).

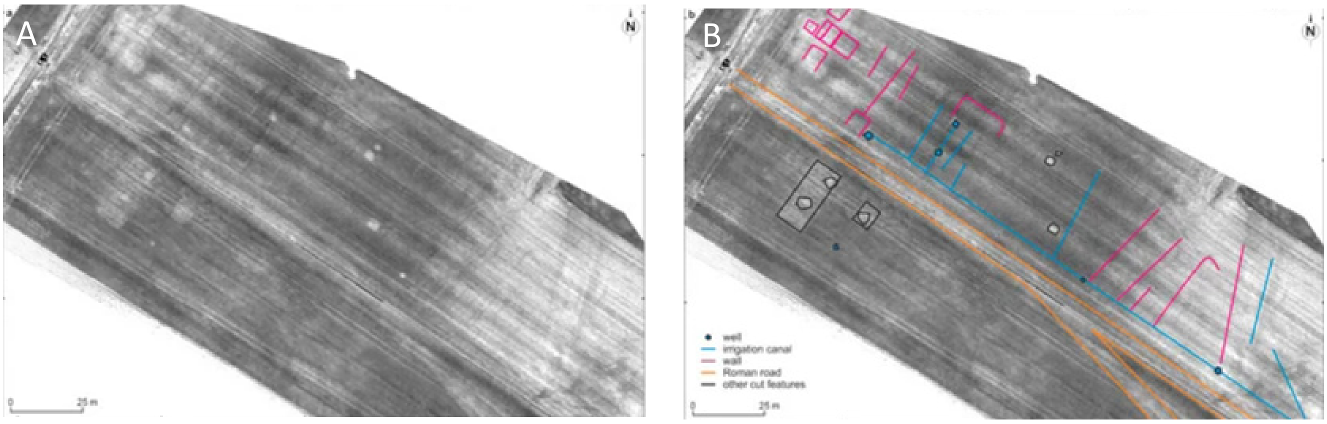

Fig. 43. NDVI orthomosaic in an archaeological site in Álava, Spain (A) and interpretation of some of the a Roman roads observed (B) (Source: Fuldain González et al. 2019)

2. Soil Indices

Apart from vegetation indices, the soil parameter should also be taken into consideration. One important feature in this type of indexes is the soil moisture, since archaeological features tend to retain different percentages comparing the rest of the area. Moreover, according to studies, the soil near archaeological remains is poor with nitrates. With the help of the soil indices, these qualities increase the capability to achieve identification of underground features and can produce a clear contrast image (Salgado Carmona et al. 2020).

A common method of ground detection is a collection of soil samples from an archaeological site for chemical analysis and identification in a laboratory. Then, after calculation of specific values for any soil spectrum, it is possible to search for 'unusual' spectral behaviour that can imply buried elements (Choi et al. 2020; Linderholm et al. 2019).

A less intrusive technique is by using soil indices, where the main bands, Red and Green from the visible range, are involved. The reason for using these bands is because they are more effective for detecting changes in the soil (Salgado Carmona et al. 2020). Interesting to mention here that the thermal water bodies in the Hierapolis site are rich in calcium carbonates that with time formed limestone (Sammartano et al. 2020). In addition, the area varies from clay to travertine stone (Negri et al. 2006). These features can imply on a specific type of soil indices that might help to find traces and discover pieces of evidence for hidden findings. According to the study of Gholizadeh *et al.*, (2018) the Red and the SWIR (a short wavelength of the InfraRed range) bands have a strong correlation with soil organic carbone and the Red-edge band affects more on clay. In order to demonstrate the logic behind the soil indexes, I will expand on one out of many other formulas:

CI – Colour Index, which related to the concentration of carbonates or sulfates in the soils. This index can be a relevant example to the site, due to the ability to display the discrimination between the carbonated areas in the soil, which might lead to a discovery of hidden structures. The formula of CI shown as follows:

$$\frac{RED - GREEN}{RED + GREEN}$$

The red band associated more with carbonite and sulfates, due to a high energy reflectance from these materials. With this ratio, the index mitigates possible illumination that can occur with the green band.

3. Water Indices

Basically, this type of indices shows visual contrast between water and non-water features. At first thought, this type of indices does not seem to be related to the case study of Hierapolis. But, due to the existence of water bodies rich with carbonate nearby the site, it can influence the archaeological area by displaying different soil textures and discovering anomalies with the earth. As a fact, water absorbs more energy in the NIR and SWIR wavelengths, and on the contrary, non-water feature reflects more energy. Although, according to several water indices introduce by the literature, it seems to be an inconsistency when more bands being considered. In addition, at times, authors use the same index name but change the band variables. For example, with NDWI (Normalized Difference Water Index):

1. $NDWI = (Green - NIR)/(Green + NIR)$
2. $NDWI = (Red - SWIR1)/(Red + SWIR1)$

While in the first formula, composed by McFeeters, the Green band has the most visual effect from the water, the second formula, constituted by Rogers and Kearney, shows that the Red band has this impact (Mondejar et al. 2019).
Figure 44 demonstrates the ability of the indexes to distinguish between different surfaces by the contrast of black and white. A true colour image (A) taken from a work done in Phewa Lake, Pokhara, Nepal, while the black and white images show the resulted indices map with a clear separation of the water (in white) with the dark background after applying the NDWI (B). As a comparison, an opposite outcome is shown here with the application of NDVI (C) which instead, emphasizes the vegetation around the lake in black. (Acharya et al. 2017).

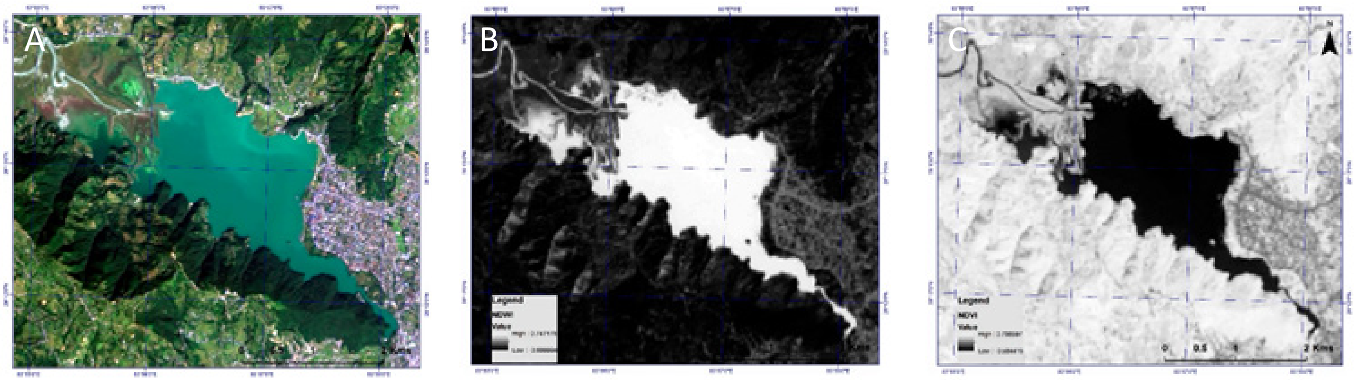

Fig. 44. A satellite true colour image of Phewa Lake in Pokhara, Nepal (A) application of NDWI index (B) and application of NDVI index as a comparison (Source: Acharya et al. 2017)

Convolution Functions

Another approach for searching supporting techniques for detecting buried features was with the Convolution filters from the Raster Functions. The aim of this operation is to improve the quality of a raster image by enhancing the features and/ or eliminating spurious data. Usually, the filters work on sharpening, blurring or detecting edges of objects by calculating predefined matrixes for each of the pixel values with relation to the weight of its neighbours[19].

A visual example to clarify this method can be seen in the images below. The grayscale image (Fig. 45) filtered by the Convolution Functions *Gradient South* and *Gradient West* (Fig 46 A and B). By comparing the two black and white images, we can see a clear distinction between the new layers. The filters were able to detect different edges and highlight in white different elements with horizontal or vertical positions.

Fig. 45. An unfiltered grayscale image, an example for the followed application of Convolution functions (Source: https://desktop.arcgis.com/en/arcmap/10.3/manage-data/raster-and-images/convolution-function.htm)

[19] Source: https://desktop.arcgis.com/en/arcmap/10.3/manage-data/raster-and-images/convolution-function.htm

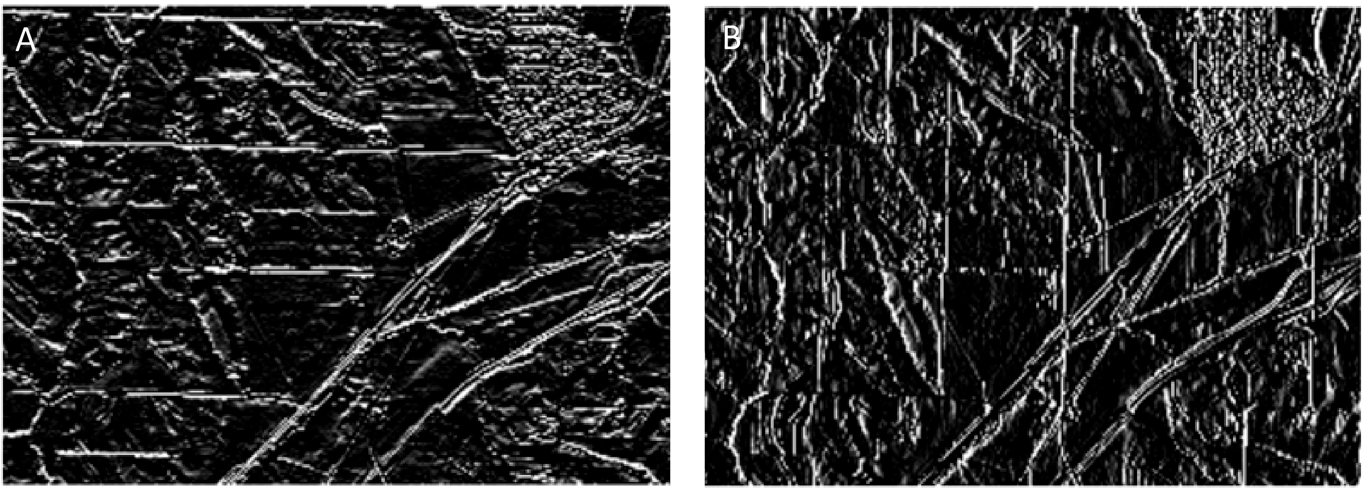

Fig. 46. A result of *Gradient South* option from the *convolution* function after applying on figure 40 (A) A result of *Gradient West* option from the *convolution* function after applying on figure 40 (B) (Source: https://desktop.arcgis.com/en/arcmap/10.3/manage-data/raster-and-images/convolution-function.htm)

In the following part of the thesis I will detail and examine some types of the Convolution filters composed from different matrixes, using the available functions in *ArcGIS Pro* software.

From Raster to Vector, Between Concept and Representation

The previous paragraphs deal with various procedures and results achieved with Raster data, while this part is dedicated to Vector data which is more compatible with graphic representation of maps and dynamic atlases. The advantage of the vector data is the facility to update, analyse, scale and store many additional information in every geometric feature that present in a map.
One of the main purposes of this thesis is to create a GIS (Geographical Information Systems) as a part of a local search engine. The main process is to digitize all the findings and the roads discovered since the 60s into one map. Then, to deal with different ways of displays and dynamic representation of temporal data, through interfacing with other geographic and non-geographic data.
The intention is to help the archaeologist to facilitate the process of the drawing, documentation, addition and update of information in a more simple, fast and sustainable way.
To understand better the advantages of the vector features and to follow processes of generating the data, cataloging and mapping, there is a need to clarify some significant terms:

Geographic Information System (GIS) – a computer framework for gathering, managing and analysing spatial data. The system characterized by the ability to integrate geospatial inputs from a wide variety of cartographic sources with emphasis on easy sharing, communicating, predicting and querying information also in real-time (Kraak 2004).

Geodatabase – in short, storage of various types of data in a common repository, with an 'information model' implemented as a series of tables containing feature classes and attributes[20].

Vector features – a data format that reflects the objects of the real world in a GIS environment and used to store spatial data. A vector feature comprised mainly of points, lines or polygons (Fig. 47) which built from 'vertices', when each vertex contains X,Y and sometimes Z coordinates that define the relative position from the other vertices and features. A series of vertices can be one for a point, two for a line and at least three for a polygon. Each object called a feature and characterized with a unique feature identifier which allows connecting all thematic and spatial characteristics related to the object[21] .

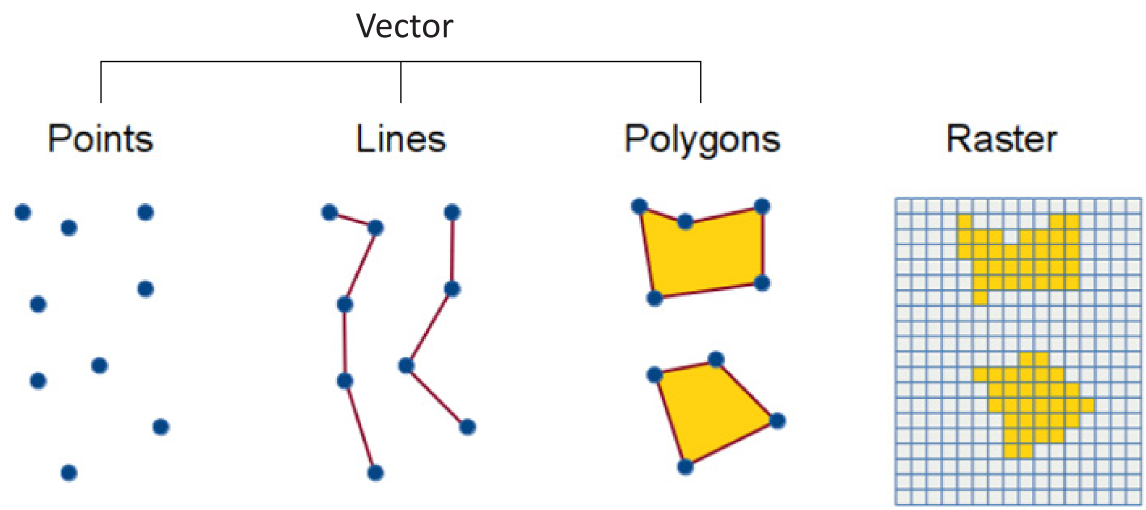

Fig. 47. Different types of the Vector formats in comparison to the Raster configuration (Source: https://ui.josiahparry.com/spatial-analysis.html)

Feature class – a collection of the same type of vector features with the same spatial representation such as type of points, lines or polygons, also share a common set of attributes stored in a database table (Fig. 48). Feature attributes are recorded in the columns and each row in the table represents one individual

[20] Source: https://pro.arcgis.com/en/pro-app/latest/help/data/geodatabases/overview/the-architecture-of-a-geodatabase.htm
[21] Source: https://geogra.uah.es/patxi/gisweb/GISModule/GIST_Vector.htm

feature. Usually, the table includes automatic, geometric attributes about each feature such as area, length and Object ID. The table, which expressed in alphanumeric format, can be expanded by the user with adding relevant and useful geometrical and thematic information about every single object.

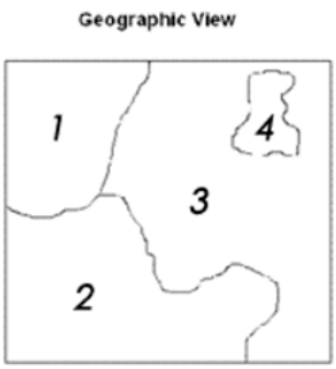

Tables View

Object ID	Shape	Name	LV Code	Management Agency
1		Shady Pines	20	Private
2		Pinewood Village	30	Pinewood Village Association
3		Sarah Park	80	City Park Board
4		Town Park	99	City Park Poard

Fig. 48. A demonstration of an attribute table containing the values of each shape in the map (Source: https://desktop.arcgis.com /en/arcmap/10.3/manage-data/geodatabases/feature-class-basics.htm).

In general, there are two different spatial representations and conception of the real world, entities can be represented by a Vector or by a Raster (Fig. 49).

In contrast to the vector representation, the raster image does not distinguish between edges of objects because it does not use points, lines or polygons, but a regular grid of cells. Values are assigned for each of these cells regardless of whether it is an object or its background, and so, no discrete boundaries can be represented. Although in raster images, the so-called 'digital topology', provides boundaries based on different neighbourhood definitions for foreground and background, yet, the procedure is neither symmetric, nor mappable when comparing to the vector representation with the same topological properties (Winter 1998).

When comparing between the two formats, some advantages can be found with the vector type when it comes to mapping. First, as already mentioned, the possibility to store information into an attribute table for each identified feature in a map, and the ability to draw, edit and change visualization into diverse thematic representations. These qualities can be very useful for the archaeological application, since it is easier to manage complex info from the site into an organized attribute table by assigning multiple data to each tomb which represented by a polyline.

Second, due to the inherent coordinates and the information available for each object, the vector data allows many operations of spatial inquiry such as proximity and networks analysis.

Third, a file size of a vector format might be smaller than a raster file because the latter records a value of digital number for each cell that covers the image, even if the cell represents the background.

Important to mention that due to its features, the vector image will appear the same even if the scale is changed- this is in contrast to raster visualization that related to the spatial resolution of an image. This characteristic is meaningful when creating vector features in a digital map. The user should know the specific nominal map scale[22] before creating those features in order to obtain a reliable map with the correct accuracy.

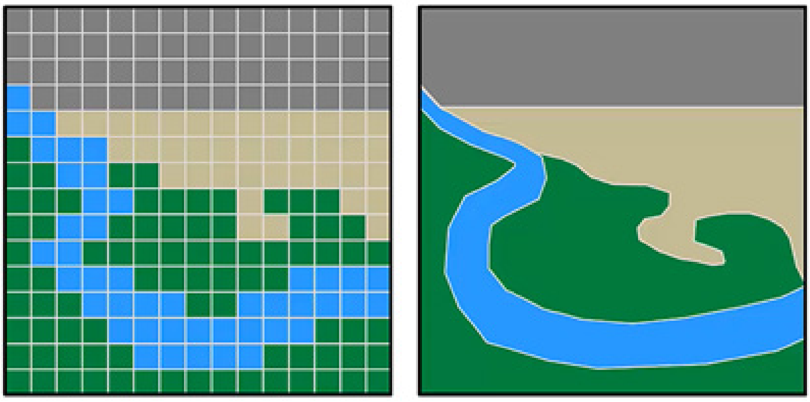

Fig. 49. A distinction between a Raster image composed of cells (left) and a Vector image composed of polylines (right) (Source: https://vimeo.com/53016715).

The option to convert raster surfaces into vector data such as polygons in the *ArcGIS* environment, can support with adding valuable data by overlaying and analysing spatial relations. This is due to the ability of the polygons to contain more information regarding each feature and each feature class.
With a connection to the next section of the thesis, some results of the Raster investigations can demonstrate the power and the benefits of converting polygons from the Raster type. One example can be the Raster Function *Contour* that was applied on the DSM, which is responsible for interpreting the topographic surface into lines, still in a raster format (Fig. 50). But, thanks to the geoprocessing tool: *Convert Raster to Polygon* or *Contour*, a new Vector layer was created with a new attribute table, with available information for each line such as the specific height. Moreover, with these lines made of polylines it is possible to use the 'Labelling' option to represent near to each line the specific height (Fig. 51). Interesting to mention that in the case of the Necropolis, when looking at these images, the vectorial lines highlight the tombs above the ground and can replace the process of drawing when quick representation is needed.

[22] Nominal map scale- the ratio between the distance on a map and the corresponding actual distance on the ground. Each map scale follows a different tolerance of accuracy.

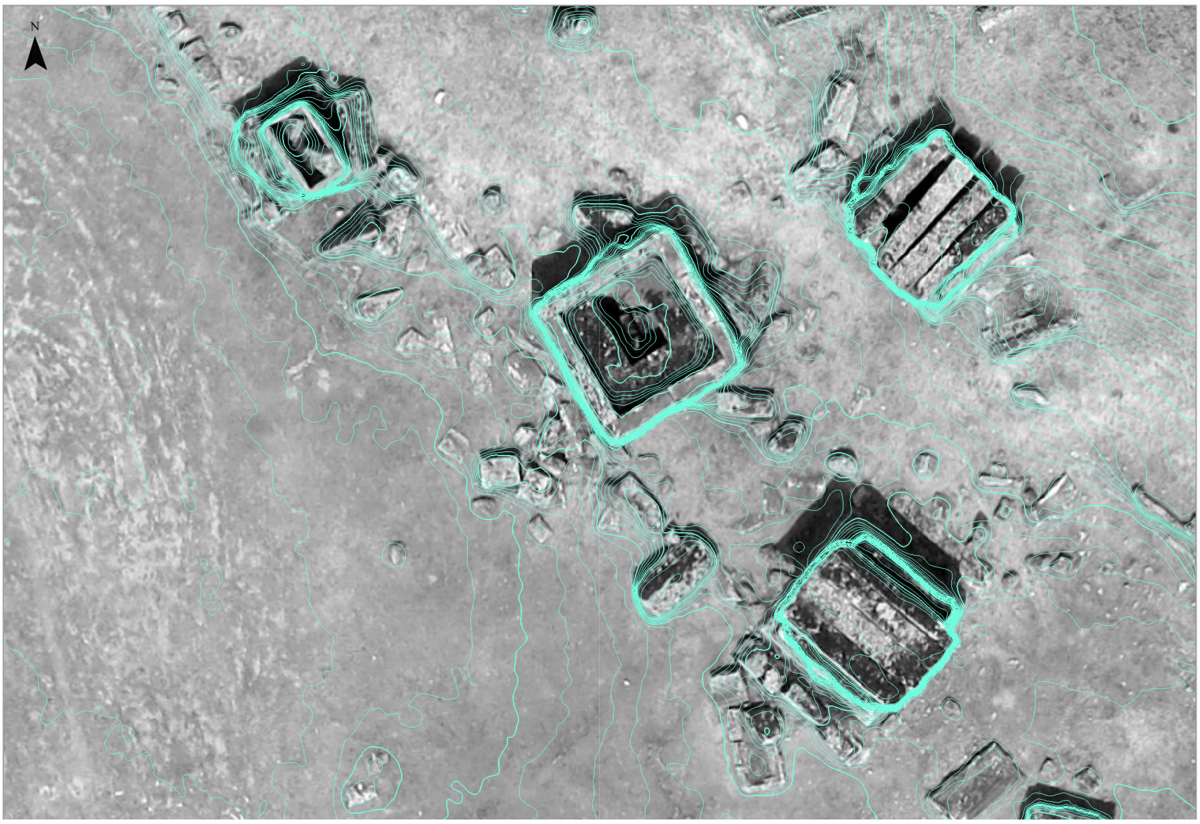

Fig. 50. Applying Raster Functions > *Contour* on DSM of 2019, Background orthoimage of 2019

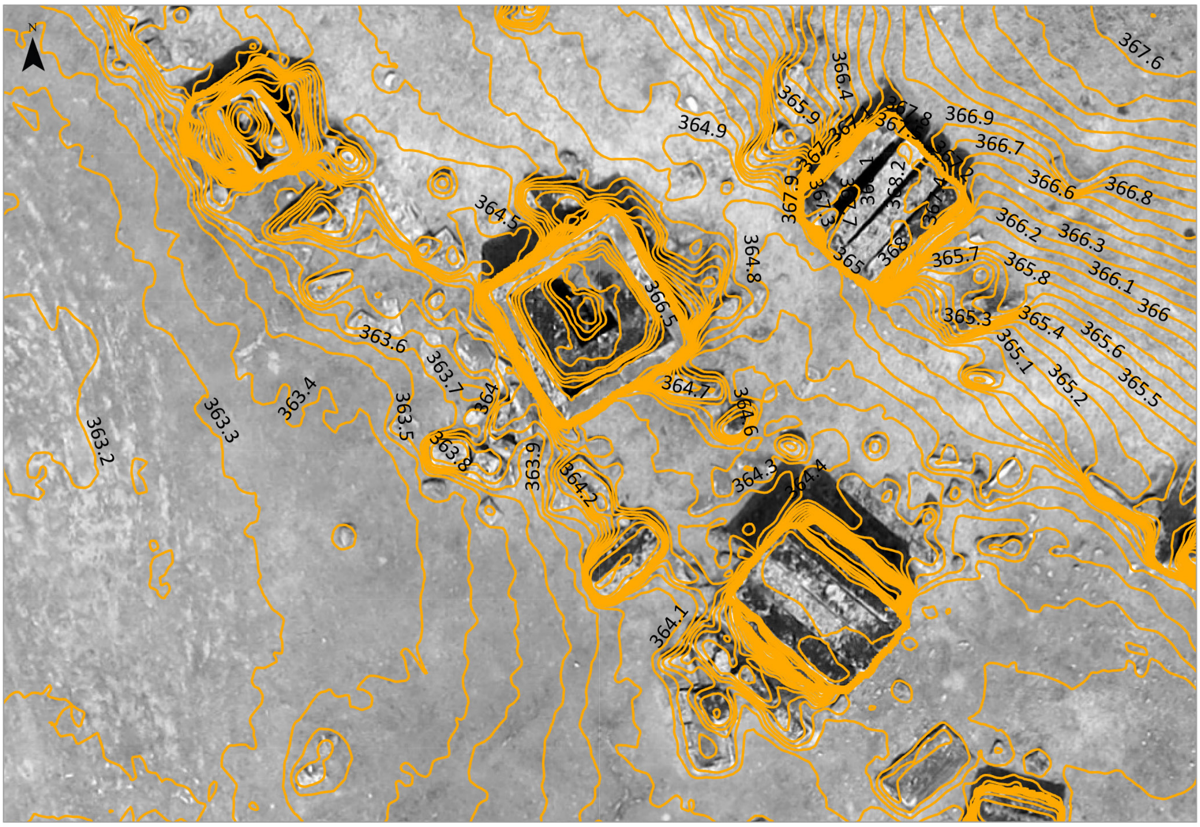

Fig. 51. Applying Geoprocessing Tool > *Contour*, Background orthoimage of 2019

Data Format Conversion

After receiving a DWG file from the Atlas of Hierapolis of Phrygia of 2008 and the subsequent version of 2015, I added the CAD feature dataset into the *ESRI ArcGIS Pro*. Thanks to the possibility of the software to interface with this kind of format, I was able to convert the different layers that appeared in the contents pane into feature classes using the geoprocessing tool: *CAD to Geodatabase,* in order to characterize each of the geometric features. The immediate result I obtained in figure 52, can be seen on the background of the orthomosaic from 2019.
From the picture, it is evident that some feature classes of the CAD dataset, are not overlapping to the UVA orthoimage with the already defined coordinate reference system.
In general, the coordinates stored in a CAD dataset are not explicitly related to a known coordinate system. Basically, by defining the coordinate system, the software can automatically reproject the dataset into another coordinate system that will integrate with the other vector and raster datasets in the project. In the case of Hierapolis, the small misalignment of the CAD is noticeable although the data automatically adjusted to the coordinates system of the current orthoimage. The reason for that can be one or more of the following causes: (1) The nominal map scales of the AutoCAD vectorial map (since each scale has different map accuracy standards) and the Raster data acquired by the drone. (2) The polygons drawn in the AutoCAD are only in an estimated location as a hypothesis because they not yet excavated. (3) The accuracy with one of the photogrammetry processes that generate the orthomosaic.

In response to some of the above issues, it is necessary to discuss some points. First, the importance of using a well-defined reference system, because, even when using various data with a different reference systems, still, conversions between datum are possible. Second, to know the nominal map scale, since each map is generated for a specific nominal map scale according to the survey requirements and so, their accuracy changes accordingly. For a large map-scale with a high level of detail, the accuracy is higher than a small map-scale with a lower level of detail. The actual values depend on the adopted regulation, for example, according to the USGS[23], a horizontal accuracy standard required that 90 percentages of points measured on the map must be within a defined distance from their actual position[24].

[23] USGS- United States geological survey, formal website: https://www.usgs.gov/
[24] Source: https://pubs.usgs.gov/fs/1999/0171/report.pdf

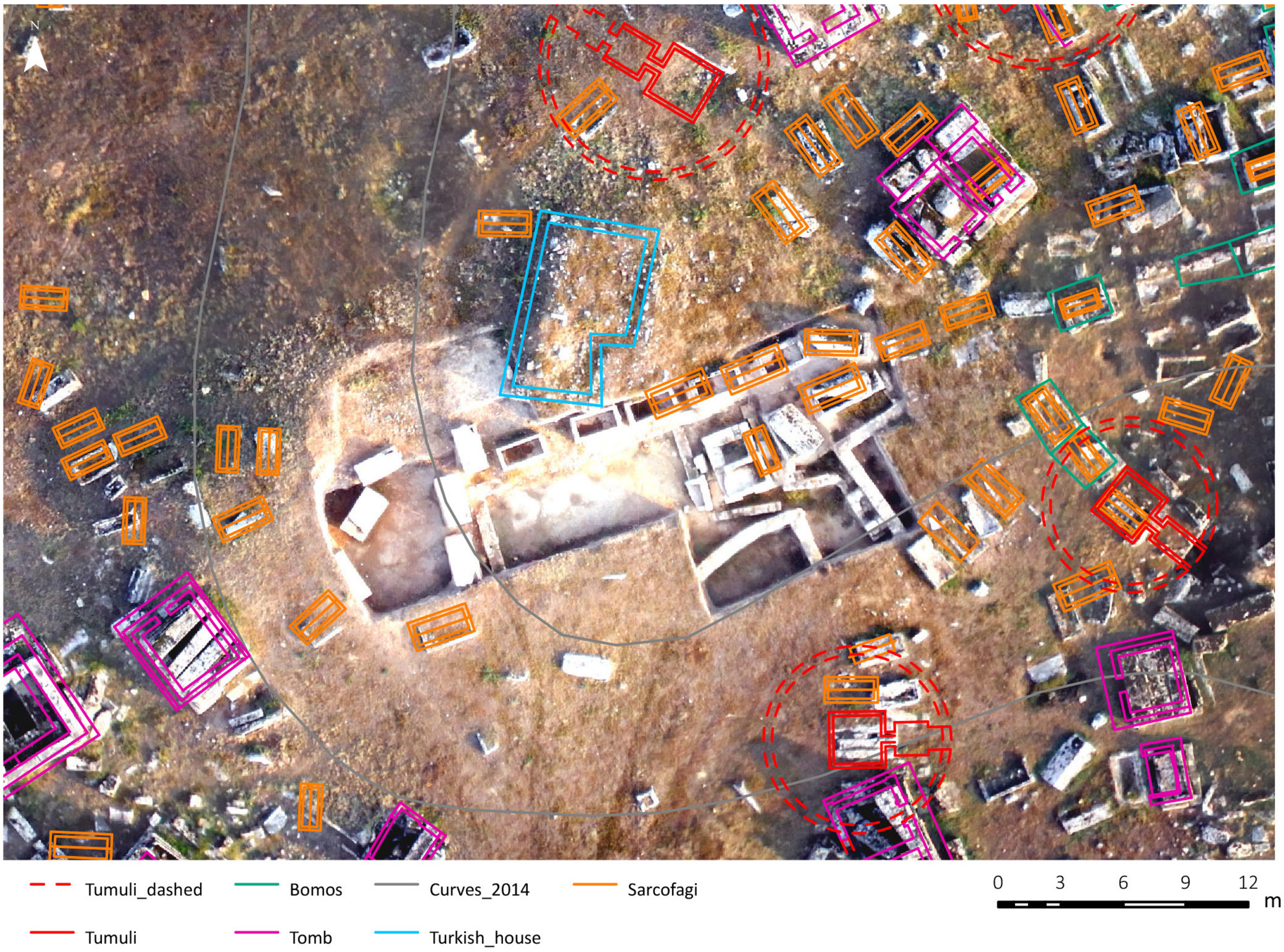

Fig. 52. Misalignment between the feature classes after conversion from an AutoCAD survey of 2015 and the orthoimage of 2019 as a background.

According to the USGS, this map accuracy adjusted to the nominal scale of the map and calculated as follows:

$$(90\%) \rightarrow 0.0005 \text{ m} * n$$

n= nominal scale factor

For example, at 1:1000 scale, 90 percentages measured on the map must be with a horizontal accuracy of 0.5 m, consequently, with smaller nominal map scale with a lower level of detail, less precision is required. For this reason, it is essential to check and update the metadata when using datasets from different sources, which contains information that describes a dataset such as creation date, last updating date, credits, reference system and the geometric resolution. From the metadata it can be clear if all the maps

are using the same nominal map scale, if not, that might cause a misalignment.
A general recommendation would be using vector datasets exploiting also low-cost applications when meeting archaeological requirements. Using geomatics to acquire and manage geospatial data would improve efficiency, save money, increase communication between the various entities and contribute to better decision making.

Generating maps from GIS environment

"From a certain point of view, cartography and Web cartography seem to be the antithesis of each other. The first discipline is over a hundred years old and deeply connected to its traditional roots. The latter is a very modern Internet information service, characterized by a continual and vertiginous evolution. However, this initially seeming paradox has turned into a truly collaborative relationship with the arrival of the map digital format and Geographical Information Systems (GIS). The Web has changed our outlook on the role of maps" (Favretto 2010).

In general, the traditional map is an abstraction of the geographic reality, that together with the Web context it gains new options and plays an important role as a web search engine that can link contents of a map like text or geometries to geographic elements in the web or can connect to other maps on the internet. This kind of map can also act as a research tool in the web or can function as a link when searching geographic data on the internet (*Ibid.*).
Generally, we can say that the vector data in the GIS application is used almost in the same way in a regular topographic map, yet, the strength of the GIS environment starts when questioning spatial analysis and attribute queries like '*How many tombs are above one meter height?*' or '*Which tombs were found in 2015?*', here the GIS plays a powerful tool to answer those type of questions when using vector format.
Besides the advantages of using vector data, there are some benefits of using it in the web environment when creating a map. First, the WebGIS version can also function as an interface to other geographic and non-geographic data on the web. Second, the map behaves like any digital map with the possibility to zoom in or-out with representing different visualization of varies stages, to switch on and off different layers, to measure areas and distances, to click on a symbol that can give access to the dataset that was added by the user and so on.

05 Results

05 Results

Visual Inspections of Temporal Changes

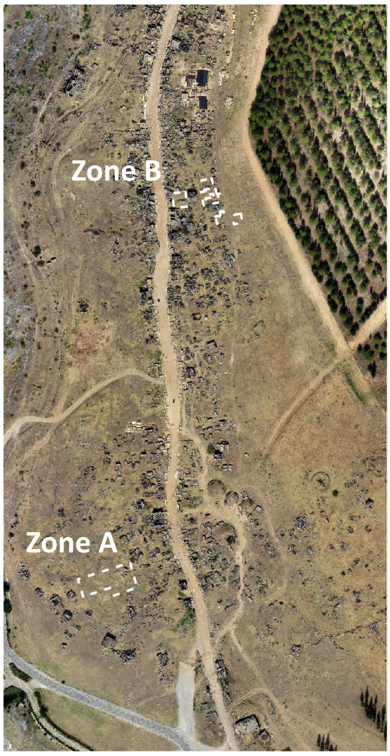

In order to compare and understand the changes between the two years, I used different approaches using the built-in Raster functions of *ArcGIS* software. The immediate act was inserting the two orthomosaic images of 2015 and 2019 as overlapped layers and simply scanning by the eyes with the '*Swipe*' option and by changing the transparency of the photos. As can be seen in figure 53, two main areas have been discovered with new excavations of clusters of tombs, one in the south of the Necropolis (A) and the second in the north (B). These zones constituted the base for my further investigations.

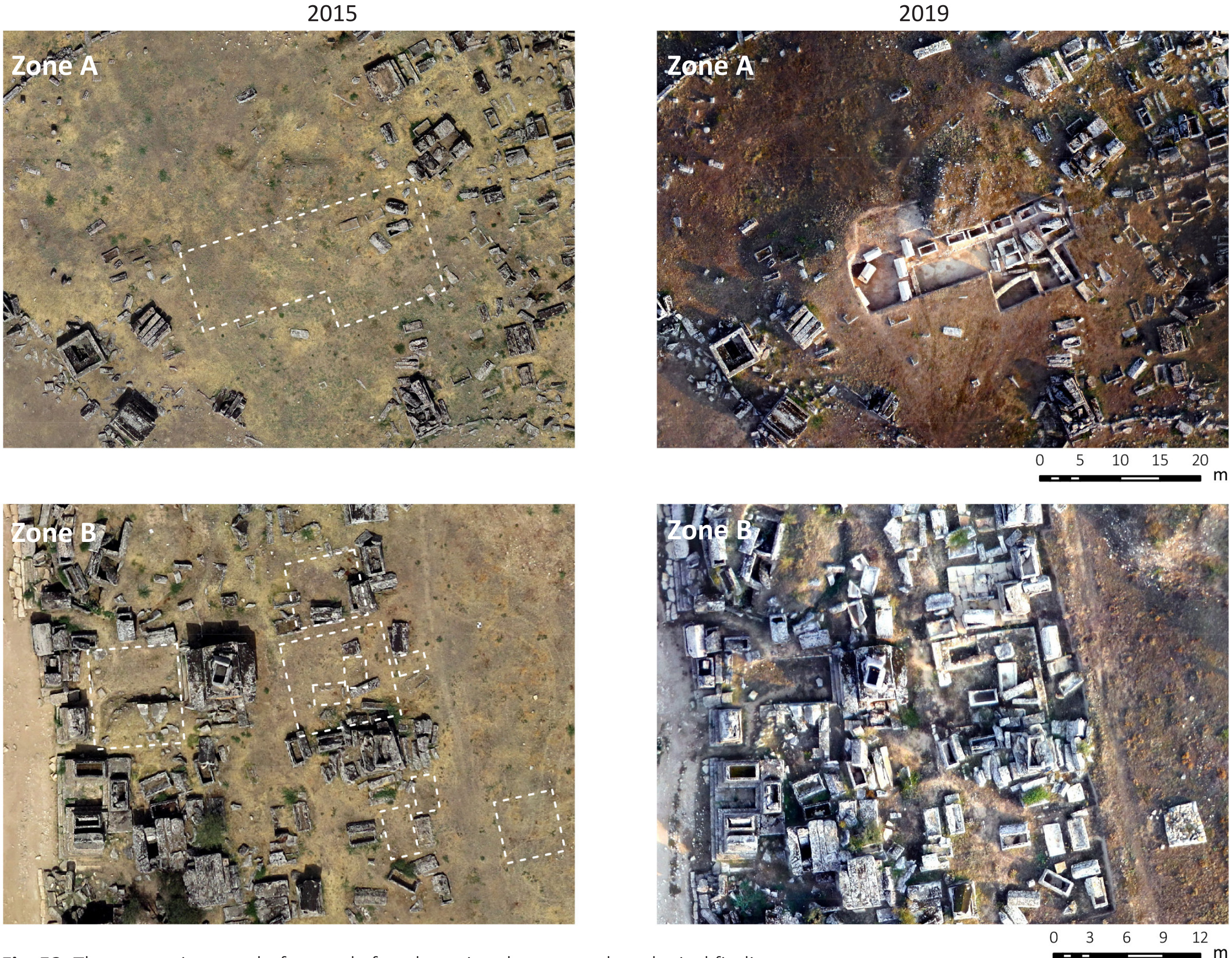

Fig. 53. The two main areas before and after detecting the new archaeological findings.

To confirm the initial results of the temporal changes and detect the site in a more precise and quantitative way I used the Raster functions. The Raster functions were useful due to their ability to calculate and display changes through time by comparing pixels of two single-band continuous raster images from different times. In our case, the availability of Z-values of the DSMs was crucial to compare the land cover of the different periods.

The first operation was computed by using the ***Compute Change*** function, located in the Raster Functions under the *Analysis* category. By inserting the two DSMs, the formula subtracts the Z value of the second input raster (DSM of 2019) from the Z value of the first input raster (DSM of 2015) using a 'cell by cell' method. In this process I used the *Stretch* style located in the *Symbology* option, so the gradual representation gave more detailed and accurate information with more classifications.

The new layer (Fig. 54) shows that the darker the colour, the greater the change of the surface with addition or losses of materials. By looking at the legends, it can be interesting to see that almost the same maximum height excavated, represented by the green colour, is almost the same maximum height piled, represented by the purple colour, especially in area B, with approximately 3.5 meters of change.

The second application I chose to calculate with the DSM was the ***Minus*** from the Raster functions under the *Math* category. In the new layer that was created, when the value of a pixel was positive, the surface was naturally removed or intentionally dug, with a negative value, the ground was filled. As shown in figure 55, the outcomes of this function support the first assumption, where the concentration of the green and the orange 'stains' represent the changes with time and are located at the same places of the estimated A and B areas of excavations.

More on the image, the main green areas symbolize the excavations carried out between the years 2015-2019 and the main orange colour represents the piles of the soil as a result from the excavations. It should be noted that after a surface analysis, I understood that the heights of the two DSM were not perfectly correlated, therefore a vertical co-registration has been done while the calculation was limited by assigning thresholds of 0.2 cm ($-0.2<X<0.2$) that were not taken into account in the new layer.

The third function applied was the ***Cut Fill***, located in the Geoprocessing 3D analyst tools with the ability to calculate the area and volume changes between two 3D surfaces (Fig. 56). The principle is the same, subtraction of one layer from the other layer using the Z-values of the DSM as the variations.

Zone A

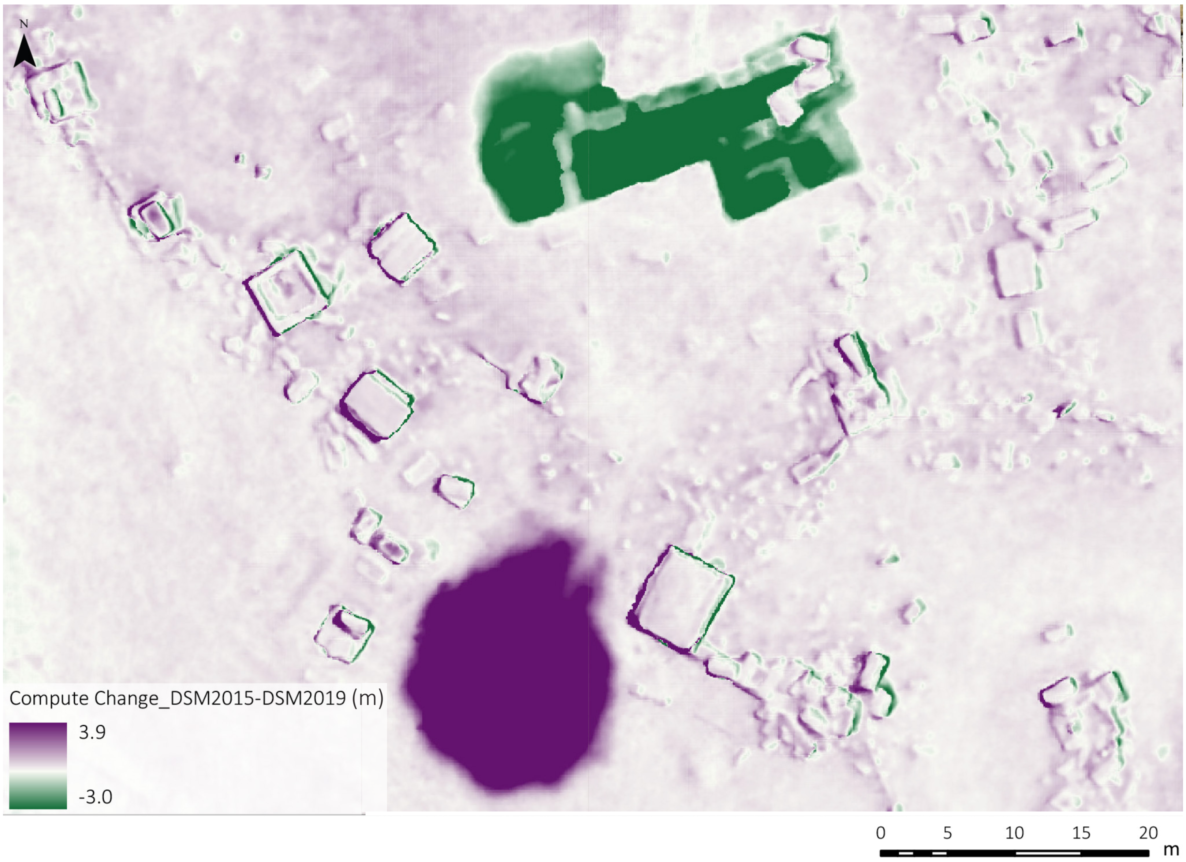

Zone B

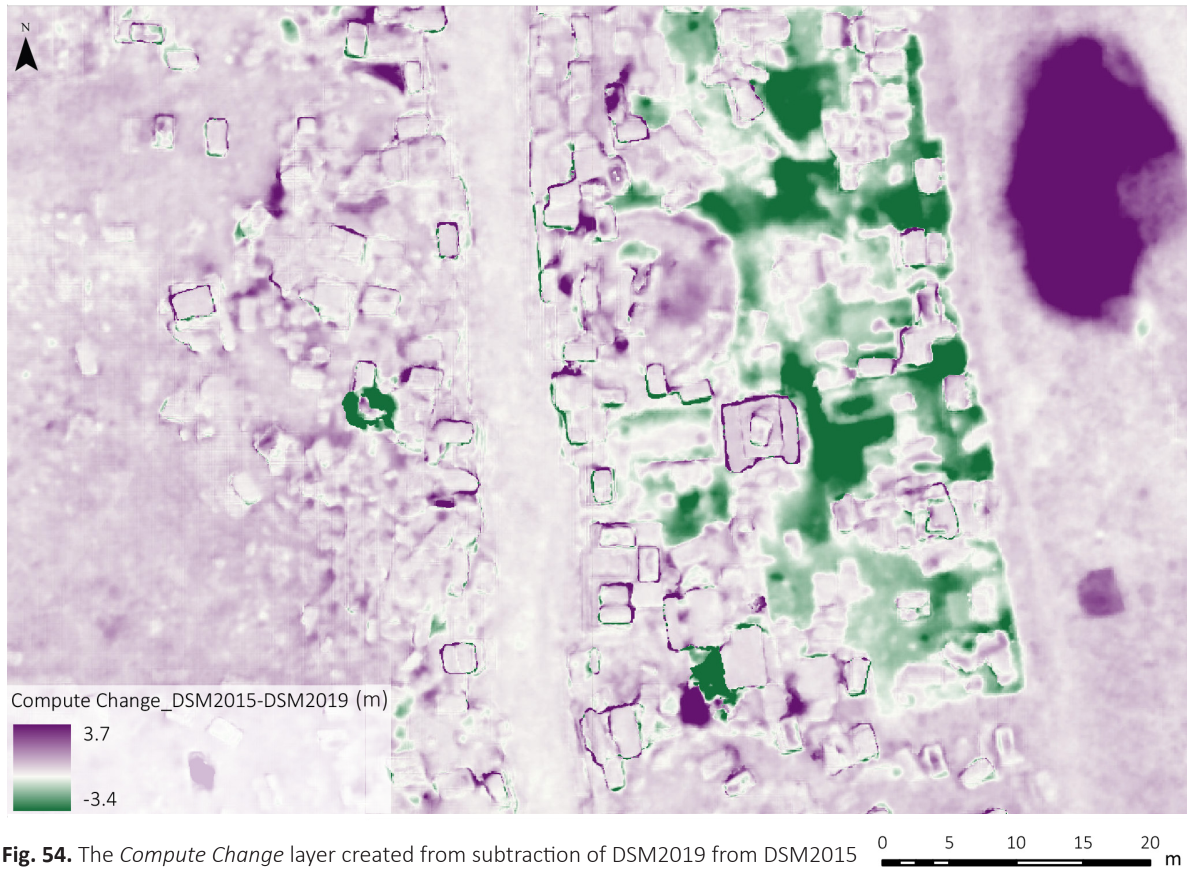

Fig. 54. The *Compute Change* layer created from subtraction of DSM2019 from DSM2015

Zone A

Zone B

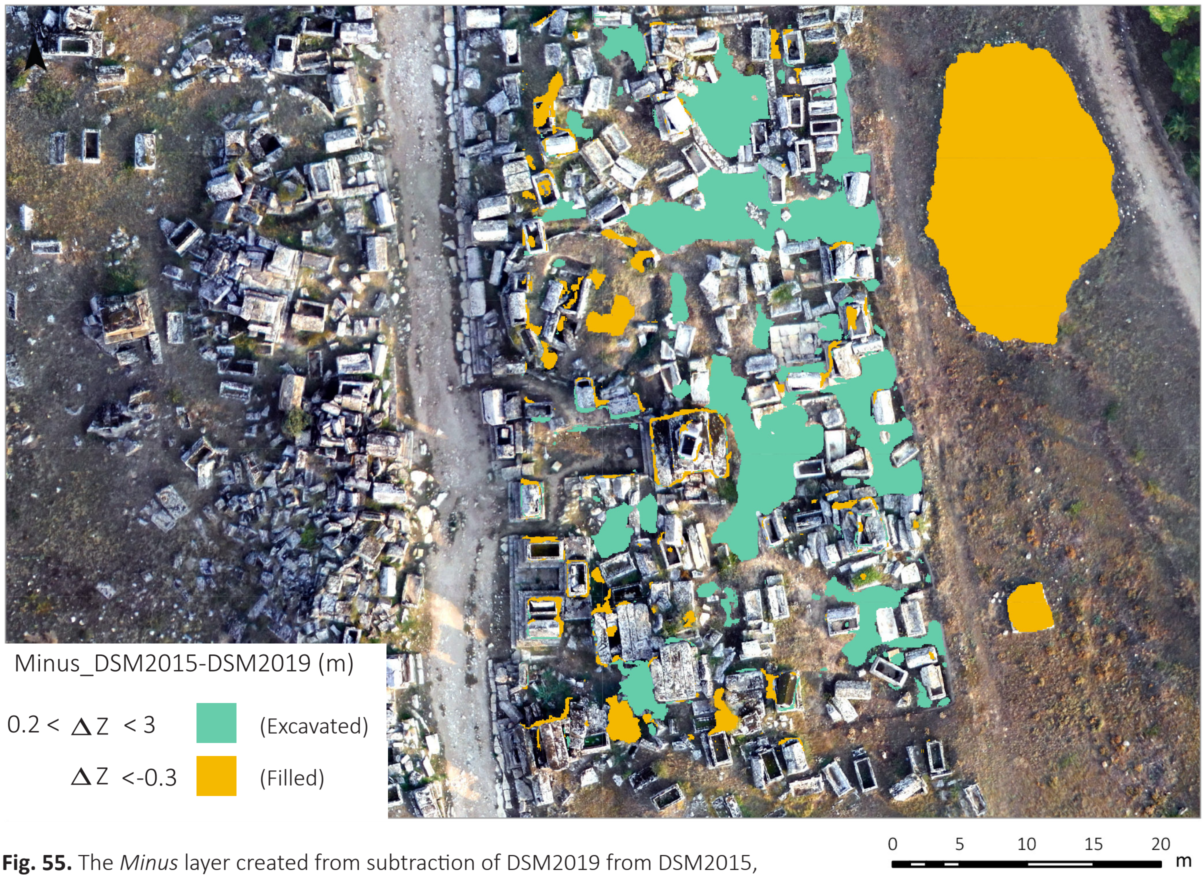

Fig. 55. The *Minus* layer created from subtraction of DSM2019 from DSM2015, background layer: orthoimage of 2019

The outcome identified regions where the surface did not change, was cut or was filled during the two different periods by comparing the elevation of the landform surfaces. From the attribute table of the new layer, I extracted the data that related to each area of interest. With analysing the attribute table of figure 56, we can say that with positive volume, the material was removed and with a negative value, the material was added. Here, in both zones, A and B, the green regions indeed compatible with the new excavations while the white areas remained without change. An exampleof a non-changing area can be seen in figure 56, when the two 'holes' in the main green region in 'zone A' resemble the sarcophagi which were already exposed in 2015.

The new layer and the categories in the tables show that this Raster function works on 'zones' of the same cut /fill/unchanged regions that already were discovered using the two previous functions. Yet here, with a more simplified way, where 'Value' represents a code for all the cells in the same region, 'Count' stands for the number of pixels in each region, 'Area' computed by calculation of the number of cells in a region multiplied by the cell size of the raster image and 'Volume' resulted from cell area duplicated with its Z-value.

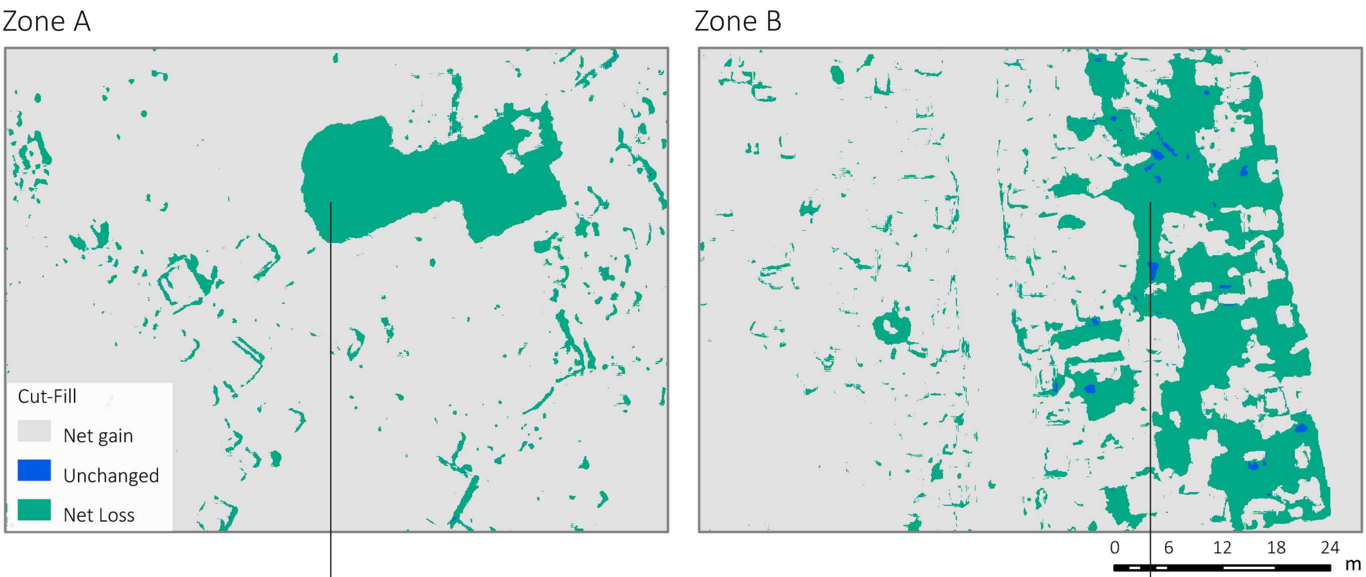

OBJECTID *	Value	Count	AREA (m²)	VOLUME (m³)
Zone A:				
36483	36483	67059	292.109004	216.296175
Zone B:				
14158	14158	136807	595.931292	129.673795

Fig. 56. *Cut Fill* layer created from subtraction DSM of 2015 and 2019 and the area and volume extracted from the attribute table for each zone.

Thanks to the Z-axis data available in *ArcGIS*, I could determine the DSM layers as ground height values and use them as a source as *elevation Surface* layer. The first main outcome was the ability to translate the landforms of the two years into *Profile Graphs* by creating a local section, using 3D line geometry (for each DSM), then to visualize, compare and analyze the elevation changes over a continuous length of time. With this method, one profile graph able to contain multiple 3D line features, in this way, the elevation lines are displayed simultaneously and assist to see more clearly the height differences (Fig. 57).

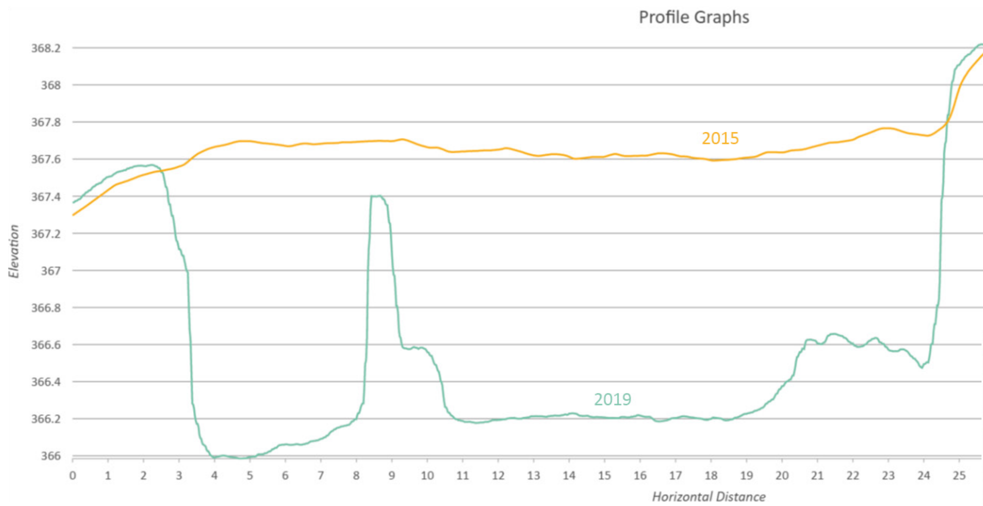

Fig. 57. A *Profile Graph* demonstrates the two landforms of 2015 and 2019, using ArcGIS Pro. From the right, orthoimage from 2019 with the location of the section that was calculated, drawn in red line.

A second important product was exploiting data in a 3D environment with its coordinate system as a local scene in the *ArcGIS* to ease the visual interpretation of the surface and to gain more geographic information about the relationship between the built structures and the land. In the case of the Necropolis area, for a more complete 3D visualization, it was better to use *Agisoft Metadata* software which contains more information regarding the elevation information. The result can be seen in figure 58.

To sum up, in the *ArcGIS* software, many tools are available for detecting and quantifying temporal changes using various Raster functions, and the overall results I obtained were satisfactory. Yet, when assessing the results of the three Raster Functions (*Compute changes, Minus, Cut-Fill*), although they are considered as quantitative operations, it seems that they are more suitable for demonstrating the changes in the site as a whole, and for getting a general idea about the location of the new excavated zones. This is in contrast to the *Profile Graph* tool which provides accurate information about the elevation for each meter on the map, and allows the generation of many sections of different times in one graph for better visualization of the changes.

In my opinion, the decision to use each tool depends on the purpose that needs to be achieved by the user. For a more global interrogation, the adoption of the Raster functions together with the 3D model can be a good starting point, while the *Profile Graph* process is more efficient in small areas with prior basic knowledge.

Zone A

2015

2019

Fig. 58. 3D representations of the situation in the years 2015 and 2019 – using *Agisoft MetaShape* software

Exploring the Surface Geometry

With the various surface tools available in the Raster functions of *ArcGIS*, I decided to experiment again with the DSM due to the content of the pixels, the Z- values, which allow analysis of the raster images with a geometric approach. In order to meet one of the main goals of the thesis: to find remote techniques that would replace the traditional, invasive excavations, I applied diverse operations with focusing on the DSM of 2015 (in zones A and B) in order to check if significant geometric anomalies would come up.
The images in the next page (Fig. 59) focus on 'zone A' of the archaeological site, and compare between a true-colour image and another three images from the same year. The three images are results of the execution of diverse Raster functions with display modifications using different visual preferences in the *Symbology*. With these new layers, I successfully obtained clear topographic irregularity that can strongly imply the presence of the known, buried sarcophagi that were found in the same place in 2019. These are optic results that are almost impossible to achieve with just the true-colour image. A theory that can strengthen and support this hypothesis is that after many years of research on the Necropolis, archaeologists deduce that sarcophagi are placed near tombs or on top of them (Teppati Losèa et al. 2021).
The anomaly in these images can be interpreted as ‘artificial hill’, which is emphasized in different representations. For the *Slope* and the *Aspect-Slope* operations (Fig. 59: B and C) the inconsistency is reflected as ‘black stains’ compared to the close surroundings, while with *Hillshade* (Fig. 59 D), the irregularity is seen as a clear hillock. Other assumption can be exploited from the images is the rectangular element located north of this ‘artificial hill’ (marked with arrow). This element seems to be hidden underground but very evident in the three images as a white contour or as a black stain. This anomaly exists also in the orthoimage and the DSM of 2019 and is probably waiting to be discovered.

Furthermore, using the *Shaded Relief* function helped me to highlight the deviation in the topographic surface that does not follow the natural one. Moreover, adding labelling of the heights with contour lines eased the reading and quantifying of the data and assisted the achievement of a more accurate analysis (Fig. 60).

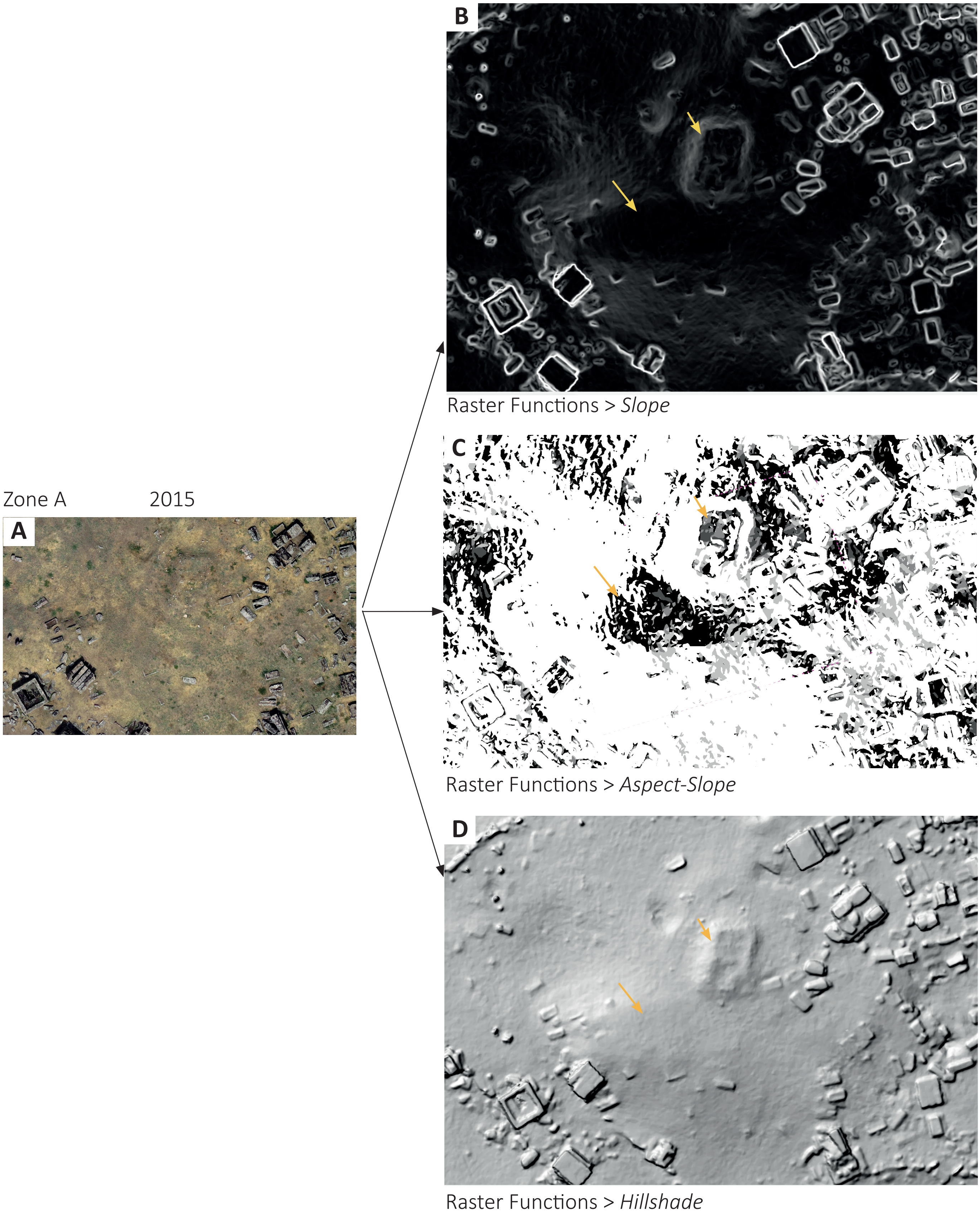

Fig. 59. Left: close-up on the area of interest A, an Orthomosaic from 2015, Right: Results after executed varies Raster Functions on zone A, using *ArcGIS Pro.*

Zone A

2015

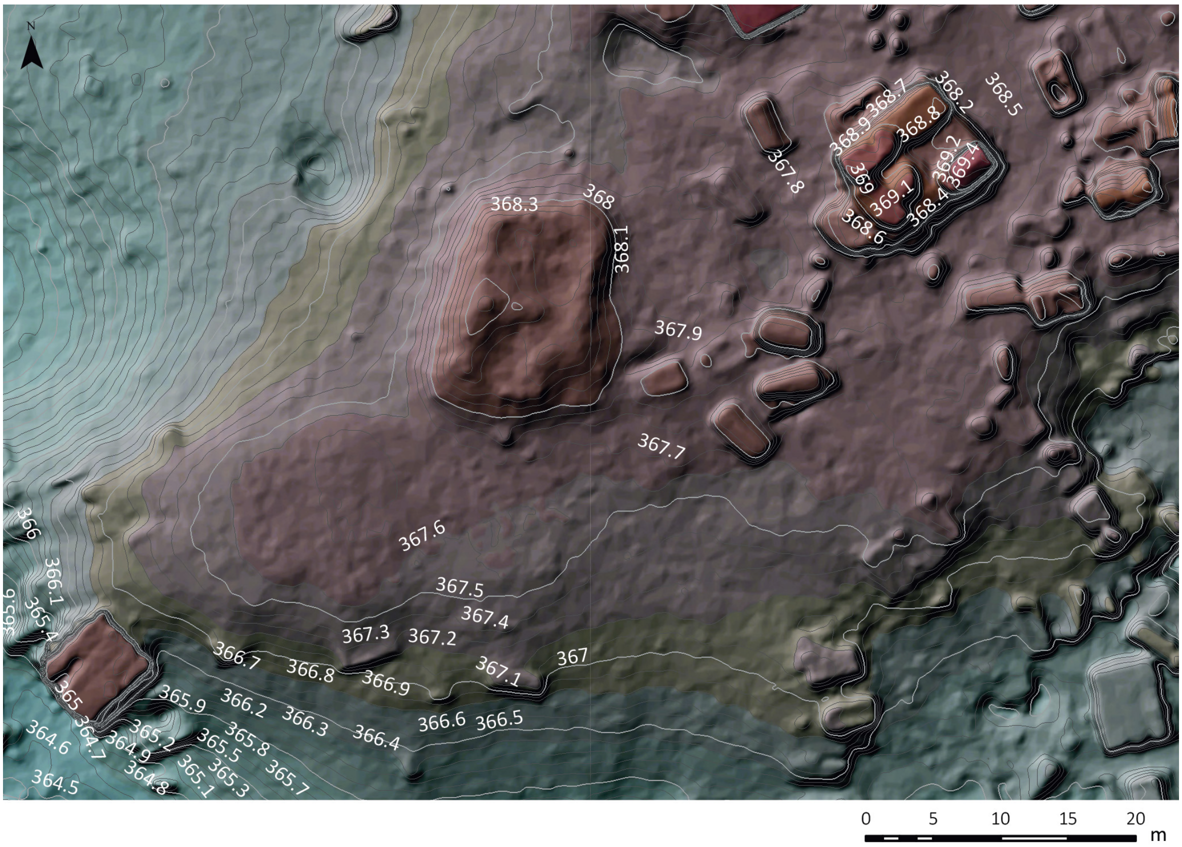

2019

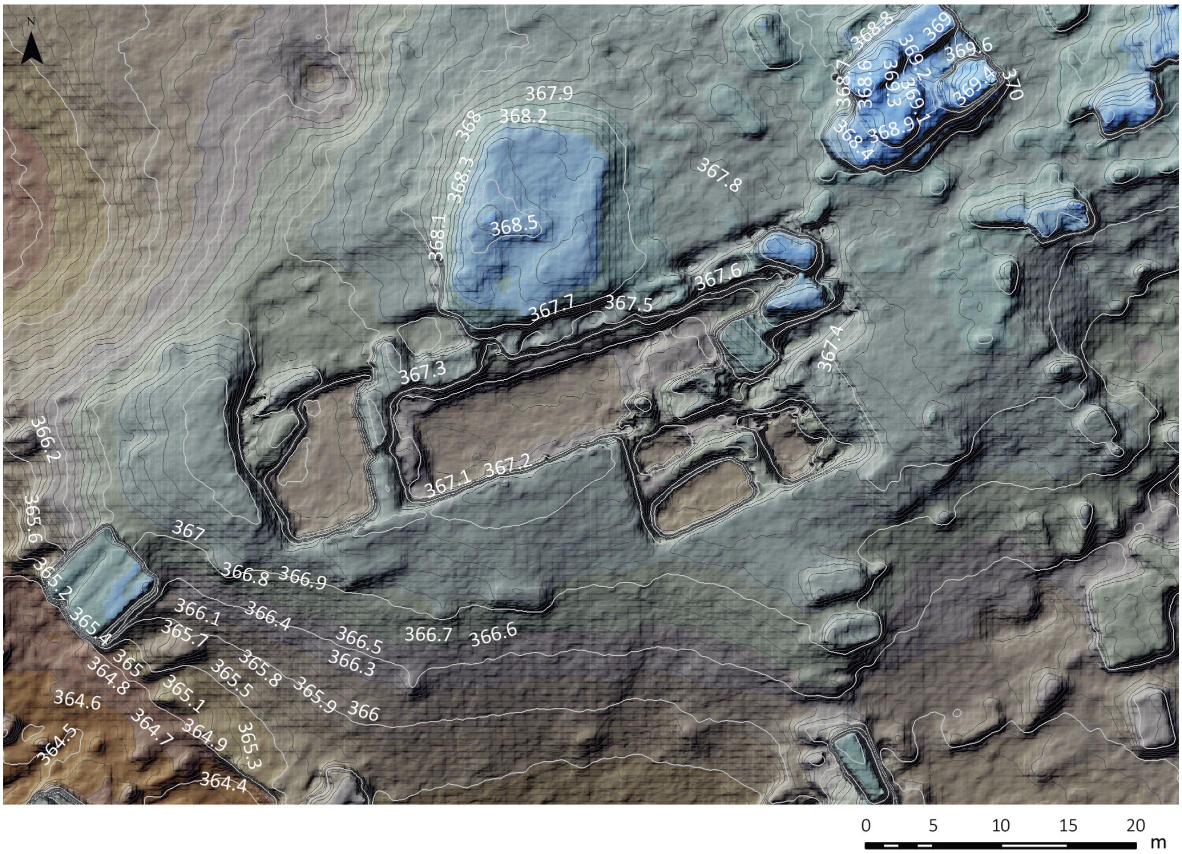

Fig. 60. A comparison between the results of 2015 and 2019, by using: Raster Function > *Contour*, on a background layer: Raster Functions > *Shaded Relief*

Applying the *Shaded Relief* from the Raster functions on the entire archaeological site helped to examine the whole picture and helped to investigate other anomalies. Besides, involving the *Symbology* tool in this operation allows one to control and add more classification of colours. One of the results represented in figure 62, might indicate the presence of other clusters of tombs. The white curved line drawn on this image highlights small hills that seem to not follow the natural topography and may indicate hidden structures like already discovered in zone A (marked in the image). In addition, this kind of display mode can imply some other circular tombs, *Tumulus* (Fig. 61 and Fig. 63) that cannot be seen in the true colour orthophoto.

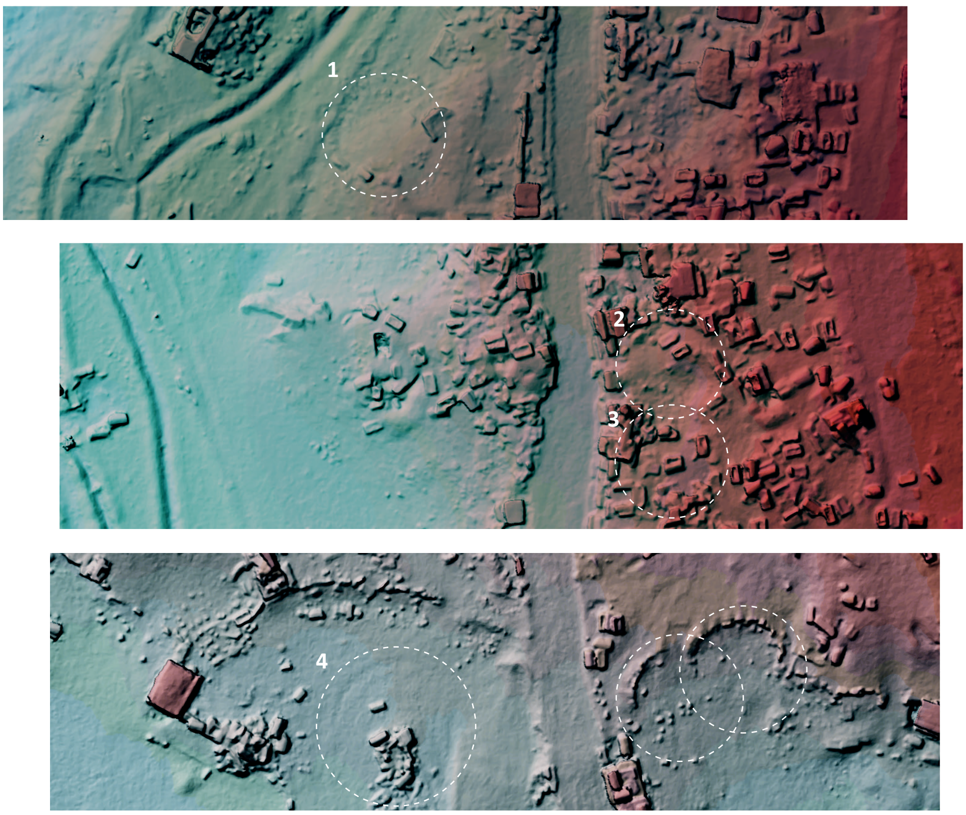

Fig. 61. Results after applying: Raster Functions > *Shaded Relief* on the whole archaeological site, estimated location of Tumulus tombs.

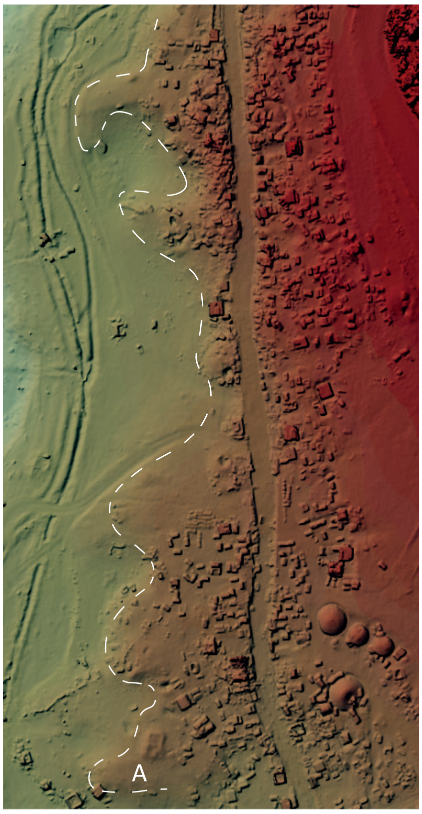

Fig. 62. Results after applying: Raster Functions > *Shaded Relief* on the whole archaeological site, representation of the inconsistency of the natural topography

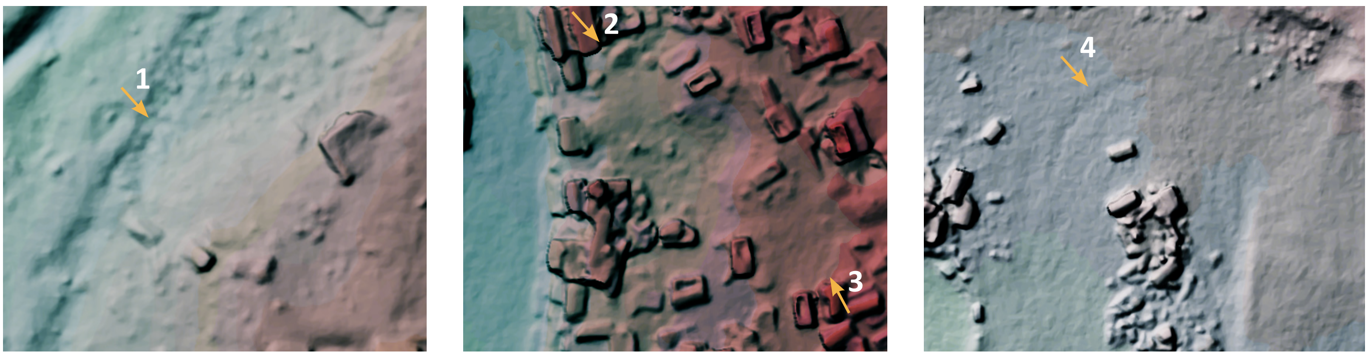

Fig. 63. A close up of some of the circular shapes marked in figure 57

An attempt for applying the same Raster functions was done also for zone B, as can be seen in the series of images below (Fig. 64). As can be seen in the photos, the density of the archaeological objects made it difficult to point out new discoveries. For a clearer demonstration, I decided to add the same images, but from 2019, with the new findings marked in yellow rectangles as a comparison to 2015.

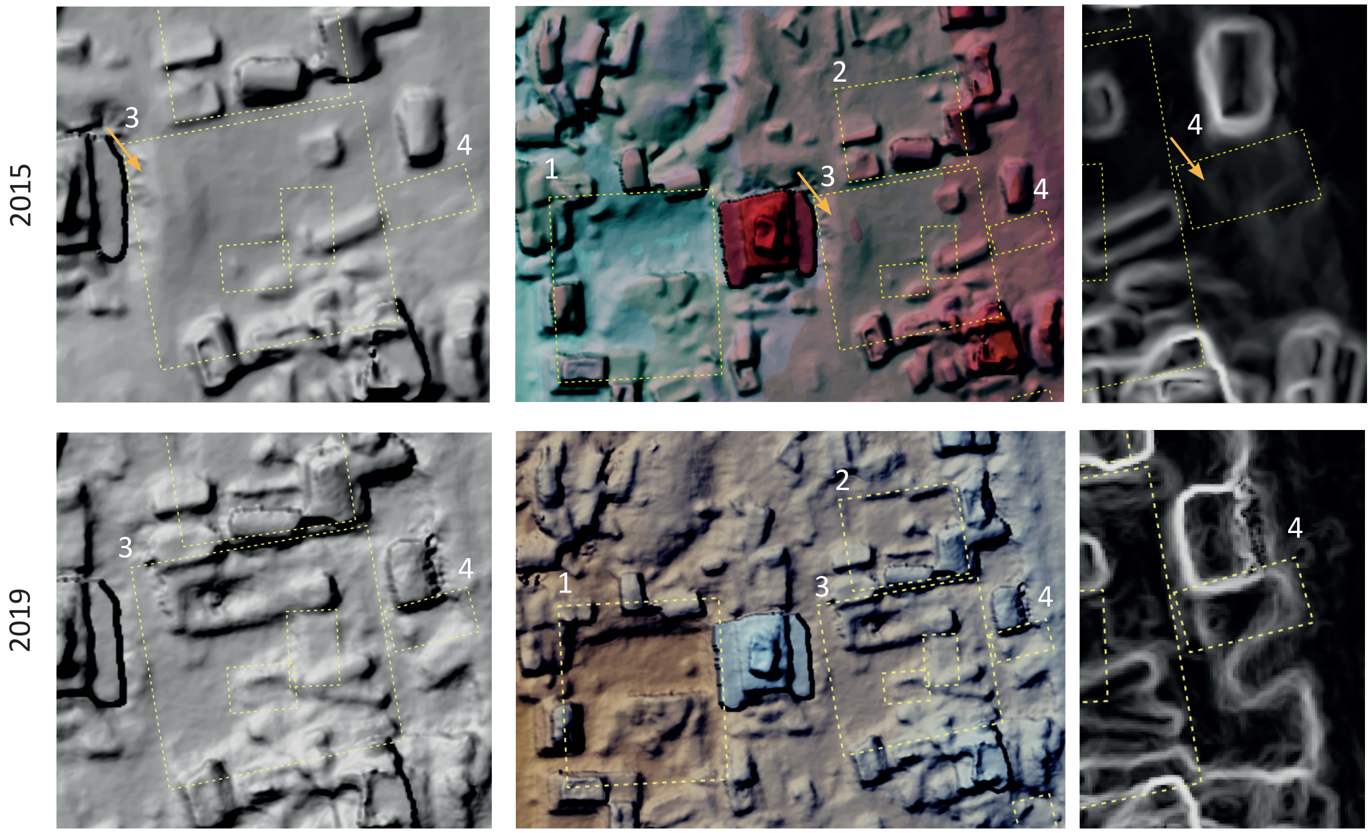

Raster Functions > *Hillshade* Raster Functions > *Shaded Relief* Raster Functions > *Slope*

Fig. 64. Results after executed varies Raster Functions on zone B, using ArcGIS Pro.

When looking at mark number 3 in the images from 2015 in both *Hillshade* and *Shaded Relief* functions, a suspicious bulge might imply a corner of a wall. Another hypothesis can be seen in mark number 4, where a rectangular white contour stressed after using the *Slope* function and can fit a tomb discovered in the same place in 2019. In general, I can say that using the Raster functions in zone B did not bring fruitful results. The reason for the uncertainty can be due to shadows from nearby structures that interrupt correctly translation of the ground in the images. 'Stains' of vegetation can also mislead the eye and can be considered by mistake as an assumption for a tomb structure.

The Near Infrared Band and False Colour Composite

The first step with the Near Infrared range of the electromagnetic spectrum was to examine it as an isolated band, so as to know if the vegetation reflected in the two main zones will be highlighted and indicate irregularity with the surface. The outcomes as seen in figure 65 show some bright and dark spots, but the texture of the soil seems quite homogeneous, therefore required further examinations.

Zone A

Zone B

Fig. 65. A pure Near infrared band extracted from the orthomosaic of 2015

As already stated, the multispectral images composed of four bands recorded with the UAV in 2015, the Red, Green, Blue from the visible range (bands 1,2,3 respectively) and the Near-infrared (Band 4) from the infrared range of the spectrum. With using the tool *Composite Bands* in the *ArcGIS,* I created a new raster database involving the Near band with the following custom band combination: the Red Channel gets the Nir (band 4), the Green channel gets the Red (band 1) and the Blue channel gets the Green (band 2). In this way, the greenery that reflects more energy with the NIR band will be highlighted in red as can be seen in figure 66.

The operation of the false colour composite can detect 'Crop marks', as already explained in the Methodologies section. The idea of the crop marks is to assist with vegetation investigation and detecting anomalies in the site that may be evidence for a hidden archaeological feature. This concept follows the fact that differences between healthy and unhealthy crops can respond to the different behaviour of the soil and the underground.

Zone A

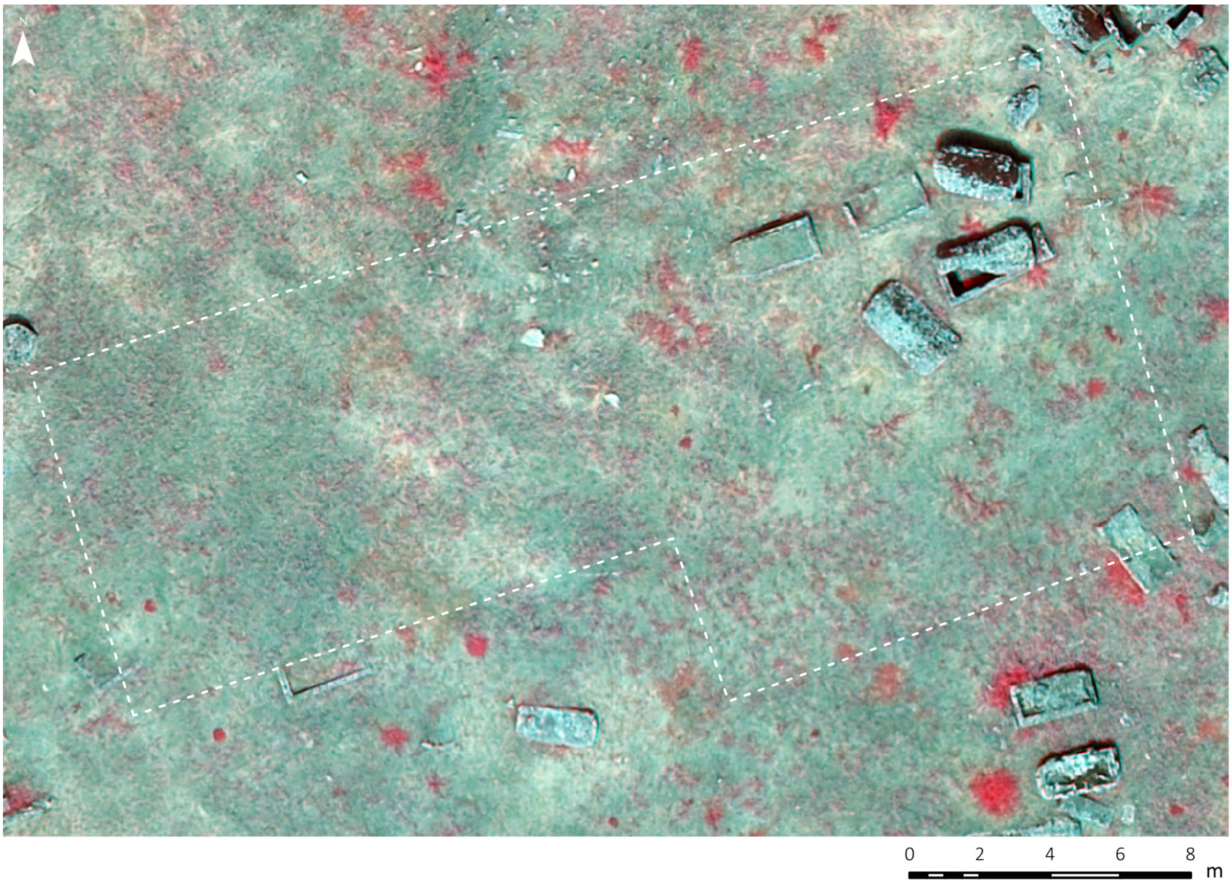

Zone B

Fig. 66. *False colour* images of 2015 composed of the Red, Green and the Near infrared bands.

The *False colour* results of the two main areas of interest from 2015, zones A and B as can be seen in figure 66, are with high contrast and clearly point out the greenery in the red colour. In order to evaluate the magnitude of this tool, I increased the scale and drew white rectangles that represent the specific areas with buried archaeological elements that will be revealed in 2019. Looking at the image of zone A (Fig 66 up), the ground with a low density of vegetation and the homogeneous soil texture made it very difficult to assume that there might be hidden elements beneath the soil. Indeed, some bright spots can be seen, but they are probably related just to the different types of soil with their different colours (see Fig. 53 and 59A to compare). Clearly, they do not give any indication about what happens under them, because they are not following the same organization and shapes of the sarcophagi under. In zone B (Fig. 66 down), the buried elements located in a number of places and enclosed in white shapes. In rectangle number 1, a black stain appears that may reflect an ancient floor founded in the new excavation (see Fig. 53 and 59A to compare), and in rectangle number 2, a dark spot can be interpreted as a corner of a wall that was discovered in a later stage. Yet, all are assumptions since the tool does not seems to provide clear and certain conclusions. This is probably due also to the fact that vegetation marks are evident in areas completely covered by vegetation/crops.

Spectral Indices

By using build-in indices from the ArcGIS and creating other relevant formulas supported by the literature (Salgado Carmona et al. 2020; Mondejar et al. 2019; Asfaw et al. 2018), I was able to manipulate, test and analyse the multispectral orthoimage of 2015 with the four bands available. I divided the work into three sections according to the different natural materials that already been extended in the Methodologies part. In theory, these materials if available in the site, are supposed to behave differently with the different bands and to show anomalies. In this part of the results, we will estimate the efficiency of this method. All the outcomes I obtained after using the indexes, included diverse modifications of the *Symbology* option in *ArcGIS* to obtain the highest contrast possible for highlighting the relevant features.

1. Vegetation Indices

NDVI - Normalized Difference Vegetation Index

By calculating the Near-infrared and the Red bands with the formula already mentioned in the Methodologies part, I generated the following black and white layer (Fig. 67). In the images, the bright areas represent the materials that reflect energy- mostly vegetation, and the dark zones demonstrate the sensitive materials for the Near-infrared like unhealthy vegetation or water bodies if present.

Zone A

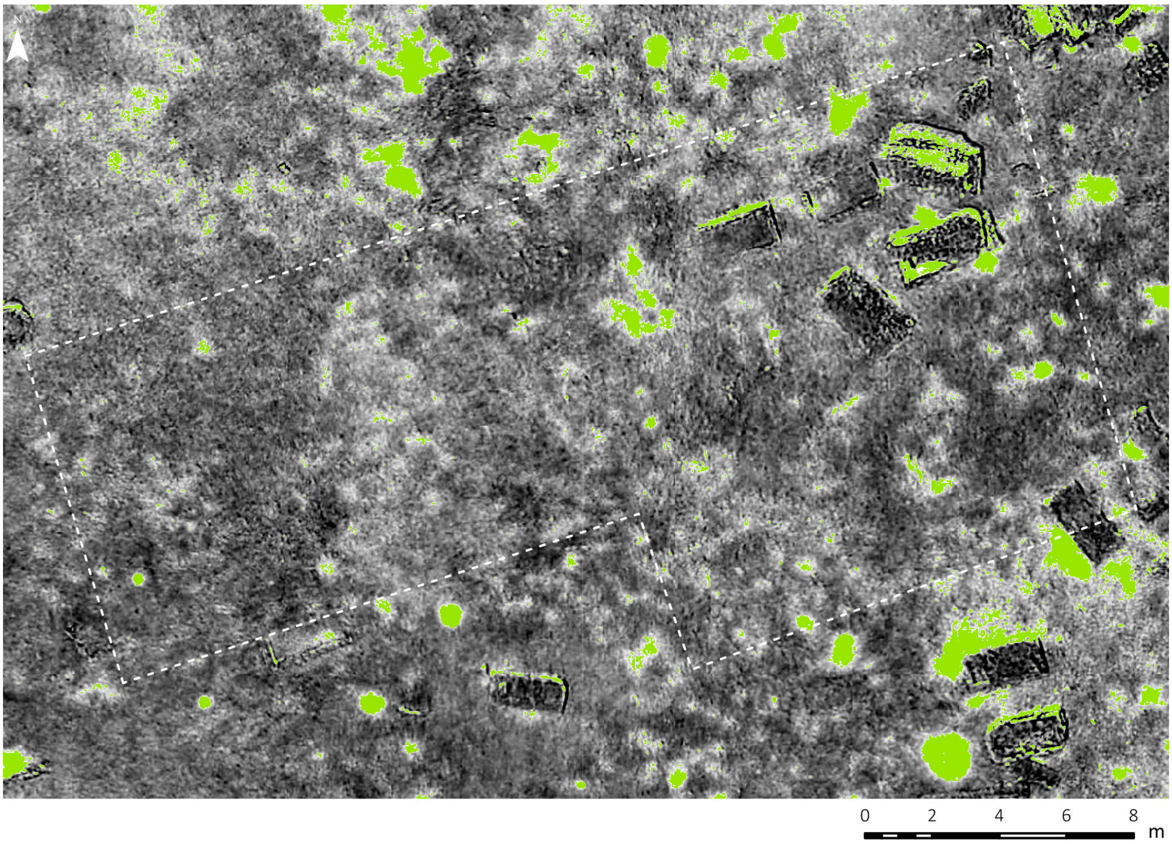

Zone B

$$\frac{NIR - RED}{NIR + RED}$$

Fig. 67. Results after applying NDVI index which stressing the vegetation using *Raster Calculator* on orthophoto from 2015.

In order to increase the contrast in the image, my next step was manually sampling pixels containing greenery, hopefully to find an irregularity related to the buried archaeological features.
For operating this process, I used the *Raster Calculator* located in the Geoprocessing tool in *ArcGIS*. The range of digital numbers inserted into the calculator was between -0.3 and 0.3, these low values can explain the negligible influence of this method, since dense, healthy vegetation can reach to 0.8. Probably this process is not suitable for the Necropolis site in certain seasons due to the dry climate and lack of green vegetation in the area. As highlighted in the pictures above, the visual results display flora as light features in the two areas of interest. Some stains like in the previous analyses are seen as dark but without consistency with the organization of the underground findings.

Many more vegetation indices were studied for the purpose of this thesis but none of them produced favourable results. The black and white areas in the images do not seem to correlate with the underground but are more connected with the shades of the soils as they were in 2015. Yet, I chose to present two more indices to support my theory:

GNDVI - Green Normalized Difference Vegetation Index: contrasts the state of the vegetation between the NIR and the Green band.

Zone A

Zone B

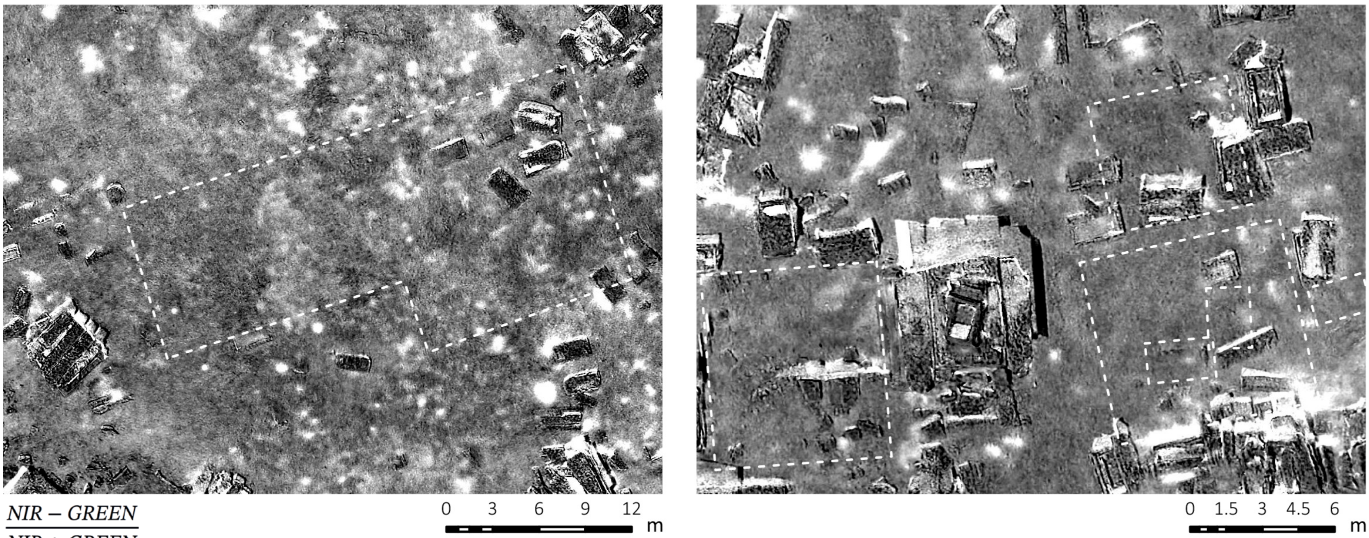

$$\frac{NIR - GREEN}{NIR + GREEN}$$

Fig. 68. Results after applying GNDVI index using *Raster Calculator* on orthophoto from 2015.

The formula of the GNDVI index (Fig. 68) is similar to the NDVI, except for the change of the Red band with the Green band in order to increase the contrast between the latter to the NIR.

SI - Salinity Index

Zone A

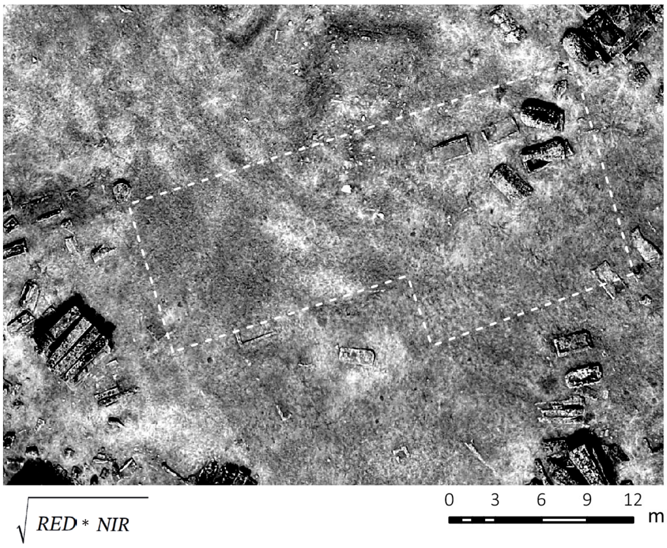

$$\sqrt{RED * NIR}$$

Zone B

Fig. 69. Results after applying SI index using *Raster Calculator* on orthophoto from 2015.

With the Salinity index an attempt had been done to check if salt sediments are present in the water bodies nearby which may be affecting the soil in the site. From figure 69 above, it can be seen that there is no influence of the material on the underground.

2. Soil Indices

The four equations I used in this study (Salgado Carmona et al. 2020) are related to the materials in the soil and the diverse states of the soil. Although the outcomes emphasized the differences, still they did not support my goal of finding evidence for underground remains. Here are the four formulas I tested and their results:

CI - Colour Index: related to the concentration of carbonates or sulfates in the soils.

Zone A Zone B

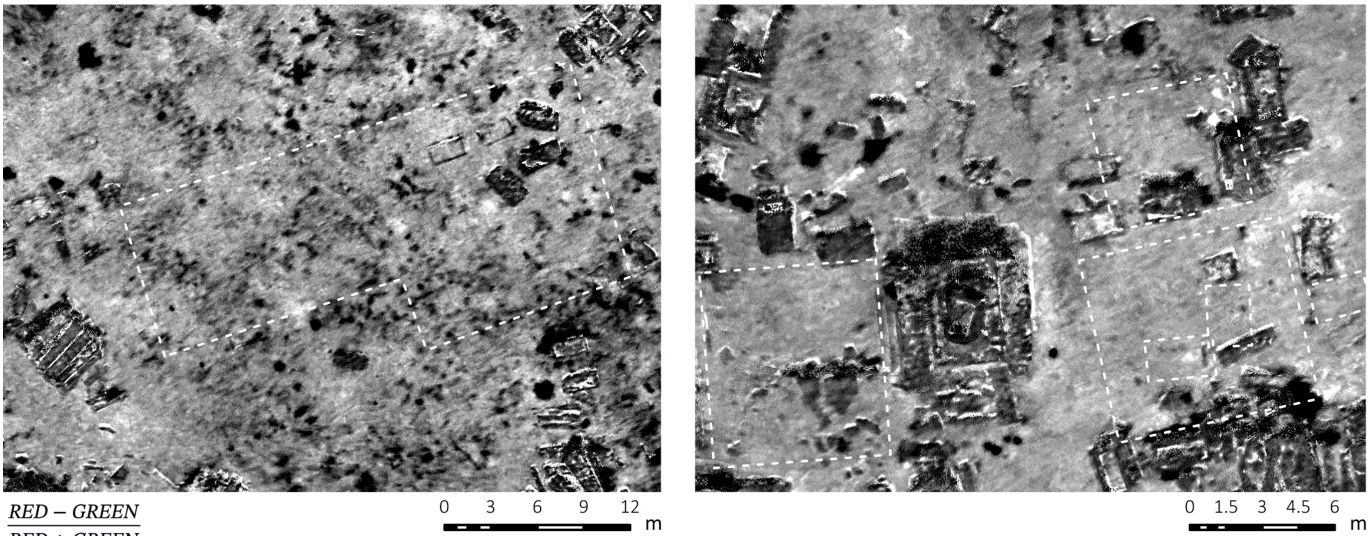

$$\frac{RED - GREEN}{RED + GREEN}$$

Fig. 70. Results after applying CI index using *Raster Calculator* on orthophoto from 2015.

RI- Redness Index: Identifies soil colour variations.

Zone A Zone B

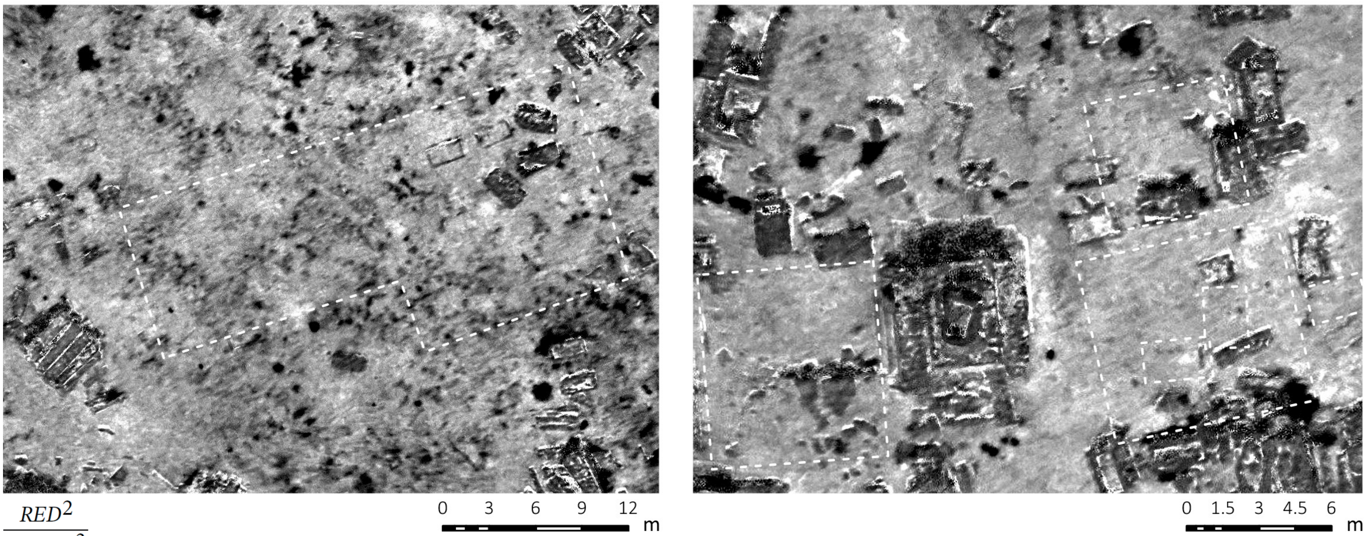

$$\frac{RED^2}{GREEN^3}$$

Fig. 71. Results after applying RI index using *Raster Calculator* on orthophoto from 2015.

BI - Brightness Index: uses the albedo of the terrestrial surface to differentiate between the vegetal covers and the soil.

Zone A

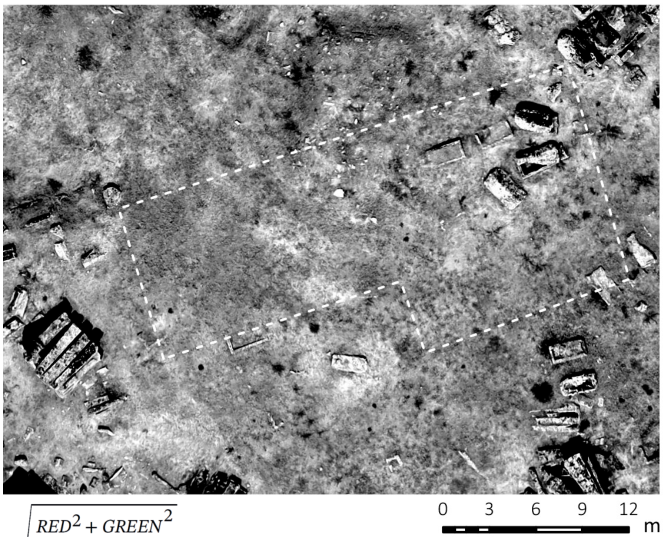

$$\sqrt{\frac{RED^2 + GREEN^2}{2}}$$

Zone B

Fig. 72. Results after applying BI index using *Raster Calculator* on orthophoto from 2015.

BI2 - second Brightness Index: sensitive to the brightness of soils which is correlated with the humidity and the presence of salts on the surface.

Zone A

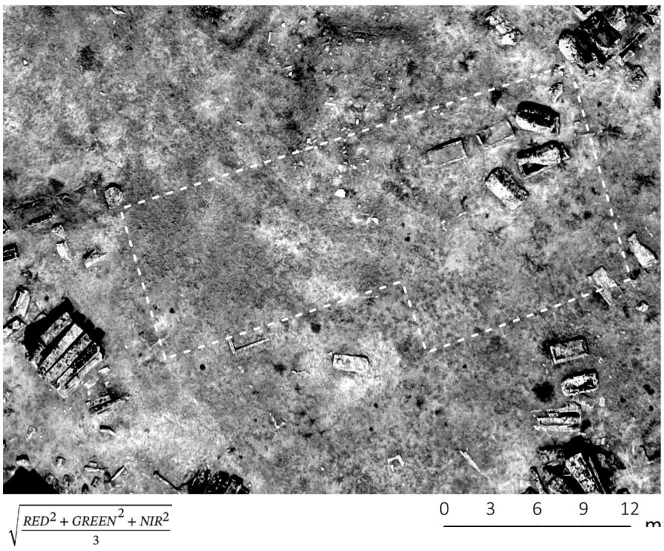

$$\sqrt{\frac{RED^2 + GREEN^2 + NIR^2}{3}}$$

Zone B

Fig. 73. Results after applying BI2 index using *Raster Calculator* on orthophoto from 2015.

3. Water Indices

Considering the presence of water elements near the site, I decided to involve also a water index to test the influence of soil moisture and to identify any potential anomaly.

NDWI - Normalized Difference Water Index

The formula below (Mondejar et al. 2019) can be compared to the GNDVI formula from the vegetation indices. In the GNDVI index (see P. 68), the NIR band is the dominant variable due to the higher reflectance of the vegetation. In contrast, in the NDWI index, the Green is the active band due to the higher reflectance of the water (see Fig. 39 'Spectral Signature'). By looking at the images in the next page (Fig. 74) – no clear argument can be declared.

$$\frac{GREEN - NIR}{GREEN + NIR}$$

To sum up, the spectral indices in the Necropolis area did not contribute much to the study. The reasons might be lack of dense vegetation or the availability of only one invisible band. I can assume that with the acquisition of more spectral bands, it would be possible to achieve more information due to the ability to involve more indices.

Zone A

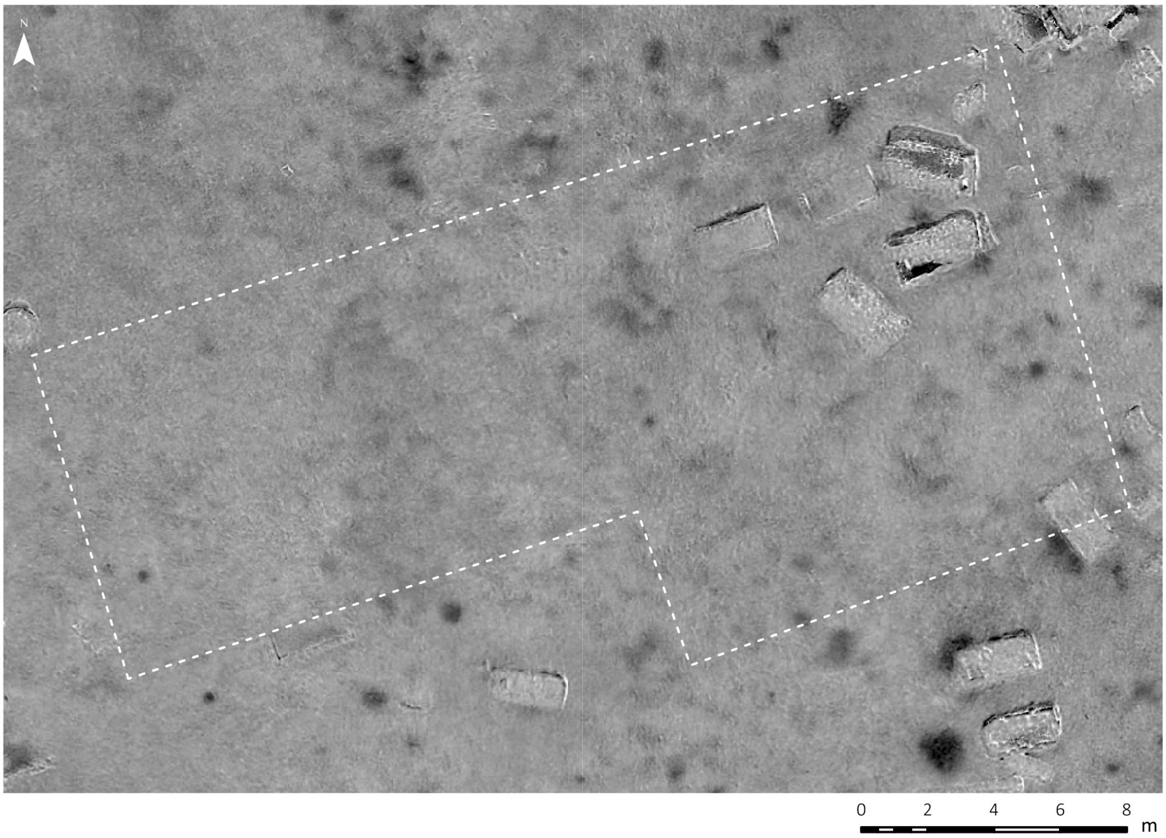

Zone B

$$\frac{GREEN - NIR}{GREEN + NIR}$$

Fig. 74. Results after applying NDWI index using *Raster Calculator* on orthophoto from 2015.

Convolution Functions

After inserting the DSM of 2015 as a Raster input into the Convolution Function in the ArcGIS Pro, a new layer was created with new features. According to a selected filter, the features highlight differently the surface with contours and shapes considering the input, in this case, the Z-value from the DSM.
The Convolution filters are applied on a moving and overlapping kernel of numeric values, for example 3 by 3. The process is continued until the kernel processed all the image.
Four main types related to Edge Detection filters were tested: *Gradient* filters, *Laplacian* filters, *Line Detection* filters and *Sobel* filters. Using these types of filters can emphasize the contour lines of the graves and perhaps even hint at evidence of remains buried under the ground.
The *Gradient* South filter for example, exploits the matrix that exhibits below:

$$\begin{matrix} 1 & 2 & 1 \\ 0 & 0 & 0 \\ -1 & -2 & -1 \end{matrix}$$

The meaning of this combination is that for each 3 on 3 pixels in an image with their digital numbers, the function multiplies this matrix respectively. In this case, the lower row, the 'southern' portion of the kernel, will be the most evident with bright colour in the new layer if it was originally dark with negative horizontal values.
The figures below (Fig. 75) demonstrate the application of this filter, the white edges define the southern side of the object and dark lines characterise the northern side. It seems that the function successfully detects the archaeological elements above the ground but not the findings below it.

Zone A Zone B

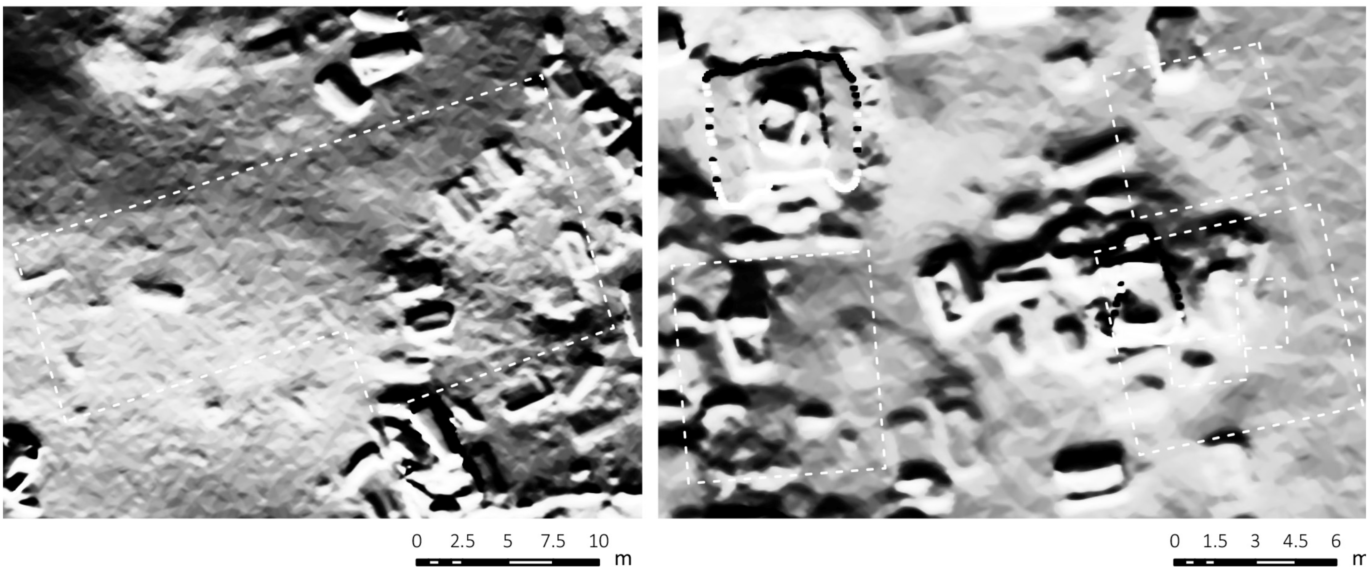

Fig. 75. Results after applying *Gradient* filter using Convolution tool from Raster functions on DSM from 2015

In the ArcGIS software six options of the *Gradient* filter are available: *North, West,East, South, North-East, and North-West.* During the study, all these filters were examined but none of them was useful for my purpose, therefore I decided to show only one example.

With the Laplacian I also used the two options available: *Laplacian 3*3* and *Laplacian 5*5*, yet, no important information came up. With the *Laplacian* filter 5*5, the software processes the following combination:

$$\begin{matrix} 0 & 0 & -1 & 0 & 0 \\ 0 & -1 & -2 & -1 & 0 \\ -1 & -2 & 17 & -2 & -1 \\ 0 & -1 & -2 & -1 & 0 \\ 0 & 0 & -1 & 0 & 0 \end{matrix}$$

In this filter the application refers to a kernel comprised of 5 by 5 cells on the input image. In the new layer, the number in the center of the matrix can be interpreted as the maximum positive or negative value while the other pixels around it creating the contrast due to the change in the algebraic sign. Applying this function to the two areas of interest emphasizes the maximum value of the digital number in the center of the objects, and the dark contours around them. The result of applying the *Laplacian 5*5* function can be seen in figure 76 below. In Zone A, the bright rectangles inside the white border are the tombs already discovered until 2015 and there is no clear evidence for other structures underground. In Zone B no traces of buried remains within the white borders were found.

Zone A Zone B

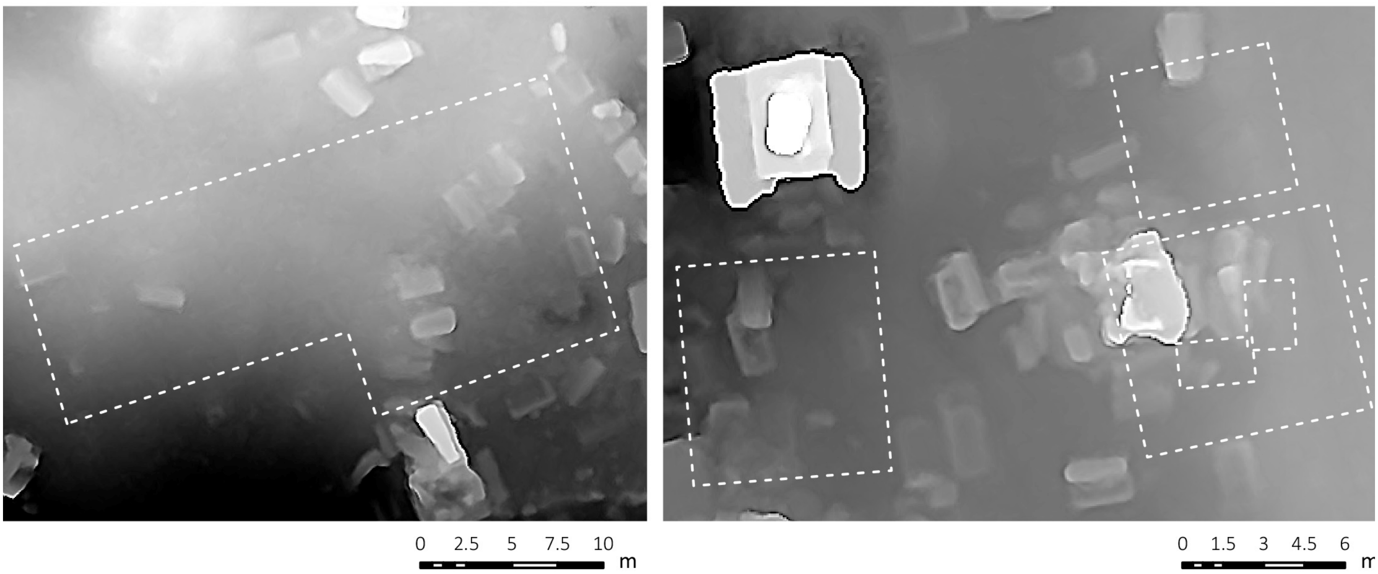

Fig. 76. Results after applying *Laplacian* 5*5 filter using Convolution tool from Raster functions on DSM from 2015

The third algorithm I processed was *Line Detection* filters. The formula below represents the *Line Detection Left Diagonal* function:

$$\begin{matrix} 2 & -1 & -1 \\ -1 & 2 & -1 \\ -1 & -1 & 2 \end{matrix}$$

With the *Line Detection Left Diagonal* function, the positive values are located in a diagonal organization while the other pixels are negative. That means that if the left diagonal was already exists and stressed in the original image, it will be more evident in the new outcome. This type of filter includes four options available in the ArcGIS software: *Horizontal, Vertical, Left Diagonal, Right Diagonal.* After study all these filters, only one was brought here as an example since the results we not useful for this study.

Zone A

Zone B

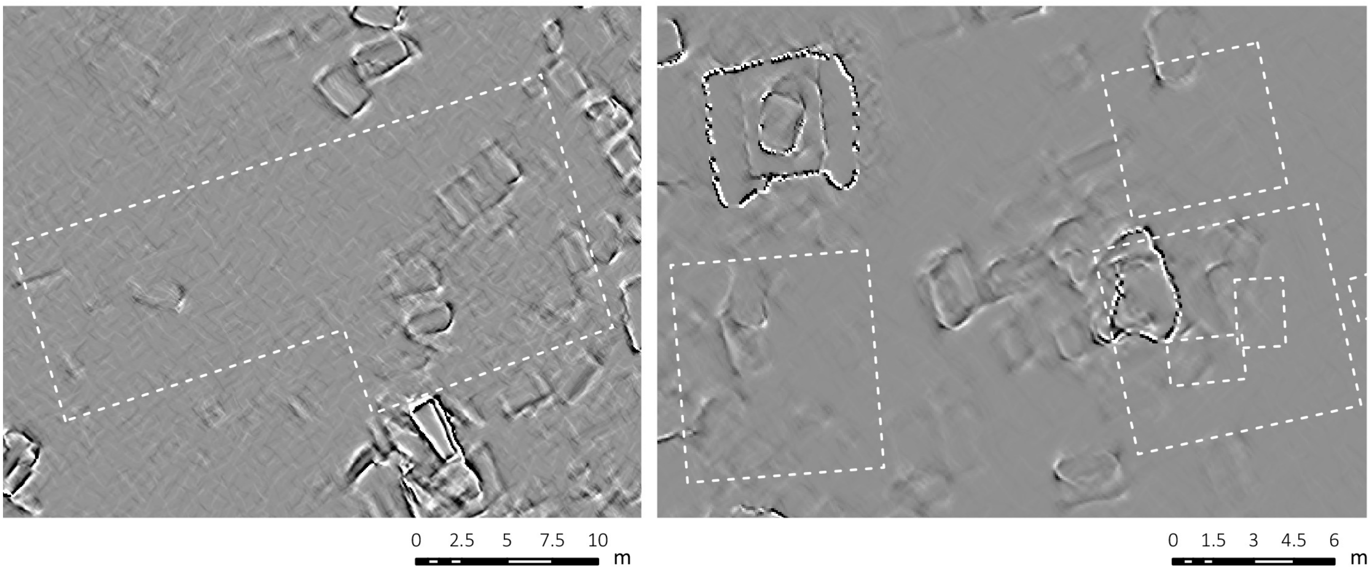

Fig.77. Results after applying *Line Detection Left Diagonal* filter using Convolution tool from Raster functions on DSM from 2015

The result of the *Line Detection Left Diagonal* filter applied for the two zones as can be seen in figure 77 above. Indeed, the texture in the pictures tends to emphasise more the left diagonal surfaces with black or white which helps to detect the objects above the ground, yet, no significant information arises under the soil.

The last manipulation on the DSM was with using the *Sobel* filters with the following matrix for the *Sobel Horizontal*:

$$\begin{matrix} -1 & -2 & -1 \\ 0 & 0 & 0 \\ 1 & 2 & 1 \end{matrix}$$

According to the values arrangement of the *Sobel* Horizontal kernel, the filter works on horizontal patterns, where the middle row will ‘neutralize’ with grey colour, the upper and the lower areas of the image will increase their values following their digital numbers.

Two options are available in the ArcGIS software for the *Sobel* filter: *Horizontal* and *Vertical*. The behaviour of the filter depends always on the digital numbers of the pixels and the reflected colours in the original photo. For example, if we take a portion of an image with dark area (which means with negative values), after applying this filter the result of upper line will be with bright colour, then, grey and after, a dark colour. The meaning is that this filter created contrast and new edges into the new layer. The filter will continue to the neighbour kernel, but the principle remains the same.

When applying the function on the two areas of interest (Fig. 78), it can be seen that the results demonstrate mostly the shadows that characterise the topography, and might be as a parallel function to the *Hillshade* procedure in the Raster functions that were mentioned before, and yet, no new evidence for hidden structures came out.

Zone A Zone B

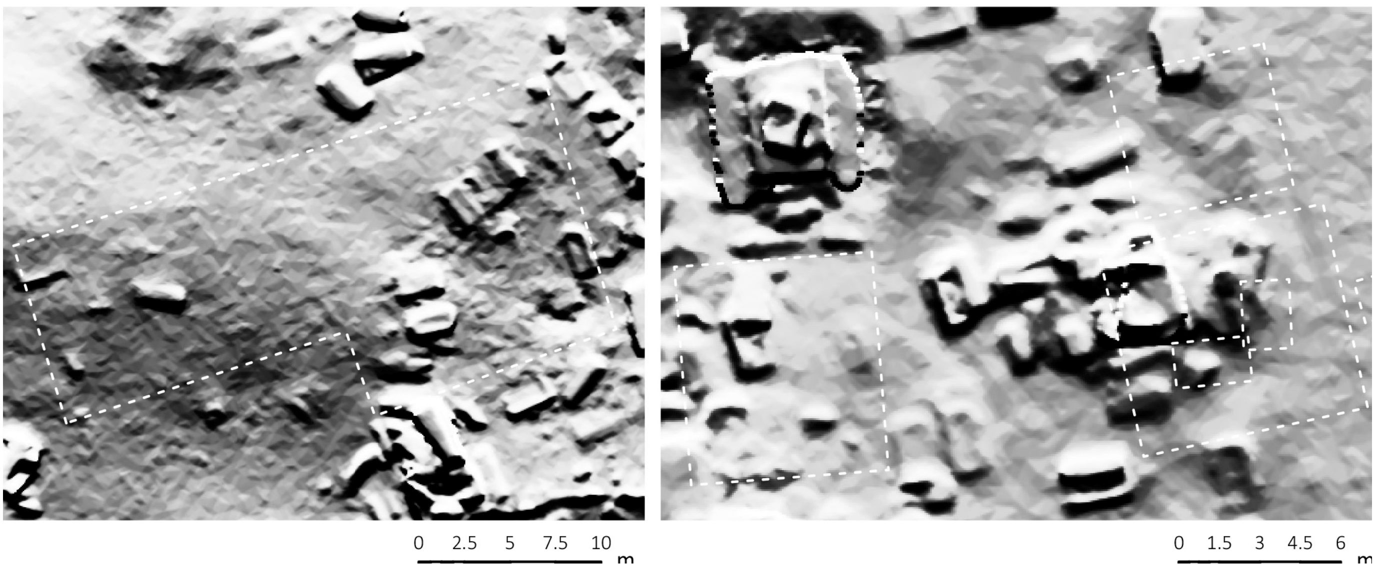

Fig. 78. Results after applying *Sobel Horizontal* filter using Convolution tool from Raster functions on DSM from 2015

Documentation Tools

Visualization

After converting the CAD data to feature classes, the software can recognize each feature with different characteristics according to the geometry type and creates attribute tables accordingly. Further, thematic information can be added as new fields in the attribute tables that are already filled with automatic geometric data. The features classes as the tombs can be controlled by the visualization and can be customised with different symbology, colour, thickness of line, continuous or dashed line.
In this way, the tombs can be classified by their typology (Fig. 79) or can be categorized according to a fine-tuned classification display. A thematic legend can be added according to the selected symbology of the classes.
Since the CAD file of the Necropolis was already identified with different layers for different types of tombs, topographic lines and roads, the work on the customised symbology was simple and fast. All that was needed was to change the colours in the symbology of each layer of the feature class. This operation is valuable when creating a map, where the goal is to classify and simplify in a very clear way the thematic differences between objects.

Fig. 79. A different visualization of the feature classes of the different elements in the map.

Documentation of New Findings

The traditional procedure of drawing and documenting in the archaeological field is based on certain rules, for example, representation of existing structures in the site with a continuous red line, while hypothesized entities are symbolised with a dashed red line (Fig. 80). A standardised symbology helps to simplify and clearly identify the different typologies of the existing tombs, as well as the new findings and future hypotheses.

In the case of the Necropolis of Hierapolis, the focus was on drawing the new main tombs excavated in 'Area A' (the southern zone of excavation, see Fig. 53) and recorded in 2019, in the GIS environment. The drawings were made by using the same standards of the traditional archaeological survey, supported by unique drawing rules established by the Hierapolis mission. The rules represent different archaeological objects and periods using different symbols in the first atlas (D'andria et al. 2008). Subsequently, the following step was to identify and relate the new findings to topologies.

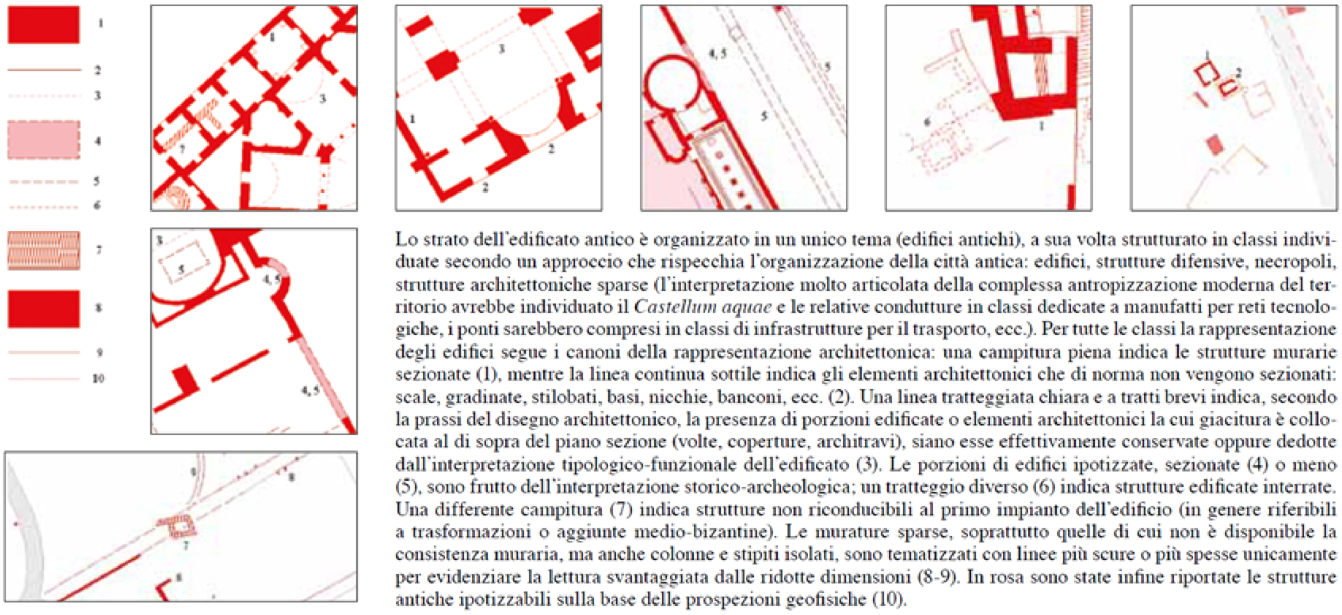

Lo strato dell'edificato antico è organizzato in un unico tema (edifici antichi), a sua volta strutturato in classi individuate secondo un approccio che rispecchia l'organizzazione della città antica: edifici, strutture difensive, necropoli, strutture architettoniche sparse (l'interpretazione molto articolata della complessa antropizzazione moderna del territorio avrebbe individuato il *Castellum aquae* e le relative condutture in classi dedicate a manufatti per reti tecnologiche, i ponti sarebbero compresi in classi di infrastrutture per il trasporto, ecc.). Per tutte le classi la rappresentazione degli edifici segue i canoni della rappresentazione architettonica: una campitura piena indica le strutture murarie sezionate (1), mentre la linea continua sottile indica gli elementi architettonici che di norma non vengono sezionati: scale, gradinate, stilobati, basi, nicchie, banconi, ecc. (2). Una linea tratteggiata chiara e a tratti brevi indica, secondo la prassi del disegno architettonico, la presenza di porzioni edificate o elementi architettonici la cui giacitura è collocata al di sopra del piano sezione (volte, coperture, architravi), siano esse effettivamente conservate oppure dedotte dall'interpretazione tipologico-funzionale dell'edificato (3). Le porzioni di edifici ipotizzate, sezionate (4) o meno (5), sono frutto dell'interpretazione storico-archeologica; un tratteggio diverso (6) indica strutture edificate interrate. Una differente campitura (7) indica strutture non riconducibili al primo impianto dell'edificio (in genere riferibili a trasformazioni o aggiunte medio-bizantine). Le murature sparse, soprattutto quelle di cui non è disponibile la consistenza muraria, ma anche colonne e stipiti isolati, sono tematizzati con linee più scure o più spesse unicamente per evidenziare la lettura svantaggiata dalle ridotte dimensioni (8-9). In rosa sono state infine riportate le strutture antiche ipotizzabili sulla base delle prospezioni geofisiche (10).

Fig. 80. Rules for drawing and documenting archaeological survey, different identification for each element in the site (Source: Atlante di Hierapolis di Frigia, 2008, P 50)

The first analysis was to understand the composition of the remains in 'Area A'. Thanks to oblique images extracted from a UAV flight from 2019 (Fig. 81 A-D) by Professor Antonia Spanò, the interpretation of the upstanding structures was more precise. The first observation from the photos was the unique grouped organization of tombs, a podium and sarcophagi that might belong to a family. A series of exposed walls that encloses the complex can support this hypothesis.

Second remark was the diagonal orientation of some of the sarcophagi. This position might point out a secondary road, that may have functioned as a segment of an ancient road network. Third remark was the small hill located north of the tombs cluster, already identified in the previous part of the thesis with the Raster functions on the DSM, that can be seen clearly also in the oblique photos. This topographic behaviour can indicate a hidden structure that is waiting to be discovered, yet, in the current map it will be defined as a hypothesis. All the elements mentioned will be represented in a new GIS map as feature classes with different graphic representations according to the various typologies.

Fig. 81 A-D. Oblique images of the Area A of the Necropolis, taken from UAV flight in 2019

After the field study , the next step was to generate a digital map using *ArcGIS* by drawing these new findings as vector data with the orthoimage of 2019 as a background. This process can be associated with CAPI (Computer Aided Photo Interpretation) technique, i.e. the process of photo-interpretation in a GIS environment.

Since the file was already composed of some feature classes (after conversion from CAD data) the following main procedures were performed:

1. Organization of each layer i.e. feature class that contains different typologies of tombs with specific *Symbology* according to the general rules of drawing an archaeological survey.
2. Drawing new geometries into the existing feature classes, by using the function *Create* from the *Edit* pane, and then choosing the relevant layer to relate the feature in the correct typology.
3. Creating new feature classes for the entities discovered lately and which are not represented yet in the map, such as the walls or hypotheses. For that, in the Catalog pane, under the project's Geodatabase folder, I set up a new Feature Class and identified it as a point, line or polygon, then assigned the suitable colour with the *Symbology* option.

Fig. 82. Drawing of the new structures discovered in 'Area A' as a GIS map

The result of the processes can be seen in figure 82, the drawing of the new discoveries identical to the graphic representation of the existing findings for achieving a united map language. In Later part of the thesis I will demonstrate other essential tools that can support the archaeological studies. One is the option to involve the time factor by setting different displays according to the periods of excavations and findings.

Functionalities of the GIS

As demonstrated, the *ArcGIS* software offers various tools to draw, display and update a map, together with the possibility to interface, correlate and eventually replace the AutoCAD data and other types of formats from different sources. But more than that, the GIS has the ability to store and add new thematic and geometric information by the user for each feature class and each feature by inserting the details into an attribute table available for each layer. With *ArcGIS* we have the possibility to communicate this information on each element with a ‘Pop-Up’ window. Another option is to use the ‘Labelling’ function for assigning and displaying specific detail near to each entity in the map, such as a number of a parcel, a name of a neighbourhood and so on.

In the new digital map I created for the Necropolis, some manual additions to the attribute table were requested for each typology. Looking at the attribute table below (Fig. 83) new fields were generated as different columns, near to the geometric data that are automatically transferred from the initial AutoCAD dataset such as the type of shape, length etc. In order to increase the amount and accessibility of information for each object in the map, it was necessary to identify relevant fields for every feature class to describe the tomb such as type of tomb, dimensions, period, geographical position and so on. Then, for each row in the attribute table of each type of tomb the content was inserted. After the two phases, turning on the ‘Labelling’ option for each layer allows the user to visually attach the Identification Number filed to each finding (see Fig. 84). Moreover, when selecting an entity in the map, a ‘Pop-Up’ window appears with all the metadata. In order to filter the data desired, there is a possibility to edit the ‘Pop-Up’ display by picking the fields that will be represented to the user and also adding images and links which communicate with other sources in the internet.

An example of a ‘Pop-Up’ window for two types of tombs can be seen in figures 85 and 86.

Field: Add Calculate **Selection:** Select By Attributes Zoom To Switch Clear Delete Copy

OBJECTID *	Elevation	Tomb Identification number	Type	Dimensions	Topographical position	Chronology	Bibliography
384	403.129	A7	Bomos	I phase - external: 6.72x4,79x2.31 m; internal: 5.74x3.81 m	The tomb defines with the adjacen...	The accuracy of the external finish...	Ronchetta 1999, 153
388	403.129	A6b	Hyposorion	external: 5.06x1.92 m	he sepulcher is obtained in the fre...	In consideration of the dating of th...	Verzone 1978, 417, fg 33
392	403.129	A6	Funerary exedra	esterno corpo centrale: 7,25x2,52x3,67 m; avancorpi: 2,02/2,00x2,39x3,67 m;	The exedra overlooks, together wit...	The inscriptions present on the cas...	Palmucci Quaglino 1977, 181, fg 12
3420	403.129	A5	Monumental gate	1.18 m	Tomb A4 and the A5 portal of acc...	The construction of the tomb and i...	Atlante di Hierapolis f 13
46	403.129	A4	Bomos	external: 4.28x3.57 m; internal: 3.47x2.75 m	Tomb A4 and the A5 portal of acc...	The construction of the tomb and i...	Atlante di Hierapolis f 13
451	403.129	A3	Bomos	external: 3.27x3.58x3.59 m; internal: 2.47x2.79 m	The sepulcher is currently isolated,...	The general compositional forms -...	Palmucci Quaglino 1977, 178
407	403.129	3	Bomos	<Null>	<Null>	<Null>	<Null>
5659	403.129	2a	Bomos	<Null>	<Null>	<Null>	<Null>
528	403.129	2	Bomos	<Null>	<Null>	<Null>	<Null>
405	403.129	1a	Bomos	<Null>	<Null>	<Null>	<Null>

Fig. 83. An attribute table of the GIS map created for the Necropolis, the columns show the categories and each raw represent a tomb.

Important to mention that the text I used here was only for demonstration in a research environment and supported mostly by the first edition of the '*Atlante Di Hierapolis Di Frigia*' and the book '*L'architettura Funeraria di Hierapolis di Frigia*'.

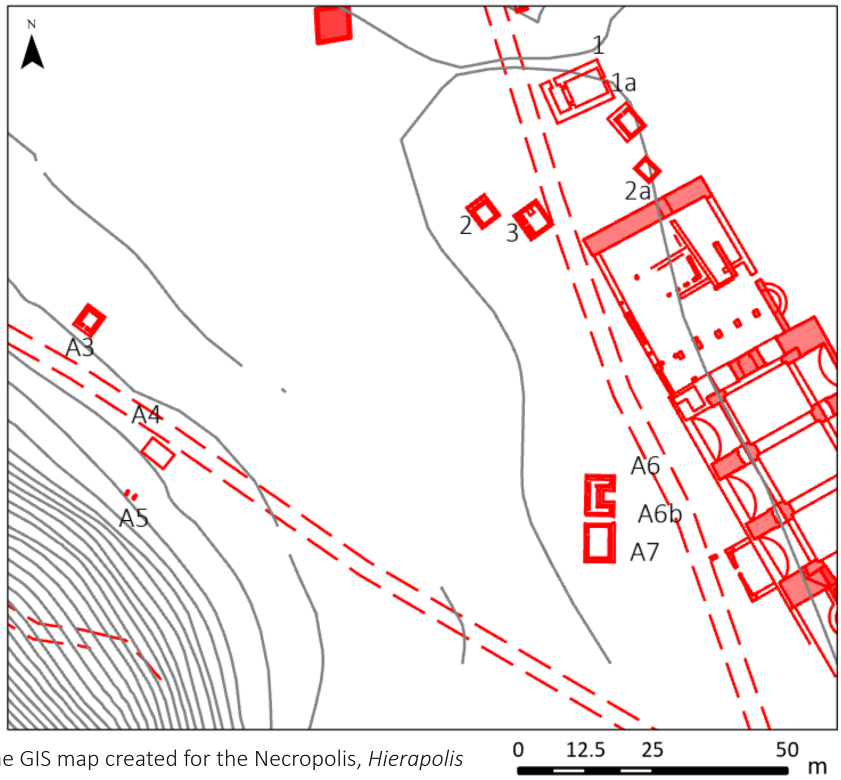

Fig. 84. A portion of the GIS map created for the Necropolis, *Hierapolis* with the labeling of the idetification number for each tomb

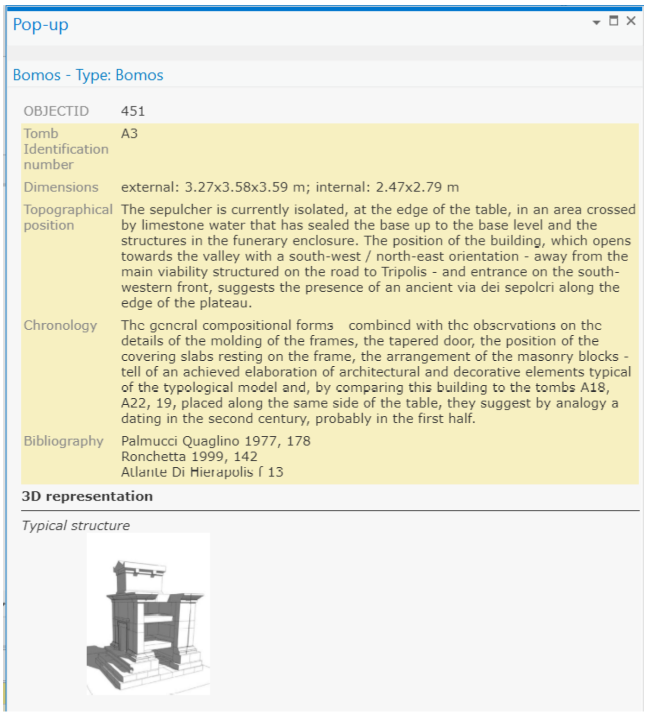

Fig. 85. An example for a 'Pop Up' for a tomb number A3: *'Bomos'* - with clicking a tomb on a map, the available data is shown according the information inserted by the user to the attriibute table.

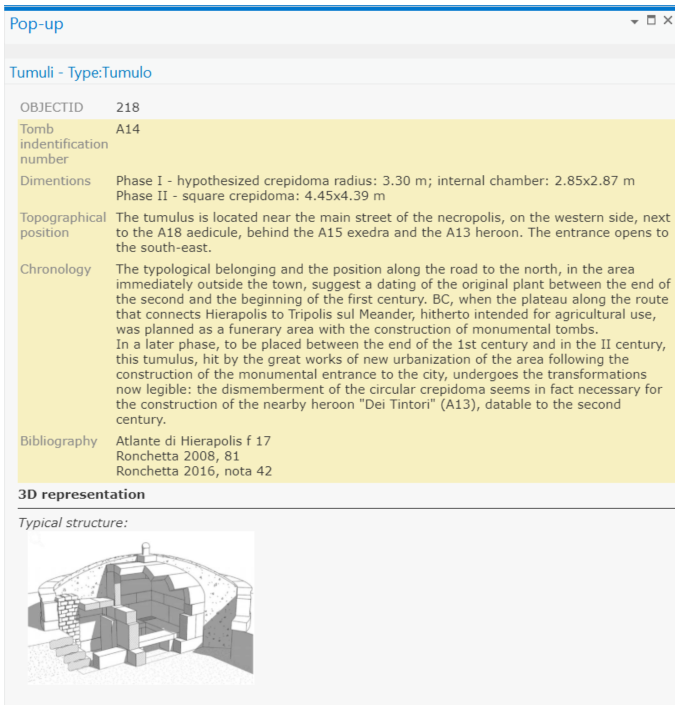

Fig. 86. An example for a 'Pop Up' for a tomb number A14: *'Tumulo'* - with clicking a tomb on a map, the available data is shown according the information inserted by the user to the attriibute table.

Visualization of Temporal Data

An important aspect in the archaeological field is the time dimension. Dating of the construction, the period of excavation works and even the restoration works is valuable to understand the story of the place in the urban context. In the Necropolis of Hierapolis, the tombs can be seen as architectural and structural evolutions that helps to organize chronologically a timeline from the late Hellenistic age to the Christian age.

My study here concentrated more on the different phases of the excavation works in the area and supported by the first edition of the '*Atlante Di Hierapolis Di Frigia*' from 2008 and the orthoimages from 2015 and 2019.

In the GIS, the time is supported spatial data in various ways. A basic demonstration of multi-temporal data can be done by storing the time as an attribute. This simple approach can easily assist archaeological studies for future excavations, and so, with the comparison between the three sources mentioned above, a new field in the attribute table (for each feature class) can be created when inserting the approximate year of excavation for each tomb in each row (for each feature).

Following the columns added and rows that filled, I could exploit the 'Year' field for separating the different displays according to different periods. But first, to control the temporal visualization at once, the first operation was to combine all the feature classes into one layer with one attribute table. Second, to implement the Geoprocessing tool *Convert Time Field* and to exploit the 'Year' value as input. Then, after modifying the 'Layer Time' for considering the time component under the properties of the new layer, a time slider appears on the screen which allows control of the visualization of three displays according to the different year of documentation: 2008, 2015 and 2019 (Fig. 87).

This process demonstrated a visual representation of the excavation phases but obviously can be applied to other parameters by setting the relevant data, for example, different displays by the estimated date of a tomb.

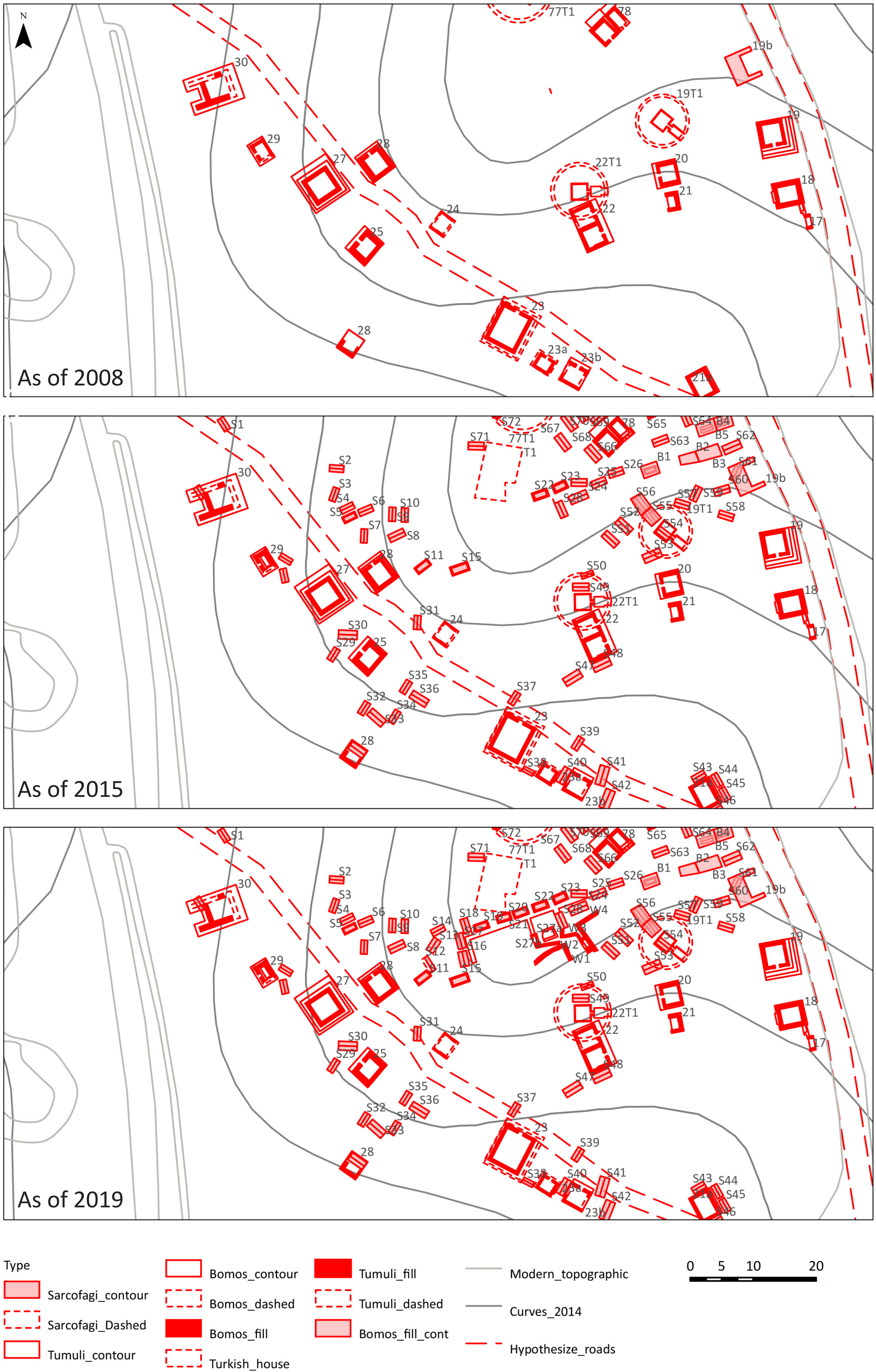

Fig. 87. Implementation of Temporal-data display for distinguish between the different period of discovery.

06 Conclusions

06 Conclusions

Approaching an archaeological site is always a complex mission as the different time layers with their various urban structures are in most cases not easy to characterize. Thanks to Geomatics and more specifically the increasing progress of UAV technology and multispectral sensors, new, relatively fast and economic techniques are available for documenting and analysing archaeological sites.

According to the workflow based on this technology, and detailly discussed in the thesis, it can be highlighted that most of the results obtained are fruitful and could contribute to future studies of the Hierapolis site and to the archaeology field in general. The main purpose of my thesis was to test the ability of geomatics to correlate with and participate in the archaeological field, supporting different phases of the archaeologist's work from a small to a large scale, assessing which of the tested techniques can be helpful.

In the first part of my work, a sequence of data processing to generate a 3D model was performed. The results undoubtedly reflect the effectiveness of UAV photogrammetry for acquiring photos with a very high level of detail (large map scales) and high positional accuracy. Moreover, by using Control Points measured in the field we can obtain a controlled positional accuracy, also enabling a proper overlapping of multi-temporal orthoimages. In relation to the goal of the first section, I would add that perceiving the whole archaeological site with drone acquisitions helps to comprehend in an immediate way all the objects and the topography at once, especially by exploring the 3D model. This is extremely relevant when physically visiting the site is challenging or impossible, as in the Covid-19 period. Thanks to the proper geomatics techniques, surveying the area in a detailed way and virtual tours are possible without physical presence.

In the second section of the thesis, the interesting results concentrated mostly on the 3D component with the visual inspection of the elevation changes and the exploration of the surface geometry. Due to the ability to inspect and measure elevation data by means of UAV photogrammetry, the contribution of the DSM was proved as highly valuable in my research. Especially when it comes to studying the topography of the site for detecting natural and artificial (such as excavations) changes over time or when searching for surface anomalies. With a simple operation of applying proper raster functions, new layers were generated with a clear representation of the new excavation areas (with respect to a reference period). Other useful thematic and quantitative information such as the area and the volume of the changes through time, were available. Furthermore, the same tool brought compelling outcomes and turned out to be a potential tool for detecting irregularity and discovering new archaeological hidden structures. However, the availability of the Near-Infrared band with the examination and the analysis of False Colour images and Spectral Indices, unsurprisingly (taking the relevant literature into account), did not come up well. Indeed, the NIR band enhances crop marks, but since our studied area, the Necropolis, suffers from a lack of vegetated areas, there was no clear impact on the soil and no additional information to exploit. Nevertheless, I am not rejecting the idea of using the Infrared band. In fact, the literature supports and proves that this band constitutes a significant component in archaeological sites with different seasons. When thinking about future surveys in Hierapolis, it will be interesting to acquire data with sensors sensitive also to other bands such as RedEdge, SWIR and thermal IR that can be exploited to derived tailored Spectral Indices. The new outcomes may contribute more information and enrich the research with new discoveries and thereby, promote the study process in the Necropolis site.

In the third part, I mostly experimented with the GIS tools that can be considered as parallel to the various documentation practices of the archaeologists' work, focusing on the vector data. By taking advantage of the possibility to digitize features and add alphanumeric attributes, I could exploit information from different sources and combine them into a GIS. Some of the strategies that I used were converting raster to vector data and adaptation of external cartographic information, such as CAD format, into the GIS environment. What I found was that the interface with many sources, the control over overlapping thematic layers, editing information and the diversified visualizations, act as key aspects in the GIS environment. These functionalities can guide the user to resolve geospatial analysis problems through a fast, well-organized, friendly application and thus, worth considering as a high priority tool.

In my opinion, this thesis was able to demonstrate that the use of new geomatics technologies definitely supports analyses and documentation of archaeological sites. The photogrammetric processing proved to be extremely effective, from the acquisition phase to the various outcomes. As a result, the information that can be exploited becomes more and more compatible with the documentation demands. Moreover, the ability to compare through time complex and dense areas, whether built or ruined, supports both the work of the archaeologists and the urban designers. The GIS, too, is found to be a highly valuable exploratory tool, which is able to implement algorithms, to store different datasets and to query thematic and geospatial analysis. Nevertheless, due to the difficulties in showing characterization of upstanding structure surfaces, the GIS technique alone is insufficient for the representation of built heritage at the architectural scale. In fact, archaeologists are constantly interested in the latest developments of BIM/GIS integration, since an archaeological site needs to be represented by fully 3D models with vertical surface information. This essential integration between these methods stresses the need for interdisciplinary cooperation. This interaction between disciplines is always useful and brings up fruitful results, such as the verification of archaeological theories from a historical point of view, or the involvement of structural engineering in a restoration project. For creating a collaborative system, many low-cost software and applications are available in the market, which meeting the diverse archaeological needs, such as cultural resource management, survey and excavations, engineering and so on. Furthermore, using one collaborative system is always more efficient for documenting, sharing and studying operations.

To sum up, compared to the traditional processes of analysing archaeological sites, geomatics offers an innovative approach that can promote advanced research and complex results. Applying this modern method has the advantages of saving money, time and minimising potential site damage.

A similar approach can certainly be exploited in different application domains, especially in the urban design world. Geomatics technologies, like in archaeological sites, can enhance the understanding of the existing urban structure and increase planning quality for the public good. In addition, the fact that this profession is focused on the interaction between a building and the environment also strengthens the collaboration between CAD, BIM (building design tools) and GIS (environmental data modelling tools).

In light of all these insights, it can be concluded that it is essential to keep exploring how geomatics can cooperate with other disciplines, by means of integrated workflows and methodologies, to support specific application domains.

Bibliography

Abate, Nicodemo, Abdelaziz Elfadaly, Nicola Masini, and Rosa Lasaponara. 2020. “Multitemporal 2016-2018 Sentinel-2 Data Enhancement for Landscape Archaeology: The Case Study of the Foggia Province, Southern Italy.” Remote Sensing 12 (8): 1309.

Aboutalebi, Mahyar, Alfonso F. Torres-Rua, William P. Kustas, Héctor Nieto, Calvin Coopmans, and Mac McKee. 2019. “Assessment of Different Methods for Shadow Detection in High-Resolution Optical Imagery and Evaluation of Shadow Impact on Calculation of NDVI, and Evapotranspiration.” Irrigation Science 37 (3): 407–29.

Acharya, Tri Dev, Anoj Subedi, In Tae Yang, and Dong Ha Lee. 2017. “Combining Water Indices for Water and Background Threshold in Landsat Image.” Proceedings 2 (3): 143.

Al-Ruzouq, Rami, Senthilkumar Venkatachalam, Abdelrahman Abueladas, & Saleh, and Abu Dabous. 2018. “Geomatics for Economic Archaeological Documentation and Management.” Applied Geomatics (2018) 10: 341–60.

Asfaw, Engdawork, K. V. Suryabhagavan, and Mekuria Argaw. 2018. “Soil Salinity Modeling and Mapping Using Remote Sensing and GIS: The Case of Wonji Sugar Cane Irrigation Farm, Ethiopia.” Journal of the Saudi Society of Agricultural Sciences 17 (3): 250–58.

Astori, B., C. Bonfanti, and A. Spano. 2003. “Integrated and Multiscale Spatial Data to Base a Gis for the Ancient City of Hierapolis in Phrygia.” International Archives of the Photogrammetry, Remote Sensing and Spatial Information Sciences- ISPRS Archives, 2003.

Boito, Camillo, and Cesare Birignani. 2009. “Restoration in Architecture: First Dialogue.” Source: Future Anterior: Journal of Historic Preservation. Vol. 6.

Castrianni, Laura, Giacomo Di Giacomo, Imma Ditaranto, and Giuseppe Scardozzi. 2008. “Integrated Technologies and Methodologies for the Reconstruction of the Ancient Topography of Hierapolis in Phrygia and Its Territory (Turkey).” In Proc. of the International Congress “Cultural Heritage and New Technologies”, Workshop 2008, 23.

Chiabrando, Filiberto, Francesco D'Andria, Giulia Sammartano, and Antonia Spanò. 2018. "UAV Photogrammetry for Archaeological Site Survey. 3D Models at the Hierapolis in Phrygia (Turkey)." Virtual Archaeology Review 9 (18): 28.

Choi, Y. J., J. Lampel, S. Fiedler, D. Jordan, and T. Wagner. 2020. "A New Method for the Identification of Archaeological Soils by Their Spectral Signatures in the Vis-NIR Region." Journal of Archaeological Science: Reports 33 (October): 102553.

D'Andria, Francesco; Scardozzi, and A.T. Spanò. 2008. "Atlante Di Hierapolis Di Frigia- 39PTO- Politecnico Di Torino." 2008.

D'Andria, Francesco. 2018. "Hierapolis in Phrygia. Tourism-Related Use and Abuse of an Archaeological Site." MIRAS 4 (HERITAGE IN CONTEXT 2-Archaeology and Tourism): 201–30.

D'Andria, Francesco and Tullia Ritti. 1985. "Hierapolis Scavi e Ricerche II. Le Sculture Del Teatro.I Rilievi Con i Cicli Di Apollo e Artemide." American Journal of Archaeology 90 (4): 499.

Daniel Câmara and Navid Nikaein. 2015. "Wireless Public Safety Networks Volume 1 : Overview and Challenges." Elsevier Ltd. 2015.

Daria De Bernardi Ferrero. 1993. "Arslantepe, Hierapolis, Iasos, Kyme. Scavi Archeologici Italiani in Turchia." BOSPHORUS BOOKS. 1993.

Djindjian, F. 1998. "GIS Usage in Worldwide Archaeology." Archeologia e Calcolatori n. IX- 1998, January.

Favretto, Andrea. 2010. "API, Cloud Computing, WebGIS and CartographyAPI, Cloud Computing, WebGIS et Cartographie." Netcom, no. 24-3/4 (December): 245–60.

Fuldain González, Juan, and Félix Varón Hernández. 2019. "NDVI Identification and Survey of a Roman Road in the Northern Spanish Province of Álava." Remote Sensing 11 (6): 725.

Gholizadeh, Asa, Daniel Žižala, Mohammadmehdi Saberioon, and Luboš Borůvka. 2018. "Soil Organic Carbon and Texture Retrieving and Mapping Using Proximal, Airborne and Sentinel-2 Spectral Imaging." Remote Sensing of Environment 218 (December): 89–103.

Granshaw, Stuart I. 2020. “Photogrammetric Terminology: Fourth Edition.” The Photogrammetric Record 35 (170): 143–288.

Jackson Davina and Simpson Richard. 2020. "Digital City: An Urban Perspective on Digital Earth". Manual of Digital Earth, editors: Huadong Guo, Michael F. Goodchild, Alessandro Annoni. Springer 2020 p. 527-564.

Kealy, Loughlin, and Stefano F Musso. 2011. EAAE Transactions on Architectural Education TRANSFORMATION.

Koucká, Lucie, Veronika Kopačková, Kateřina Fárová, and Martin Gojda. 2018. “UAV Mapping of an Archaeological Site Using RGB and NIR High-Resolution Data.” Proceedings 2 (7): 351.

Kraak, Menno Jan. 2004. “The Role of the Map in a Web-GIS Environment.” Journal of Geographical Systems 6 (2): 83–93.

Kumsar, Halil, Ömer Aydan, Celal Şimşek, and Francesco D’Andria. 2016. “Historical Earthquakes That Damaged Hierapolis and Laodikeia Antique Cities and Their Implications for Earthquake Potential of Denizli Basin in Western Turkey.” Bulletin of Engineering Geology and the Environment 75 (2): 519–36.

Lasaponara, Rosa, and Nicola Masini. 2007. “Detection of Archaeological Crop Marks by Using Satellite QuickBird Multispectral Imagery.” Journal of Archaeological Science 34 (2): 214–21.

Linderholm, Johan, Paul Geladi, Nathalie Gorretta, Ryad Bendoula, and Alexia Gobrecht. 2019. “Near Infrared and Hyperspectral Studies of Archaeological Stratigraphy and Statistical Considerations.” Geoarchaeology 34 (3): 311–21.

Mondejar, Jeremy P., and Alejandro F. Tongco. 2019. “Near Infrared Band of Landsat 8 as Water Index: A Case Study around Cordova and Lapu-Lapu City, Cebu, Philippines.” Sustainable Environment Research 1 (1): 16.

Negri, Sergio, and Giovanni Leucci. 2006. “Geophysical Investigation of the Temple of Apollo (Hierapolis, Turkey).” Journal of Archaeological Science 33 (11): 1505–13.

Nikolakopoulos, Konstantinos G., Konstantina Soura, Ioannis K. Koukouvelas, and Nikolaos G. Argyropoulos. 2017. “UAV vs Classical Aerial Photogrammetry for Archaeological Studies.” Journal of Archaeological Science: Reports 14 (August): 758–73.

Nuzzo, Luigia, Giovanni Leucci, and Sergio Negri. 2009. “GPR, ERT and Magnetic Investigations inside the Martyrium of St Philip, Hierapolis, Turkey.” Archaeological Prospection 16 (3): 177–92.

Pillay, Sharlene. 2015. “Introduction Aerial Photogrammetry.” www.wisegeek.com/what-.
Pohl, C, and J L Van Genderen. 1998. “International Journal of Remote Sensing Review Article M Ultisensor Image Fusion in Remote Sensing: Concepts, Methods and Applications.” Int. j. Remote Sensing 19 (5): 823–54.

Pohl, C, and J L Van Genderen. 1998. “International Journal of Remote Sensing Review Article M Ultisensor Image Fusion in Remote Sensing: Concepts, Methods and Applications.” Int. j. Remote Sensing 19 (5): 823–54.

Ritti, Tullia, Klaus Grewe, and Paul Kessener. 2007. “A Relief of a Water-Powered Stone Saw Mill on a Sarcophagus at Hierapolis and Its Implications.” Journal of Roman Archaeology. Journal of Roman Archaeology L.L.C.

Ronchetta, Donatella. 2017. “L’ARCHITETTURA FUNERARIA DI HIERAPOLIS DI FRIGIA Le Tombe A Della Necropoli Nord.”

Salgado Carmona, José Ángel, Elia Quirós, Victorino Mayoral, and Cristina Charro. 2020. “Assessing the Potential of Multispectral and Thermal UAV Imagery from Archaeological Sites. A Case Study from the Iron Age Hillfort of Villasviejas Del Tamuja (Cáceres, Spain).” Journal of Archaeological Science: Reports 31 (June): 102312.

Sammartano, G., F. Chiabrando, and A. Spanò. 2020. “OBLIQUE IMAGES AND DIRECT PHOTOGRAMMETRY WITH A FIXED WING PLATFORM: FIRST TEST AND RESULTS IN HIERAPOLIS OF PHRYGIA (TK).” ISPRS - International Archives of the Photogrammetry, Remote Sensing and Spatial Information Sciences XLIII-B2-2020 (B2): 75–82.

Scardozzi, Giuseppe. 2007. “Remote Sensing and Archaeological Survey in the Hierapolis of Phrygia Territory, Turkey.” In Remote Sensing for Environmental Monitoring, GIS Applications, and Geology VII, edited by Manfred Ehlers and Ulrich Michel, 6749:674904. SPIE.

Scardozzi, Giuseppe. 2008. “Old High Resolution Satellite Images for Landscape Archaeology: Case Studies from Turkey and Iraq.” In Remote Sensing for Environmental Monitoring, GIS Applications, and Geology VIII, edited by Ulrich Michel, Daniel L. Civco, Manfred Ehlers, and Hermann J. Kaufmann, 7110:711004. SPIE.

Semeraro Grazia. 2016. "The Sanctuary of Apollo in Hierapolis: building activities and ritual paths". In: Ancient quarries and building sites in Asia Minor.Research on Hierapolis in Phrygia and other cities in south-western Anatolia:archaeology, archaeometry, conservation. p. 777-785, BARI:EDIPUGLIA

Spanò, A. "Le ragioni dell’intervento di natura topografica a Hierapolis- 1999", In: Hierapolis scavi e ricerche IV– Saggi in onore di Paolo Verzone, a cura di: D. Ferrero De Bernardi, Giorgio Bretschneider (ITALIA), 2002.

Spanò, A., B. Astori, C. Bonfanti, and F. Chiabrando. 2004. “GIS Applications for Knowledge and Preservation of Hierapolis of Phrygia Site.” International Archives of the Photogrammetry, Remote Sensing and Spatial Information Sciences- ISPRS Archives 35.

Spanò, A., F. Chiabrando, G. Sammartano, and L. Teppati Losè. 2018. “Integrated Imaging Approaches Supporting the Excavation Activities. Multi-Scale Geospatial Documentation in Hierapolis (TK).” In International Archives of the Photogrammetry, Remote Sensing and Spatial Information Sciences- ISPRS Archives, 42:1075–82. International Society for Photogrammetry and Remote Sensing.

Suárez, Lola, J A J Berni, P J Zarco-Tejada, L Suárez, V González-Dugo, and E Fereres. 2008. “Remote Sensing of Vegetation from UAV Platforms Using Lightweight Multispectral and Thermal Imaging Sensors SPECCHIO Spectral Information System View Project UAV-Borne Spectroscopy to Detect Tomato Diseases View Project REMOTE SENSING OF VEGETATION FROM U.”

Teppati Losèa, Lorenzo, Antonia Spanò, and Anna Anguissola. 2021. “GEOMATICS ADVANCED TESTINGS FLANKING ARCHAEOLOGICAL RESEARCH. A NOTEWORTHY AREA IN THE NORTHERN NECROPOLIS OF HIERAPOLIS OF FRIGIA (TK).”

Themistocleous, K, A Agapiou, B Cuca, and D G Hadjimitsis. 2015. “UNMANNED AERIAL SYSTEMS AND SPECTROSCOPY FOR REMOTE SENSING APPLICATIONS IN ARCHAEOLOGY.”

Verhoeven, Geert Julien, 2007. “Becoming a NIR-Sensitive Aerial Archaeologist.” In Remote Sensing for Agriculture, Ecosystems, and Hydrology IX, edited by Christopher M. U. Neale, Manfred Owe, and Guido D’Urso, 6742:67420Y. SPIE.

Verhoeven, Geert Julien, Philippe F. Smet, Dirk Poelman, and Frank Vermeulen. 2009. “Spectral Characterization of a Digital Still Camera’s NIR Modification to Enhance Archaeological Observation.” IEEE Transactions on Geoscience and Remote Sensing 47 (10): 3456–68.

Verhoeven, Geert Julien, 2012. “Near-Infrared Aerial Crop Mark Archaeology: From Its Historical Use to Current Digital Implementations.” Journal of Archaeological Method and Theory 19 (1): 132–60.

Vettori, Silvia, Susanna Bracci, Emma Cantisani, Claudia Conti, Marilena Ricci, and Maria Piera Caggia. 2019. “Archaeometric and Archaeological Study of Painted Plaster from the Church of St. Philip in Hierapolis of Phrygia (Turkey).” Journal of Archaeological Science: Reports 24 (April): 869–78.

Waterson, Merlin, and Ian Morrison. 2019. Rescue & Reuse: Communities, Heritage and Architecture. Riba.

Wenn, Camilla Cecilie, Sven Ahrens, and Johann Rasmus Brandt. 2017. “Romans, Christians, and Pilgrims at Hierapolis in Phrygia. A Funerary Journey of Mental Changes.” 9781785703591, 196–216.

Winter, Stephan. 1998. “Bridging Vector and Raster Representation in GIS.”, Proceedings of the 6th ACM international symposium on advances in geographic information systems, 1998-11-01, p.57-62

First of all, I would like to thank Professor Giulio Tonolo Fabio and Professor Spanò Antonia for the guidance and the support they gave me from the beginning with their promptness in responding with always great availability in presence and in remote. I also sincerely thank to Dr. Patrucco Giacomo and Dr. Sammartano Giulia for assisting and solving technical issues during my work on the thesis.

I would like to express my gratitude to the Politecnico di Torino for having me in their master's program and for giving me the chance to pursue my dream to study architecture in Italy, and the opportunity to enrich my academic education and skills. I also thankful to all my teachers in the Architecture Construction City Master of Science degree program who shared their knowledge and experience with me and to my friends from around the world that I had a chance to meet during my studies.

I am the most thankful to the ones who never left my mind and thoughts, my parents who are not among the living but have always accompanied me in my heart, to my siblings for their support and advices and to my friends who were always there to listen and encourage.

Thank you.